IDENTIFICATION OF ALTERED RAS SIGNALING AND INTERMEDIATE FILAMENT HYPERPHOSPHORYLATION IN GIANT AXONAL NEUROPATHY

Kyle Benjamin Martin

Submitted to the faculty of the University Graduate School
in partial fulfillment of the requirements
for the degree
Doctor of Philosophy
in the Department of Medical and Molecular Genetics,
Indiana University

May 2015

Accepted by the Graduate Faculty, Indiana University, in partial fulfillment of the requirements for the degree of Doctor of Philosophy.

_____
R. Mark Payne, M.D., Chair

_____
Theodore R. Cummins, Ph.D.

Doctoral Committee

_____
Nuria Morral, Ph.D.

December 17, 2014

_____
Ronald C. Wek, Ph.D.

ACKNOWLEDGMENTS

First and foremost, I would like to thank my advisor Dr. R. Mark Payne for his continued guidance and support. Although my project was not directly related to his other research interests and outside his clinical expertise, Dr. Payne's patience and encouragement allowed this project to fully develop into what it is today. I would also like to thank the members of my research committee, Dr. Ronald Wek, Dr. Nuria Morral, and Dr. Theodore Cummins, for their help and constructive criticism over the years. I am also grateful for the continual guidance of Dr. Brittney-Shea Herbert, whose advice on academics and the Ph. D. process have been invaluable to my matriculation through the program.

Next, I would like to thank all the current and former members of the Payne Lab, of which I am particularly grateful to Sam Beard, Loren Nelson, and Kelsey Loden for their contributions to this work. I also am especially thankful for the help of Malgorzata "Gosia" Kamocka and Seth Winfree of the Indiana Center for Biological Microscopy for their training and troubleshooting for all the microscopy contained in this work.

I am also grateful to Lori and Matt Sames for organizing multiple Giant Axonal Neuropathy conferences, which I attended with other researchers from around the world. In addition to learning about other critical GAN research, these conferences provided me a forum to meet the Sames family, whose daughter, Hannah, suffers from GAN. Meeting the Sames family and experiencing their

resolve was truly moving and provided me with more than enough motivation to complete this research.

Finally, I would like to thank all my friends and family for their support throughout my tenure in graduate school. In particular I would like to thank my parents who, despite not understanding the science of what I was doing, were always there to support me. Without them, none of this would have been possible.

Kyle Benjamin Martin

IDENTIFICATION OF ALTERED RAS SIGNALING AND INTERMEDIATE FILAMENT HYPERPHOSPHORYLATION IN GIANT AXONAL NEUROPATHY

Giant axonal neuropathy (GAN) is a rare genetic disease that causes progressive damage to the nervous system. Neurons in GAN patients develop an abnormal organization of cytoskeletal proteins called intermediate filaments (IFs), which normally provide strength and support for the overall cell structure. The irregular IF structure in GAN patient neurons leads to a progressive loss of motor skills in children and subsequent death in adolescence. GAN is caused by reduced levels of the gigaxonin (Giga) protein. Giga functions to control the degradation of other cellular proteins, and the loss of Giga in GAN cells results in significantly elevated levels of the galectin-1 (Gal-1) protein. Gal-1 stabilizes the active form of the Ras signaling protein, which functions as a molecular switch to regulate the phosphorylation and subsequent organization of IFs. The connection between these pathways led us to propose that Giga regulates IF phosphorylation and structure by modulating Ras signaling through the degradation of Gal-1. Using GAN patient cells, we demonstrated that restoring Giga reduced Gal-1 protein levels, decreased IF phosphorylation, and reestablished normal IF organization. Similar effects of reduced IF phosphorylation and improved IF structure were also obtained in GAN cells by directly decreasing the protein levels of either Gal-1, or downstream Ras

signaling proteins. Taken together, these results demonstrate that the loss of Giga induces Gal-1 mediated activation of Ras signaling, thereby leading to the increased IF phosphorylation and abnormal IF structure observed in GAN cells. Identification of aberrant Ras signaling is significant because it is the first to specify a mechanism by which the loss of Giga leads to the development of GAN and provides targets for novel drug therapies for the treatment of this currently immedicable genetic disease.

R. Mark Payne, M.D., Chair

TABLE OF CONTENTS

LIST OF FIGURES

LIST OF ABBREVIATIONS

BTB	broad complex, tramtrack, and bric-a-brac
CNS	central nervous system
CRL	cullin-RING ligase
Cul3	cullin-3
DMEM	Dulbecco's modified Eagle's medium
EBS	epidermolysis bullosa simplex
eGFP	enhanced green fluorescent protein
FBS	fetal bovine serum
Gal-1	galectin-1
GAN	Giant Axonal Neuropathy
GAPDH	glyceraldehyde-3-phosphate dehydrogenase
GAPs	GTPase-activating proteins
GDP	guanosine diphosphate
GEFs	guanine nucleotide exchange factors
GFAP	glial fibrillary acidic protein
GFP	green fluorescent protein
Giga	gigaxonin
GTP	guanosine triphosphate
HECT	homologous to E6-AP C-terminus
HGPS	Hutchinson–Gilford progeria syndrome
HVR	hypervariable region

IFs	intermediate filaments
IRES	internal ribosome entry site
kDa	kilodalton
MAPs	microtubule-associated proteins
MAP1B	microtubule-associated protein 1B
MAP8	microtubule-associated protein 8
MATH	meprin and TRAF homology
MEK1	mitogen-activated protein kinase kinase 1
MEK2	mitogen-activated protein kinase kinase 2
NF-H	neurofilament heavy chain
NF-L	neurofilament light chain
NF-M	neurofilament medium chain
NFs	neurofilaments
PBS	phosphate buffered saline
PHD	plant homeodomain
PI3K	phosphoinositide 3-kinase
PKA	protein kinase A
PNS	peripheral nervous system
PVDF	polyvinyl difluoride
RING	really interesting new gene
Ser	serine
siRNA	small interfering ribonucleic acid
TAT	transactivator of transcription

TBCB	tubulin-folding cofactor B
UPS	ubiquitin-proteasome system
VFA	vimentin free area

CHAPTER I: INTRODUCTION

Giant Axonal Neuropathy: description and clinical overview

Giant Axonal Neuropathy (GAN) is a rare autosomal recessive disease characterized by early onset and progressive neurologic dysfunction in both the peripheral nervous system (PNS) and central nervous system (CNS). GAN patients are undiagnosed at birth due to the apparent lack of symptoms at this time. Patients demonstrate slightly delayed motor development through the first years of life, but they usually begin to walk in a time frame commensurate with their peers (1-3). As the disease progresses, however, GAN patients slowly develop PNS dysfunction that presents as a gait disorder around the age of two to five years old (3). The ambulatory ability of GAN patients slowly deteriorates until a walking aid is needed around the age of eight to twelve years old, and the neurologic dysfunction eventually progresses to a point where they become confined to a wheelchair in middle to late adolescence (3). Eventually, multiple functions of the autonomic nervous system fail in patients, thus necessitating the use of feeding tubes and ventilators in the advanced stages of the disease (4). GAN patients ultimately die of respiratory failure, usually in their second decade of life (5, 6).

Throughout the progression of the disease, motor and sensory neuron abnormalities are observed as most patients exhibit distal muscle weakness, distal sensory impairment, nystagmus, and areflexia (6-8). Other less common symptoms include optic atrophy, epilepsy, dysarthria, and developmental delay

(6, 8, 9). Upon electrophysiological examination, these symptoms were shown to be the result of decreased nerve conduction velocities and massively reduced motor and sensory nerve action potentials (9, 10). In addition to the PNS defects, additional tests demonstrated CNS dysfunction through irregular electroencephalography readings and magnetic resonance imaging of diffuse white matter abnormalities in these patients (2, 7, 11, 12). Further CNS involvement in GAN was confirmed by magnetic resonance spectroscopy, which showed significant demyelination and neurodegeneration in white matter as well as a proliferation of glial cells in both white and gray matter (13, 14).

These clinical findings are not inherently unique to GAN as similar symptoms are observed in multiple other childhood disease involving chronic polyneuropathy. There are two characteristics, however, that are distinctive features of this disease. The first is the presence of tightly curled, or sometimes referred to kinky, hair that is observed in most GAN patients (1-3, 7, 9, 12, 15, 16). In each case, the tightly curled hair is observed on the head, eyelashes, and eyebrows, and is distinctly different from that of the parents. GAN patients have been observed in many different ethnic backgrounds, including Japanese, Indian, and European descent, with each having this remarkably curly hair (6, 17). Ultrastructural examination of hair samples from multiple GAN patients were mostly unremarkable, but revealed the presence of unusual longitudinal grooves throughout the hair (2, 10, 18). Although this remains an interesting finding, the mechanism of altered hair structure and its relevance to GAN remains unknown.

In addition to this unique hair phenotype, GAN patients also have a second distinctive characteristic of enlarged, or so-called “giant,” neuronal axons from which the name of the disease was derived (1). These enlarged axons measure 30-50 μm in diameter in sural nerve cross sections (6, 18, 19) and are significantly larger than the 3-6 μm diameter axons observed in unaffected individuals (20). Axonal enlargements are not uniform throughout the entire length of the neuron, however, as longitudinally dissected nerve fibers reveal segmental swellings with intermittent areas of normal axon diameter (1, 2, 11, 21). The distended segments tend to be more abundant in the proximal region of the axon, with swellings near the axon hillock, and are less commonly found in distal region (18, 22). Each enlarged axonal segment is also noted as having an abnormally thin or completely absent myelin sheath (11, 12, 17, 19). In addition to the irregular neuronal structure, patient biopsies also reveal reduced nerve fiber populations, thus indicating axonal loss and neurodegeneration (1, 17, 21). This phenotype of giant axons, thin myelin sheaths, and neurodegeneration is observed throughout the entire nervous system, with similar observations noted in the peripheral nerves, spinal cord, and cerebral cortex (18, 23).

Ultrastructural analysis of the enlarged axonal segments revealed the presence of densely packed and disorganized neuronal intermediate filaments, termed neurofilaments (1, 7, 12, 21). Neurofilaments, along with actin and microtubules, comprise the cytoskeletal structure needed to maintain neuron organization and function. The abnormal accumulation of neurofilaments, however, impedes GAN patient neuronal function by occupying all the axonal

space and displacing other organelles (6, 17, 23). Mitochondria and microtubules are particularly affected, as they are excluded from the central neurofilament mass and found only sparingly in the periphery of each enlarged axonal segment (1, 19, 24, 25). Conversely, the intermittent narrow portions of the axon contain only microtubules and mitochondria and are devoid of neurofilaments (1, 22). This interesting observation demonstrates that the accumulation of neurofilaments is responsible for the giant axons observed in patients, and prompted GAN to be classified as a disease of the intermediate filaments.

Function and dynamics of intermediate filaments

Intermediate filaments (IFs) were initially described nearly a half century ago and the name was derived from their diameter (10 nm) being intermediate in size compared to that of microfilaments (7 nm) and microtubules (24 nm) (26). In contrast to microfilaments and microtubules, which are composed of highly conserved globular actin and tubulin proteins, respectively, IFs are constructed from a highly divergent family of filamentous proteins. Each member of the IF family contains a prototypical three domain structure that includes a non-α-helical amino-terminal head domain, a central α-helical rod domain, and a non-α-helical carboxyl-terminal tail domain (27, 28). Although the central rod domain is largely conserved between IF proteins, high variability in both the head and tail domains has led to the identification of at least 67 different IF proteins that share as little as 20% sequence identity (27). This large group of divergent proteins was

eventually classified into five distinct types based on sequence similarity, assembly properties, and expression patterns (29).

Type-I and type-II IFs are comprised of the acidic and neutral-basic keratins, respectively, and are expressed mainly in epithelial cells (30). Four different proteins: vimentin, desmin, glial fibrillary acidic protein (GFAP), and peripherin, are classified together as type-III IFs. Vimentin is the most widely expressed of all IFs and is found in endothelial cells, epithelial cells, and mesenchymal cells such as fibroblasts (31). The other members of the type-III IFs have a limited distribution, with desmin in muscle cells, GFAP in glial cells, and peripherin in the neurons of the PNS. Type-IV proteins include nestin, syncoilin, α-internexin, and the neurofilament triplet proteins that together comprise the neuronal IF network (32). The individual triplet proteins were initially described based on their molecular weight; therefore, they were called the neurofilament light (NF-L), neurofilament medium (NF-M), and neurofilament heavy (NF-H) proteins (29). Type-V IFs are composed of the lamin proteins, which form the nuclear lamina on the interior of the nuclear envelope (33). In contrast to the other four types of cytosolic IFs, the type-V lamins are restricted to the nucleus.

Despite vast differences in head and tail domain amino acid sequence, the conserved central rod domain allows all classes of IF to assemble in a similar stepwise process to form the filamentous network of the cell. For each type of IF, the α-helical rod domains of two proteins associate in a parallel and non-staggered manner to form a coiled-coil dimer (34-37). Two dimers then pair

together in an antiparallel and half-staggered fashion to create a soluble tetramer that functions as the basic IF subunit (28). Next, eight tetrameric subunits associate laterally to form a unit length filament, which then progressively anneal end-to-end to eventually form the full length immature IF structure (38-42). Once the structure is in place, the filaments undergo an internal reorganization by radially compacting to form the mature 10 nm diameter filaments (43, 44). These discrete mature filaments then coalesce to create an extensive and complex IF network that spans the entire cytosolic space from the nucleus to cell membrane (45-47).

Once this intricate array is formed, IFs generally function as the primary structural elements of the cell and are critical to maintaining the overall cellular shape (35, 48). Goldman and colleagues (49) demonstrated this function in fibroblasts by using a peptide mimetic that bound to the central α-helical rod domain of native vimentin IFs and inhibited the dimerization of vimentin monomers . Without the ability to construct full length filaments, the vimentin network in these fibroblasts was destabilized and eventually disassembled. Concurrent with this disassembly, the fibroblasts drastically changed their overall structure by retracting their filopodia and acquiring an exclusively rounded shape. Similar shape alterations have also been demonstrated in cells of the nervous system, as depleting the IF network through knockdowns of GFAP in glial cells and peripherin in PC12 cells inhibited each cell line's ability to form peripheral processes and neurites, respectively (50, 51). Collectively, these experiments indicated a universal function of cell shape determination for all classes of IFs.

In addition to their function in maintaining overall cellular shape, IFs have also been shown to regulate the intracellular shape by controlling the distribution of multiple organelles such as the nucleus, Golgi apparatus, and mitochondria (52-54). This IF-mediated distribution is especially critical for mitochondria, as studies in mice have shown that mice lacking the expression of the muscle-specific desmin IF have altered mitochondrial morphology and distribution. The mitochondria defect eventually leads to cardiovascular lesions and a dilated cardiomyopathy (54-56). These experiments demonstrate that all classes of IFs function as both mechanical integrators of intracellular space and primary determinates of cellular shape.

For many years, the role of maintaining overall cellular architecture was attributed to IFs being stable and static structures. These assumptions were based on the unique biochemical properties of IFs in relation to the other highly dynamic microfilaments and microtubules. During protein extraction, high concentrations of salts and detergents solubilize most cellular proteins, including actin and tubulin, but only small pools of soluble IFs were recovered (57). The remaining IF structure could be isolated as full length, insoluble filaments (58). These unique biochemical properties demonstrated that the polymerization of IFs creates an extremely stable structure and led to the assumption that there was little subunit exchange on the mature filament due to the lack of soluble IF intermediaries.

Despite the initial labeling as a static structure, more recent experiments revealed a more dynamic and mobile IF network than had previously been

hypothesized. The dynamic properties of IFs were demonstrated by monitoring the ectopic expression of IFs in transfected cells by immunofluorescence at different time points. These studies revealed that newly synthesized IFs are incorporated into the endogenous network at numerous discrete sites throughout the entire length of each filament in a process termed dynamic subunit exchange (59-61). Additional time-lapse observation using green fluorescent protein (GFP) fusion proteins further confirmed this process of dynamic subunit exchange, and also showed that individual filaments and smaller IF subunits are in perpetual motion without changing the overall cellular shape (62, 63).

The constant flux of IFs was also shown to involve the fast and discontinuous movement of IF subunits that could not be explained by simple diffusion alone (64). Instead, an intact microtubule network was required for this dynamic movement as microtubule disassembly disrupted the motion of IF subunits and forced the majority of IFs into juxtanuclear cap (65, 66). This dependence on microtubules and rate of motion suggested that the microtubule-based motors kinesin and dynein were responsible for IF subunit motility. Indeed, moving IF subunits were shown to colocalize both motor proteins and disrupting this interaction had dramatic effects on the IF network (65, 67). By blocking the association between microtubules and kinesin, all kinesin-mediated plus-end transport was disrupted, and a subsequent collapse of the IF network into a compacted perinuclear aggregate was observed (65, 68). In contrast, enhanced kinesin binding resulted in increased plus-end transport and accumulation of IFs in the cellular periphery (67). Taken together, these findings demonstrate that IFs

compose a constantly fluctuating network that is mediated by microtubule based motors and is critical for the structural integrity of the cell.

Generalized IF dysfunction in GAN

As the principal structural elements of the cell, IFs are indispensable for proper cellular function and abnormalities in the IF network have debilitating consequences. Dysfunction of the IFs has been described as the primary determinant for many genetic diseases, such as epidermolysis bullosa simplex (EBS). EBS is a rare autosomal dominant disease characterized by bullous skin lesion that occur in response to minor injuries or abrasions (69). The disease is caused by mutations in the keratin intermediate filament protein, which is expressed in the keratinocyte cells that compose the epidermis (70). During keratin network assembly, the abnormal keratin expressed from the mutant allele binds to the normal keratin expressed from the normal allele and prevents any further IF polymerization (71). The lack of polymerization impedes the formation of the mature IF network and causes the basal keratinocytes to become fragile and easily damaged in response skin perturbations (69). This disease demonstrates the structural importance of IFs and shows that mutations in one type of IF can have devastating effects.

Abnormal IF structure serves as the genetic basis for a multitude of other diseases including NF-L mutations in Charcot–Marie–Tooth disease type-2 (72), NF-H mutations in amyotrophic lateral sclerosis (73), and lamin-A mutations in Hutchinson–Gilford progeria syndrome (HGPS) (74). HGPS is a rare genetic

disease characterized by the appearance of marked premature aging. The mutant lamin-A produced in patients is improperly processed and becomes permanently affixed to the inner nuclear membrane, thus preventing its incorporation into the normal nuclear lamina (33). Acting in a dominant gain-of-function manner, the mutant lamin disrupts the normal lamin structure and eventually leads to severely disrupted nuclear structure and function (75). Collectively, these diseases are caused by mutations in one type of IF, which proceeds to compromise the mechanical integrity of any cell expressing that particular IF.

Unlike these other IF disorders, GAN is unique in that multiple classes of IFs are abnormal in numerous different cell types. In addition to the neurofilament accumulations in neurons, GAN patients also display aggregated IFs in other cells of the nervous system such as astrocytes, Schwann cells, endoneurial fibroblasts, and perineurial cells (10, 11, 76, 77). Abnormal IF structure has also been observed in cells outside the nervous system, for instance, muscle fibers, endomysial fibroblasts, endothelial cells, and pericytes (11, 19, 78, 79). In addition, altered keratin IFs are believed to cause the remarkably curly hair phenotype of GAN patients (16, 80). Since these affected cells express several different types of IFs, this suggests that GAN is not a disease of a single IF class, but rather that GAN is a disorder of generalized cytoplasmic IF disorganization.

This overall IF disorganization is also observed in dermal fibroblasts isolated by skin biopsy, which display a collapsed IF network that is retracted from the cell periphery and gathered into a discrete cytoplasmic mass near the

center of the cell, as determined by fluorescence microscopy (77, 81, 82). This mass is composed of the type-III IF protein, vimentin, and forms either an aggregate adjacent to the microtubule-organizing center, or a perinuclear ring that encircles the nucleus (83, 84). In normal growth conditions utilizing medium containing over 2% fetal bovine serum (FBS), vimentin aggregates are only observed in an average of 3% to 15% of GAN fibroblast cells (82, 84). Although this collapsed vimentin network is constitutively apparent in a subset of GAN fibroblasts grown in normal culture conditions, the phenotype is aggravated upon serum starvation. GAN cells grown in low serum conditions (0.1% FBS) exhibit a retraction of the vimentin network away from the cell periphery and vimentin aggregation is enhanced in an average of 48% to 88% of GAN cells, depending on the patient cell line (82, 84, 85). Similar induction of vimentin aggregates is also observed upon prolonged culture confluency and as a function of passage number, with a higher percentage of cells containing aggregates as the passage number increases (84, 86).

Despite this dramatic induction of vimentin rearrangement, the actin and microtubule networks are unaltered in GAN cells and remain indistinguishable from control fibroblasts in any of the previously described conditions that affect IF structure (82-86). In all conditions, IF aggregates appear to form from a distinct subpopulation of vimentin filaments that normally populate the IF network. When assayed by immunoblotting or quantitative proteomics, there is no increase in vimentin synthesis and no significant difference in the amount of vimentin between GAN and control fibroblasts (86-89). These quantitative techniques

demonstrate that the formation of vimentin aggregates in GAN fibroblasts is not a result of increased IF protein levels, but rather result from a disorganization of the existing vimentin structure. This disorganized vimentin structure resembles the altered neurofilament network observed in GAN neurons and allows GAN fibroblasts to be used as a cell culture model to study the molecular mechanisms of the disease. Altogether, the generalized IF abnormalities in multiple GAN cell types suggests a defect in a more ubiquitously expressed protein that regulates IF structure, as opposed to a single defect in one class of IF.

The *GAN* gene and encoded gigaxonin protein

Although GAN was classified as a genetic disease soon after its initial description in the 1970's, the genetic defect causing these IF abnormalities remained elusive (1, 78). Homozygosity mapping of three patient families in 1997 confirmed the autosomal recessive inheritance of GAN and localized the gene locus to chromosome 16q24.1 (90). Further refinement by Bomont and colleagues (91) lead to the identification of a single gene responsible for the disease, simply called the *GAN* gene, which was found to encode for a novel 68 kilodalton (kDa) protein that was named gigaxonin (Giga) . Giga is a ubiquitous low abundance protein that is expressed evenly throughout the PNS and CNS; lower levels of expression are also seen in the heart, muscle, liver, and kidneys (85, 92, 93). After identification of the gene and encoded Giga protein, more than 40 distinct mutations have been identified in the *GAN* gene of patients (94). These mutations are distributed evenly throughout the entire coding sequence

and include missense and nonsense mutations, insertions, and deletions (3, 9, 25, 91, 95-97). Although the type and location of the mutation are variable between cases, all GAN patients have greatly decreased Giga protein levels ranging from 0.7% to 36.6% of unaffected controls (16, 85, 93). The deceased Giga protein levels are not the result of altered transcription since GAN patients have Giga mRNA levels commensurate or even higher than controls, but are rather caused by the mutant Giga in all GAN cases being highly unstable (16, 95). This instability is the result of a shorter protein half-life for GAN-linked mutations, as mutant Giga exhibits a half-life ranging from 1 to 3 hours, whereas control Giga has a half-life of about 10 hours (16). Although GAN-linked mutations were shown to confer Giga protein instability, the function of Giga and its role in the pathogenesis of the disease remained elusive.

The first insights into Giga function came from bioinformatics analyses, which identified Giga sequence similarity to the ‘Broad complex, Tramtrack, Bric-a-brac’ (BTB)-Kelch family of proteins. Like other members of the BTB-Kelch family, Giga contains an N-terminal BTB domain and a C-terminal domain composed of six kelch motifs (91). In a prototypical BTB-Kelch protein, the BTB domain mediates protein-protein interactions and regulates homomeric or heteromeric dimerization (98, 99). Similarly, the Kelch repeats assemble in a β-propeller structure that also facilitate protein-protein interactions (100). With both N- and C-terminal domains mediating protein-protein interactions, members of the BTB-Kelch family have been shown to function as substrate adaptors that play a critical role in the ubiquitin-proteasome system (101).

Regulation of the ubiquitin-proteasome system

The ubiquitin-proteasome system (UPS) is a highly regulated cascade that allows temporal and specific degradation of proteins through targeted proteolysis. Targeting of proteolytic substrates occurs via the energy dependent conjugation of ubiquitin, a highly conserved 76 amino acid polypeptide, to the ε-amino group of a substrate lysine residue (102, 103). Multiple ubiquitin proteins can be added to the substrate to form a ubiquitin chain in a process called polyubiquitination. Polyubiquitinated proteins are then selectively targeted to the proteasome, which is a multisubunit energy dependent protease responsible for protein degradation (102, 104). This regulated protein degradation provides an irreversible process to promptly and specifically decrease target protein levels.

Regulation of the UPS is required to prevent nonspecific proteolysis and involves several steps to ensure targeted protein degradation (105). The first step in the cascade is ubiquitin activation by the E1 ubiquitin-activating enzyme, whose active-site cysteine forms a thiol ester with the C-terminal carboxylate of ubiquitin in an energy dependent reaction (106, 107). Activated ubiquitin is then receptive to nucleophilic attack by the E2 ubiquitin-conjugating enzyme that transiently transports the activated ubiquitin as a thiol ester using its active-site cysteine (102). The third step involves the E3 ubiquitin ligase specifically binding the proteolytic substrate and the subsequent formation of a complex between the substrate bound E3 and the E2 with the activated ubiquitin (104). Once the complex is formed, the E3 catalyzes the transfer of activated ubiquitins from the E2 to a substrate lysine residue, thus resulting in a polyubiquitinated substrate

(108). In the fourth step of the cascade, the polyubiquitinated substrate is delivered to the proteasome, which recognizes the polyubiquitin chain as a signal to degrade the substrate (108). Once it is received by the proteasome, the substrate is unfolded in an energy dependent manner, the proteasome removes the polyubiquitin chain, and the unfolded substrate enters the proteasome by facilitated diffusion (109). Degradation occurs when the substrate enters the central chamber of the proteasome, which contains the protease active sites that degrade the substrate into short polypeptides that are subsequently recycled for new protein synthesis (104). This cascade utilizing multiple enzymes allows for efficient degradation of a diverse population of substrates in a targeted and specific manner.

The enzymes of the UPS cascade are organized in a hierarchical fashion to allow for the increasing specificity needed to facilitate targeted ubiquitination. This hierarchy contains a single E1 that activates ubiquitin for all downstream conjugating enzymes (110). More diversity is observed for the E2 enzymes, with 35 human versions identified so far (111). All E2 enzymes share a conserved core domain of about 150 amino acids, but variable N- and C-terminal regions allow each E2 to associate with several different E3 enzymes (111). Compared to the single E1, the increased number of E2 enzymes allows the activated ubiquitin to be distributed in an efficient manner to the most diverse portion of the hierarchy, which is composed of the E3 ubiquitin ligases. E3 enzymes are responsible for targeting the proteolytic substrate, therefore conferring substrate specificity to the UPS. This specificity is reflected in the number of E3s, as almost

a thousand have been characterized (112). Despite the vast array of E3s, all can be categorized into one of four classes based on their specific structural motif: HECT (homologous to E6-AP C-terminus)-type, PHD (plant homeodomain)-finger-type, U-box-type, or RING (really interesting new gene)-finger-type (112). The largest of these classes is the RING-finger-type E3s, which itself is divided into subclasses that include the cullin-RING ligases (CRLs).

CRLs are multisubunit E3 complexes that are assembled onto a cullin protein that functions as a scaffold on which the rest of the E3 is assembled (113). Human cells express seven highly homologous cullin proteins that have similar structures containing an elongated protein with a central core domain that is flanked by distinct protein binding domains located on N- and C-terminal (101, 114). The C-terminal of the cullin scaffold has a highly conserved domain that binds to the RING protein, which in turn functions as a binding site for an activated E2 ubiquitin-conjugating enzyme (114, 115). On the opposing end of the cullin, the N-terminal domain contains a variable sequence that interacts with specific adaptor proteins (114, 115). These adaptor proteins function to bind specific targeted substrates and chaperone them into the CRL complex where ubiquitin can then be transferred from the cullin-RING-bound E2 to the adaptor-bound substrate (116). Therefore, the substrate adaptors provide the CRL with the substrate specificity needed for targeted and precise degradation.

In addition to conferring specificity to the CRL, the utilization of substrate adaptors also allows for the central cullin-RING complex to associate with numerous different adaptors that can target diverse substrates to the common

core E3 (101). This targeting of adaptors and bound substrates to the core CRL is not universal, however, as not all classes of substrate adaptors can bind to each type of cullin. Instead, the cullin-substrate adaptor interaction is mediated by the variable cullin N-terminal domain and limits each cullin to only interacting with a specific class of substrate adaptors (117). Although their associations are restricted to one class of substrate adaptors, each cullin can interact with numerous substrate receptors of the same class (101). For example, the cullin-3 (Cul3) protein specifically interacts with numerous substrate adaptors that contain an N-terminal BTB domain (99, 118-122). These various BTB proteins also have a C-terminus comprised of either a zinc finger, meprin and TRAF homology (MATH), or Kelch domain that facilitates substrate binding (117). Therefore, these BTB proteins contain an N-terminal domain that permits binding to Cul3 and a C-terminal domain that recruits substrates for ubiquitination. Collectively, this domain structure allows for these BTB proteins to function as efficient substrate adaptors (98). Indeed, numerous BTB proteins have been validated as substrate adaptors for CRL, with one class being the BTB-Kelch proteins that includes Giga (100, 123). The sequence similarity of Giga to other BTB-Kelch proteins supports the hypothesis that Giga functions as substrate adaptor in a multisubunit CRL to facilitate the UPS-mediated degradation of currently unknown substrates (Figure 1).

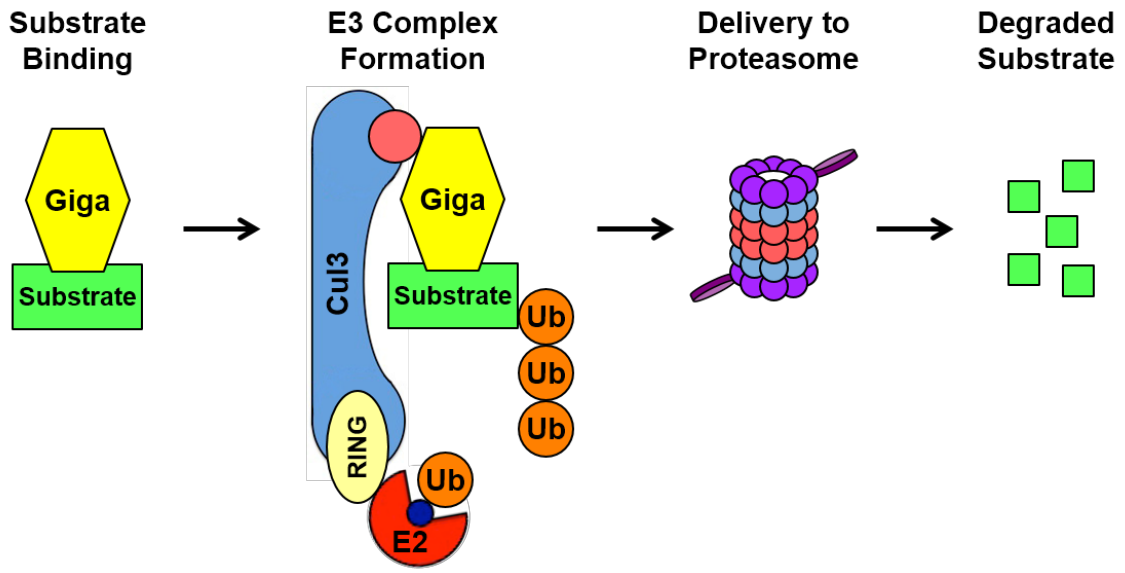

Figure 1: Giga functions as a substrate adaptor for an E3 ubiquitin ligase. Giga binds substrates through its C-terminal Kelch repeat domains and subsequently assembles into the E3 complex via its N-terminal BTB domain. Once the E3 complex is formed, multiple ubiquitins are transferred from the E2 ubiquitin-conjugating enzyme to the substrate. The polyubiquitinated substrate is then delivered to the proteasome and degraded. Figure modified from Petroski and Deshaies, "Function and regulation of cullin–RING ubiquitin ligases" (101).

Gigaxonin functions as a substrate adaptor

Although Giga contains the protein binding domains of a canonical substrate adaptor, verification of this function requires experimental evidence for Giga binding to both Cul3 and targeted substrates via its BTB and Kelch domains, respectively. Confirmation of these associations, however, has proven to be difficult due to the transient nature of the CRL complex formation and the low expression levels of native Giga (85, 121). Despite these difficulties, the BTB domain of Giga has been shown to bind Cul3 and facilitate Giga's assembly into a CRL, thus supporting its role as a substrate adaptor (120, 123). Further validation of Giga's substrate adaptor function came when three different proteins were reported as substrates of Giga (93, 124-126). This ability to bind multiple

substrates is not unique to Giga, as many other substrate adaptors demonstrate the ability to facilitate the ubiquitination and degradation of multiple proteins within a similar pathway (127-133).

The first Giga-mediated substrate interaction was identified when Giga was shown to bind microtubule-associated protein 1B (MAP1B) (93). The MAP1B protein functions in microtubule dynamics by binding tubulin subunits, promoting their polymerization into microtubules (134). By increasing tubulin polymerization, MAP1B has a stabilizing effect on the microtubule structure and is critical in complex cells such as neurons (135, 136). Accordingly, MAP1B deficient neurons display inhibited axon formation due to a delay in axon outgrowth; this axonal phenotype made MAP1B an intriguing possible substrate of Giga in the context of GAN (137, 138). Interactions between Giga and MAP1B were first identified using a yeast two-hybrid system and were subsequently verified by co-immunoprecipitations (93). Additionally, the binding of MAP1B was shown to occur via the Kelch substrate binding domain of Giga, thus further confirming MAP1B as a Giga substrate (93). As substrate adaptors control the degradation of their targets, the protein levels of the two are inversely related; that is, as protein levels of the adaptor decrease, a consequential increase in substrate is observed due to its impaired degradation. This relationship was demonstrated for Giga and MAP1B, as the absence of Giga in GAN knock-out mice led to significantly increased MAP1B protein levels (124). The inverse was also shown by Giga overexpression, which resulted in a protein clearance of MAP1B that was dependent on the proteasome (124). Together, these experiments support

the model that Giga functions as a substrate adaptor that targets MAP1B for proteasome mediated degradation.

A second substrate of Giga is tubulin-folding cofactor B (TBCB), which is one of several tubulin-folding cofactors that controls microtubule dynamics by promoting the depolymerization of microtubules (139, 140). Specifically, TBCB dissociates the α and β tubulin heterodimer and subsequently sequesters the free α-tubulin subunit to prevent reformation of the functional tubulin dimer (141, 142). The association of TBCB and Giga was initially identified with a yeast two-hybrid screen and verified by co-immunoprecipitation, which further showed the Giga Kelch domain was responsible for the interaction (125). As predicted for adaptor and substrates, these proteins were found to be inversely related, as elevated protein levels of TBCB were observed in gigaxonin-null mice (125). Additionally, Giga overexpression in cell culture resulted in significantly decreased TBCB protein levels that were dependent on proper proteasome function (125). These results also demonstrate all the necessary elements of an adaptor-substrate interaction and indicate that TBCB is a substrate of Giga.

A third Giga substrate is microtubule-associated protein 8 (MAP8) (126). Akin to the previously described member of microtubule-associated protein, MAP8 binds tubulin subunits and stabilizes the overall microtubule structure (143, 144). Giga binds to MAP8 and controls its proteasome mediated degradation in a similar fashion as the other identified substrates (126). Taken together, the three identified Giga substrates of MAP1B, TBCB, and MAP8 are all classified as microtubule-associated proteins (MAPs) due to their ability to bind

microtubules and alter microtubule dynamics, thus suggesting a role for Giga in controlling the microtubule structure through the degradation of these three MAPs.

The implied role for Giga in microtubule dynamics, however, does not appear to conform to experimental observations, as the microtubule structure is unaltered in GAN cells (82, 83). The only reported GAN cytoskeletal defect is disorganized IF structures, and no changes in tubulin protein levels or microtubule organization have ever been reported (84-86, 145). This lack of a connection between Giga and the microtubule structure led to further scrutiny of the purported Giga substrates and the emergence of conflicting reported experiments. The original experiments identifying MAP1B, TBCB, and MAP8 as Giga targets all used either GAN knockout mice or overexpression systems to confirm Giga-substrate binding, show substrate accumulation in the absence of Giga, and demonstrate proteasome mediated degradation of the substrates (93, 124-126). Multiple other studies have since attempted to reproduce these results in primary GAN patient cells, but none have been successful. In contrast to the original studies, the protein levels of TBCB and MAP1B were found to be unaltered in GAN cells, thus minimizing the likelihood that they are Giga substrates (85, 86, 145). These conflicting results may be the result of non-native associations that occur with Giga overexpression or defects in the GAN knockout mouse model used to identify the substrates. To date, three GAN mouse models have been created but each exhibit only moderate behavioral, motor, and sensory deficits that do not recapitulate the severity of the human disease (92,

126, 146). Additionally, independent analysis of these knockout mice failed to demonstrate the significant increases of MAP1B, TBCB, and MAP8 that were originally described (92). This discrepancy in reported protein levels, coupled with the lack of microtubule phenotype in GAN, has brought into question the validity of MAP1B, TBCB, and MAP8 as Giga substrates.

To obtain a better understanding of Giga substrates, Mussche and colleagues (89) utilized differential proteomics in conjunction with mass spectrometry to compare protein levels between control and GAN fibroblasts . This strategy was reliant on the substrate adaptor function of Giga, as the loss of Giga in GAN cells would result in impaired substrate degradation and ultimately lead to their accumulation which could be quantified in the assay. The results from these experiments identified 72 known structural cytoskeletal proteins, but no significant differences in protein abundance were observed between control and GAN cells. Among the quantified cytoskeletal proteins, both vimentin and MAP1B were not found to be accumulated in GAN cells. The assays failed to identify either TBCB or MAP8, however, most likely due to their low expression in fibroblasts. Although the proteomic approach failed to implicate any proteins previously associated with GAN, five other proteins were found to have a significantly higher abundance in GAN cells and are potential substrates of Giga. The most significantly upregulated protein was galectin-1, and analysis of its function demonstrated an intriguing possibility for galectin-1 involvement in the IF abnormalities of GAN.

Galectin-1 and Ras stabilization

The galectins are a conserved family of β-galactoside binding proteins that share a consensus carbohydrate recognition domain responsible for their inherent ability to bind polysaccharides (147). Galectins are ubiquitously expressed, as almost all cells express at least one of the fifteen mammalian galectins that have been identified (148, 149). Although the galectin family of proteins is highly conserved, each member differs in their affinity for different polysaccharide chains (150, 151). This lectin function leads to galectin interaction with a wide variety of glycoproteins, and allows galectins to modulate a diverse group of biological pathways such as homeostasis, apoptosis, and embryogenesis (152-156).

The galectin family member of interest in the context of Giga-targeted protein ubiquitination is galectin-1 (Gal-1), as Gal-1 protein levels were found to be significantly elevated in GAN cells (89). Like other galectins, Gal-1 is widely expressed and high protein levels of Gal-1 were noted in the PNS and CNS (149, 157-159). The function of Gal-1 is dependent upon its localization, as Gal-1 exhibits dual localization in the intracellular and extracellular space (160, 161). In the extracellular space, Gal-1 function is dependent on its lectin activity and Gal-1 has been shown to bind to various polysaccharides and glycoproteins (162, 163). For example, extracellular Gal-1 has been show to bind specifically to N-glycosylated β-integrins and transiently promote activation of the integrin complex (164). In contrast to the lectin based extracellular activity, the intracellular function of Gal-1 has been demonstrated to be independent of

polysaccharide binding and has been attributed to specific protein-protein interactions (149). The most prolific of these intracellular protein based interactions involve the lactose-independent binding of Gal-1 to the Ras proteins (165).

Ras proteins function as molecular switches in the plasma membrane that transduce extracellular signals into different intracellular signaling cascades. This activity of the Ras switch is controlled by guanosine triphosphate (GTP) binding, as Ras proteins alternate from an active GTP-bound state to an inactive guanosine diphosphate (GDP)-bound state (166). The formation of activated Ras is catalyzed by guanine nucleotide exchange factors (GEFs), which are recruited to the plasma membrane in response to activated receptor tyrosine kinases. This membrane localization facilitates their interaction with Ras and allows the GEFs to activate Ras by catalyzing the exchange of GDP to GTP (167, 168). The binding of GTP induces conformational changes in Ras that permit Ras interaction with a variety of downstream effects for the duration of the Ras-GTP interaction (169, 170). To inactivate Ras signaling, hydrolysis of GTP is necessary. Although Ras has an intrinsic GTPase activity, its activity is too low to allow efficient termination of the signaling cascade (168, 171). Therefore, Ras inactivation requires the activity of GTPase-activating proteins (GAPs), which enhance the intrinsic Ras GTPase activity and allow Ras to cycle back to its inactive GDP-bound form (168). The utilization of GEFs and GAPs allows Ras to function as a binary switch that controls the rapid and transient transduction of

signals to intracellular effectors. These effectors are involved in multiple cellular process, including homeostasis, differentiation, and survival.

The Ras protein family is composed of three ubiquitously expressed isoforms: H-Ras, K-Ras, and N-Ras. The Ras isoforms are highly homologous, with each sharing 85% amino acid sequence identity. This similarity allows all the Ras isoforms to transmit their signals through similar effector proteins, such as Raf, phosphoinositide 3-kinase (PI3K), and Ral-GDS (166, 170). Despite many mechanistic similarities, the Ras isoforms possess distinct cellular functions. This idea was best demonstrated using individual Ras isoform knockout mouse models, which showed that only K-Ras was essential for normal mouse development, whereas both H-Ras and N-Ras were dispensable (172-175). These biological differences are attributed to a 25 amino acid variable domain in the C-terminus of each isoform, termed the hypervariable region (HVR), for which the Ras isoforms share as 15% sequence identity (176). This region is essential for interaction with downstream effector proteins, and the differences in the HVR are believed to cause isoform-specific effector interactions that activate distinct intracellular signaling cascades with varying affinities (177-182).

In addition to its role in effector binding, the HVR has also been shown to be critical for the proper membrane localization of all Ras proteins. The HVR contains a common tetrapeptide CAAX (C-cysteine, A-aliphatic amino acid, and X-any amino acid) sequence that is essential for a series of post-translational modifications required for Ras membrane localization (183). In the first step of this sequence, a farnesyl group is attached to the cysteine residue of the CAAX

tetrapeptide by the farnesyltransferase enzyme (184). This farnesylation then targets the Ras protein to the endoplasmic reticulum, where the Rce1 endopeptidase removes the AAX tripeptide, and the newly generated C-terminal farnesylcysteine is subsequently methylated by isoprenylcysteine carboxyl methyltransferase (185-189). Following methylation, the Ras isoforms take one of two pathways to become fully integrated into the plasma membrane, which is reliant upon a second C-terminal targeting signal. The first pathway involves the palmitoylation of upstream cysteine residues in the HVR of H-Ras and N-Ras (190). This transfer of a palmitoyl moiety allows H-Ras and N-Ras to be trafficked through the exocytic pathway via the Golgi and permits subsequent anchoring in the plasma membrane (185, 191). The second pathway involves K-Ras, which lacks the HVR cysteine residues required for palmitoylation, but instead contains a positively charged polylysine sequence that permits the Golgi-independent trafficking of K-Ras to the membrane in an unknown mechanism (190, 192). This finding demonstrates that the HVR of the Ras isoforms provides subtle differences in sequence that can lead to substantial differences in effector binding and traffic to the membrane.

The HVR not only alters Ras trafficking to the membrane, but also alters the localization of each Ras isoform in the plasma membrane, which is a complex system of microdomains. Microdomains are highly ordered areas of the membrane that contain distinct lipid and protein compositions which allow the isolation of different signaling molecules to increase signaling efficiency (193). Ras microdomain localization has proven to be dependent on its post-

translational modifications, as the palmitoylated H-Ras and N-Ras are found in lipid rafts while the non- palmitoylated K-Ras is localized to the disorganized bulk membrane outside of the lipid microdomains (194, 195). Once attached to the membrane, the Ras proteins are highly dynamic and continuously moving between different membrane microdomains by lateral diffusion (196). This dynamic motion has especially been demonstrated for H-Ras, as its microdomain localization is dependent on its activation state. The majority of inactive H-Ras-GDP is found in lipid microdomains, but the exchange of GDP for GTP redistributed the activated H-Ras from the lipid raft to the disorganized bulk membrane, which therefore is the primary site of H-Ras signaling (194, 195, 197, 198). This dynamic motion of H-Ras is dependent on the HVR, and particular protein interactions with this domain have been shown to influence H-Ras localization and function.

One such H-Ras interacting protein is Gal-1, which was previously shown to be significantly elevated in GAN cells. Gal-1 specifically binds the membrane bound H-Ras isoform, while K-Ras and N-Ras show minimal association with Gal-1 (165). Additionally, the specific interaction between Gal-1 and H-Ras is dependent upon activation state, as the GTP bound H-Ras binds Gal-1 more efficiently than the inactive form (199). Once bound, Gal-1 stabilizes activated H-Ras by attenuating the GAP-facilitated GTP hydrolysis and driving the formation of transient nanoclusters in nonraft microdomains (200-202) (Figure 2). These H-Ras nanoclusters contain six to eight closely associated activated H-Ras proteins that serve as a signaling platform to efficiently transmit signals to downstream

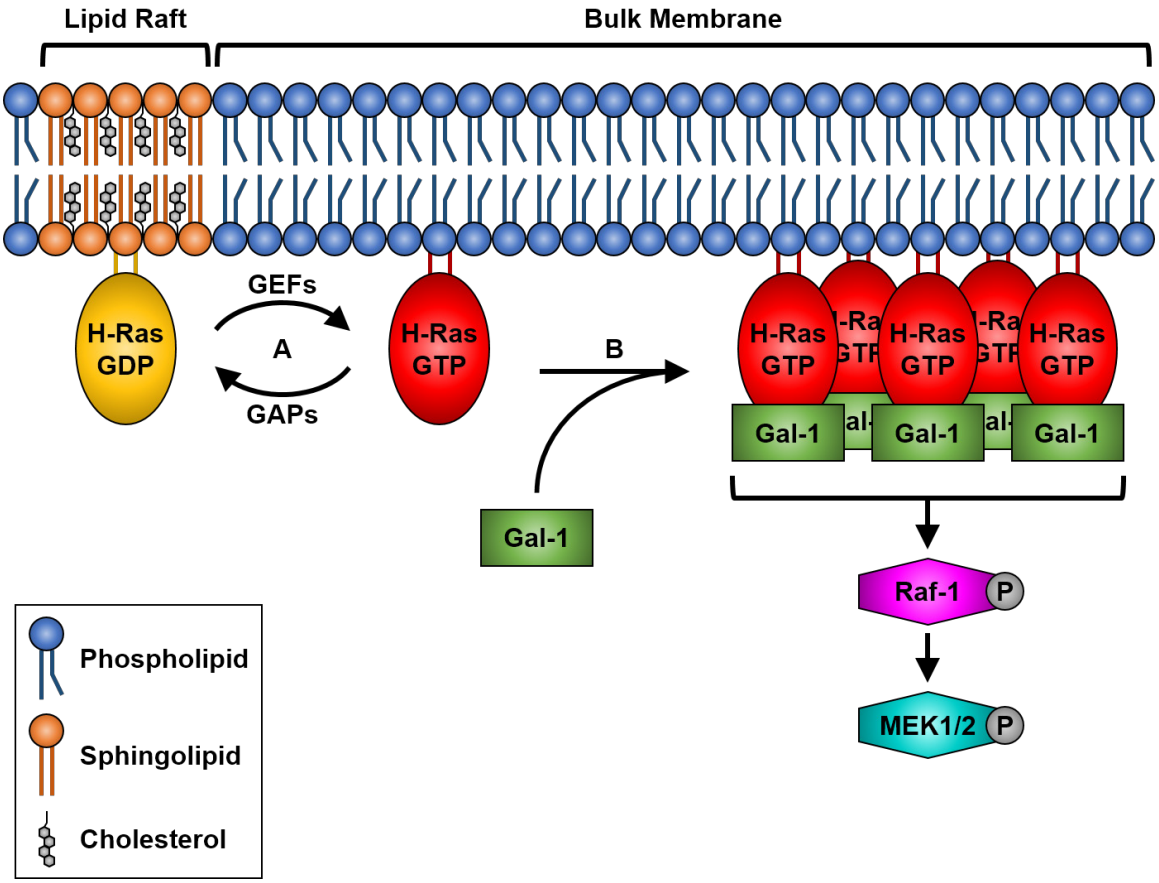

Figure 2: Gal-1 stabilizes GTP bound H-Ras and forms activated Ras nanoclusters. (A) Inactive H-Ras-GDP is found primarily in lipid rafts, which are enriched with sphingolipids and have high concentrations of cholesterol. The GEF-catalyzed activation of H-Ras redistributes the H-Ras-GTP into the bulk membrane, which is composed of mostly phospholipids. (B) Gal-1 stabilizes activated H-Ras in the bulk membrane and drives the formation of transient H-Ras nanoclusters. These nanoclusters serve as platforms to efficiently transmit the activated H-Ras signal to downstream effector proteins.

effector proteins (203). Therefore, increased Gal-1 levels lead to a stabilization of H-Ras nanoclusters that ultimately result in increased effector activation.

In addition to increasing the effector output, Gal-1 also alters H-Ras association with its two main effector proteins, Raf-1 and PI3K. Specifically, activated H-Ras that is stabilized by Gal-1 has been shown to promote Raf-1 activity while inhibiting signaling through PI3K (165, 199). This selectivity is due

to a conformational change in H-Ras which occurs during Gal-1 binding and permits binding to Raf-1 but disrupts binding to PI3K (199). Together this suggests a dual role for Gal-1 in Ras signaling, as Gal-1 not only specifically stabilizes the H-Ras isoform, but also provides effector selectivity by diverting downstream signaling to Raf-1 at the expense of PI3K. Once activated by Gal-1 and H-Ras interactions, increased Raf-1 pathway signaling can potentially have a multitude of effects on the cell. One potential outcome of interest in the context of GAN is the phosphorylation of IFs, as Raf-1 associated kinases have been demonstrated to phosphorylate IFs at multiple sites (204).

Role of intermediate filament phosphorylation

IF phosphorylation generally promotes the reorganization of the filament structure and modulates their dynamic movement in order to accommodate various physiological events. Phosphorylation mainly occurs on serine and threonine residues in the variable head and tail domains of the IF (205, 206). In most cell types, this modification inhibits IF subunit polymerization and promotes the disassembly of the preexisting IF structure (204, 207-209). Although this outcome has been demonstrated for various IFs in numerous cell types, the process of IF phosphorylation is best understood in the context of vimentin phosphorylation in fibroblasts (210-213). Vimentin contains 40 identified phosphorylation sites, which are modified by numerous protein kinases (206, 209, 214, 215) (Figure 3). The effect of vimentin phosphorylation was first demonstrated by Lamb and colleagues in 1989 when they microinjected a known

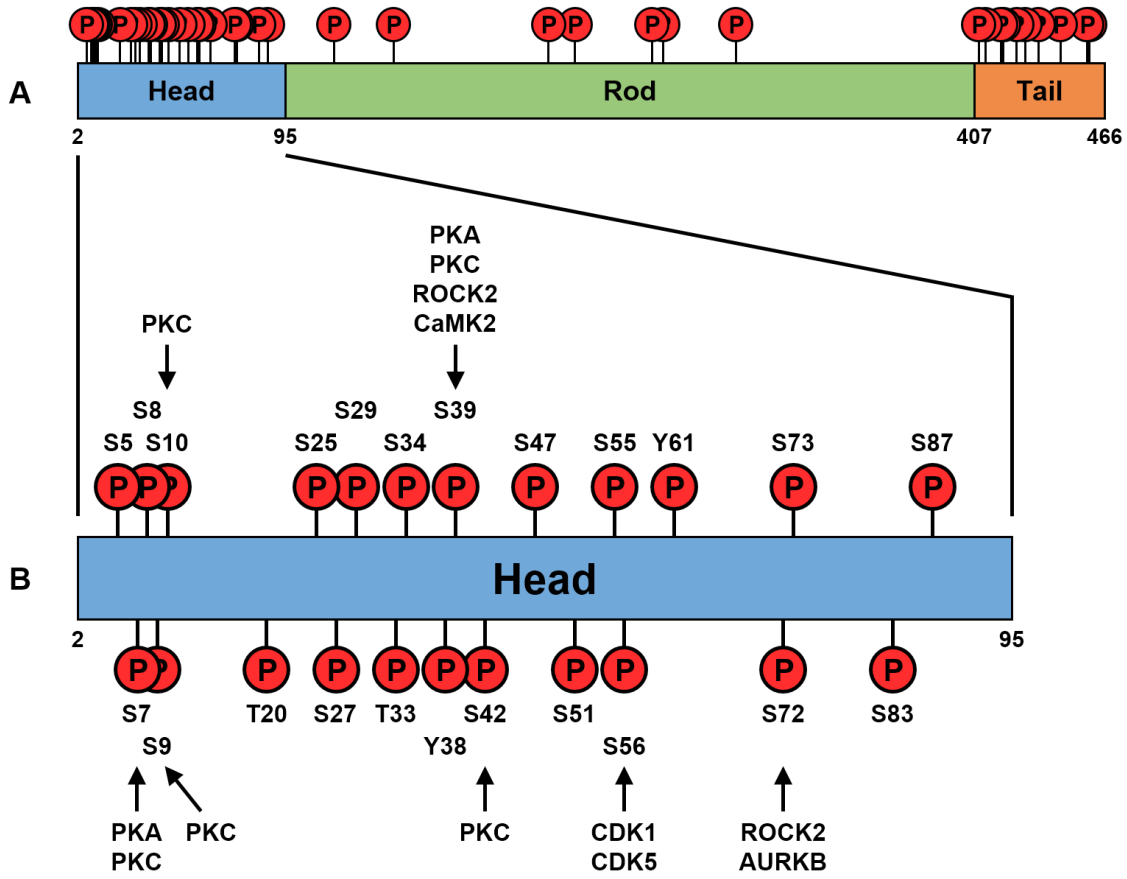

Figure 3: Map of identified vimentin phosphorylation sites. (A) Distribution of vimentin phosphorylation sites on the N-terminal head domain, the central rod domain, and the C-terminal tail domain. (B) Magnification of the vimentin N-terminal head domain noting the specific phosphorylation sites. All identified kinases responsible for each phosphorylation event are listed and noted by an arrow.

vimentin kinase, protein kinase A (PKA), into fibroblasts and observed a prolific rearrangement of the vimentin structure (216). Succeeding the PKA injections, the filaments retracted from the periphery of the cell in a time dependent manner and eventually collapsed around the nucleus to form a tight perinuclear bundle. This phenotype occurred concurrently with a significant increase in PKA-mediated vimentin phosphorylation, and led to the conclusion that vimentin

phosphorylation stimulates dynamic rearrangement of the IF structure. Similar results were also obtained by overexpressing other protein kinases, thus demonstrating the phenotype of phosphorylation-induced vimentin redistribution was not specific to one kinase or phosphorylation site but instead represented a more inclusive function of IF phosphorylation (204, 217, 218).

The vimentin network has also been shown to be modified via phosphorylation during normal cellular processes, such as mitosis (219). As cells enter mitosis, vimentin phosphorylation increases and the IF network is depolymerized to form non-filamentous cytoplasmic aggregates (208, 220-223). This drastic reorganization is required to disassemble the vimentin structure and thus allow partitioning of the constituted IF proteins into the daughter cells (224). To permit mitotic disassembly and subsequent reassembly in daughter cells, the phosphorylation of IFs is spatiotemporally regulated by distinct kinases (225, 226). As the cell enters prophase, IF phosphorylation increases and the widely distributed IF network of interphase is retracted from the cellular periphery to form a centrosomal IF aggregate (206, 224). Subsequent phosphorylation on separate residues dissolves this aggregate into IF subunits that form a finely speckled pattern throughout the cytoplasm during metaphase (224, 227, 228). Next, the progression into anaphase and telophase coincides with a general decrease in vimentin phosphorylation and the reformation of short filaments, which are then reassembled into longer filaments that are concentrated in a juxtanuclear cap (206, 224, 229). Finally, phosphorylation at cleavage furrow-specific sites during cytokinesis promotes the segregation of the IFs into

separate daughter cells (214, 224, 230). This dynamic disassembly and reorganization of IFs demonstrates the spatiotemporal control of IF structure by phosphorylation during vital cellular processes such as mitosis.

In addition to controlling the reversible polymerization of the IF structure in dividing cells, IF phosphorylation also contributes to cytoskeletal function in post-mitotic cells such as neurons. The neuronal intermediate filament network is composed of neurofilaments (NFs) that form a stable structure after synaptogenesis that is not disassembled and reassembled like the IF network of a mitotic cell (231, 232). Although the NF structure is never completely reorganized, individual NFs are still dynamic and undergo extensive subunit exchange that allows the structure to be maintained (233, 234). This movement of NFs displays some similarities to the IF reorganization observed in mitotic cells, as phosphorylation also controls the dynamics of NFs through two related mechanisms.

The first mechanism altered by NF phosphorylation is the transportation of NFs, which move along the axonal microtubule structure by associating with the kinesin and dynein molecular motors (235, 236). Although NFs are transported using the conventional molecular motors, their movement proceeds at a significantly slower rate than any other cargo due to interrupted associations of the NF and motor (237). This dissociation results in periods of long pauses when the NF is unattached to the motor, followed by short intermittent bursts of rapid movement when they are attached that ultimately generates an overall slow rate of transport (238, 239). The rate of transportation is further modulated by NF

phosphorylation, which progressively restricts association with kinesin and promotes elongated transportation pauses (235, 240, 241). By promoting dissociation from kinesin, NF phosphorylation generates an anterograde rate of transport that is inversely correlated with its phosphorylation state (242, 243). In addition to inhibiting anterograde transport, NF phosphorylation also promotes retrograde transport by promoting NF association with dynein (236). Therefore, NF phosphorylation leads to accumulation of NFs in the proximal region of the axon by restricting anterograde transport and promoting retrograde transport.

The second mechanism by which phosphorylation alters NF dynamics is by increasing protein-protein interactions between the C-terminal domains of NFs (244). These domains contain multiple serine residues that extend from the filament to form side arms when phosphorylated (205, 243). The lateral projections conferred by the side arms normally control the spacing between adjacent full length filaments, but hyperphosphorylation of NFs disturbs these interactions and promotes attraction between the side arm and the core of adjacent polymers NF (245, 246). The NF attractions result in the formation of a bundle, which is a large NF accumulation that specifically contains phosphorylated NFs and selectively excludes non-phosphorylated forms (244, 247, 248). Concurrent with the formation of these bundles, NF phosphorylation increases the axon caliber, as enlarged axons are observed in distinct regions containing increased NF phosphorylation and accumulation (232, 249).

Collectively, NF phosphorylation promotes bundling and inhibits anterograde transport, thus leading to increased axon caliber due NF

accumulation in the proximal region of the neuronal axon. This phenotype is remarkably similar to that observed in GAN patient neurons and potentially could explain the 'giant' axons filled with disorganized neurofilaments. The phosphorylation of NFs in the context of GAN, however, has not been widely investigated. One report observed an increased phosphorylation in enlarged axons but the state of IF phosphorylation has not been documented in any other GAN cells type (19). This is of particular interest since a mechanism causing systemic IF hyperphosphorylation could explain the generalized IF disorganization that is observed for numerous *in vivo* GAN patient cell types.

Summary and hypothesis

GAN is characterized by generalized IF abnormalities that result from Giga mutations. Giga normally functions as an E3 substrate adaptor in the UPS, and the loss of Giga function leads to accumulation of its substrates. One potential Giga substrate is Gal-1, which stabilizes activated Ras and promotes signaling through Raf-1 at the expense of PI3K. Raf-1 associated kinases phosphorylate IFs at multiple distinct sites and generally promote the disassembly or aggregation of IFs (Figure 4). This phosphorylated IF phenotype is reminiscent of the IF abnormalities observed in GAN patient fibroblasts and neurons. Taken together, this led us to hypothesize that Giga regulates IF phosphorylation and structure by modulating the Ras pathway through the degradation of Gal-1 (Figure 5).

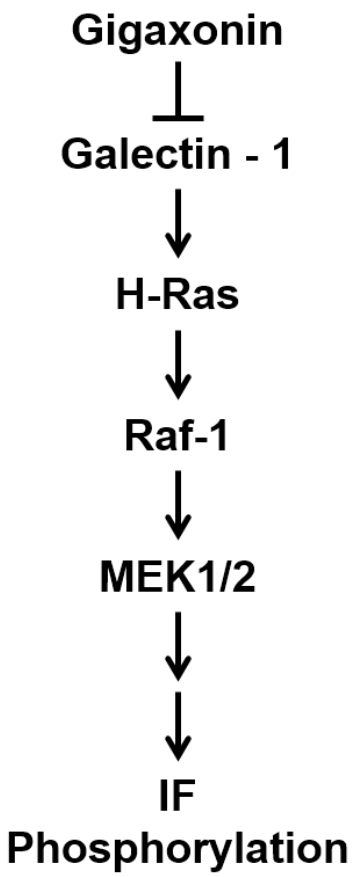

Figure 4: Schematic of the proposed Giga-mediated signaling pathway. Giga controls the protein degradation of Gal-1, which normally stabilizes the activated form of H-Ras. The Giga-mediated degradation of Gal-1 allows for the maintenance of activated H-Ras levels in the cell and regulates the signaling to downstream effectors that can phosphorylate intermediate filaments.

The objectives of this study were therefore fourfold: 1) Ascertain the IF phenotype of GAN patient cells and its relationship to an alteration in IF phosphorylation state, 2) Determine if replacing Giga can correct IF phenotype and phosphorylation, 3) Confirm Gal-1 as a substrate of Giga, and 4) Determine if the Gal-1 mediated Ras signaling pathway generates the IF abnormalities in GAN.

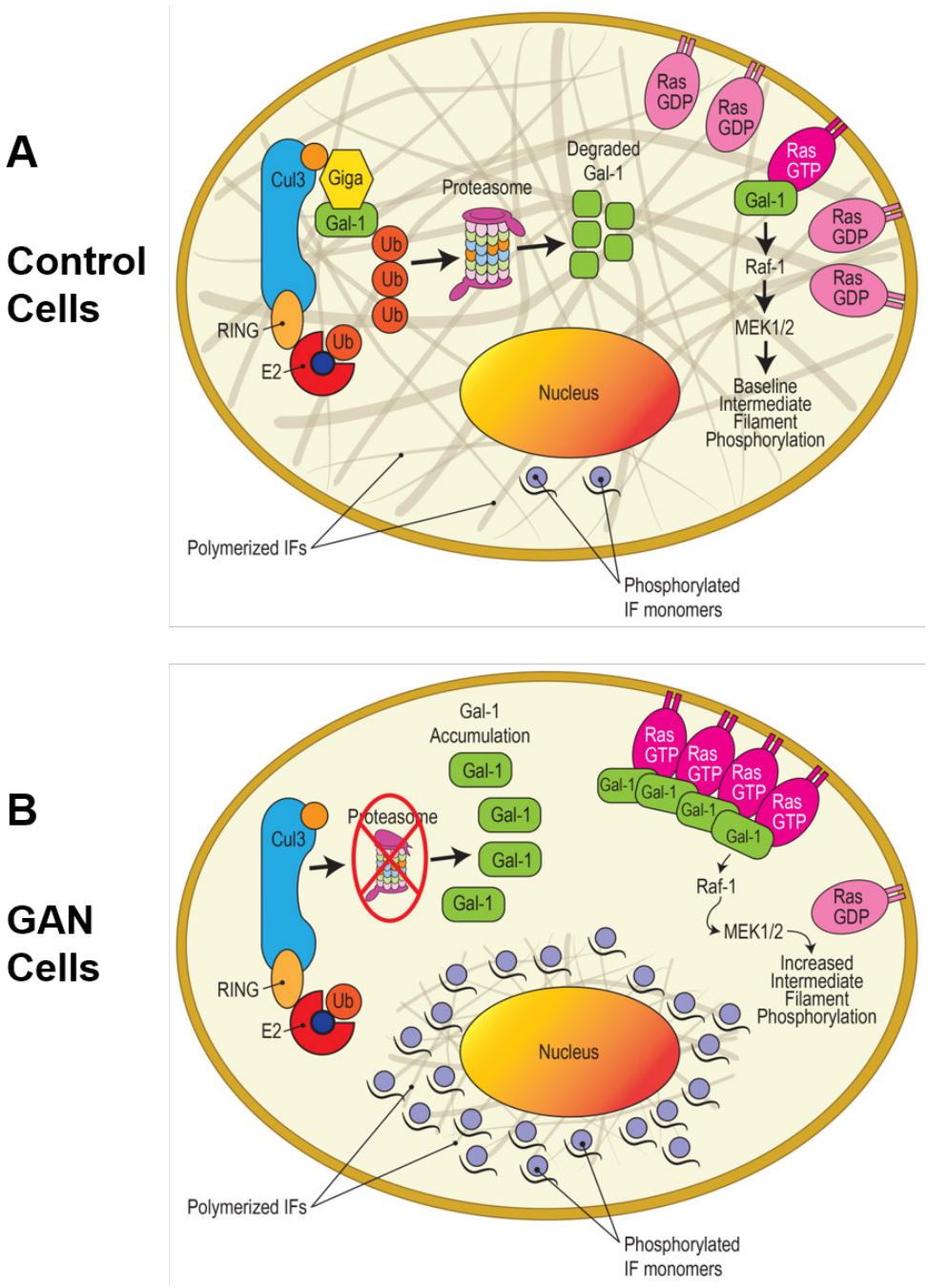

Figure 5: Illustration of the proposed signaling pathway in GAN. (A) In control cells, Giga is expressed and can degrade Gal-1. Low levels of Gal-1 permits the hydrolysis of Ras-GTP to inactive Ras-GDP. This leads to low levels of vimentin phosphorylation, which maintains normal vimentin polymerization and distribution. (B) In GAN cells, Giga is not expressed and Gal-1 accumulates. Increased levels of Gal-1 stabilize Ras-GTP and increase downstream vimentin phosphorylation. This increased phosphorylation promotes the disassembly of vimentin filaments and results in the formation of phosphorylated vimentin subunits that accumulate in the perinuclear region of the cell.

CHAPTER II: MATERIALS AND METHODS

Cell culture

Fibroblasts used included the de-identified GAN patient cell lines of 10-W145 (GAN cell line 1) and F3245 (GAN cell line 2) (both gifts of Dr. Steven Gray, University of North Carolina at Chapel Hill School of Medicine). GAN cell line 1 was used as the representative GAN cells in all experiments unless otherwise noted. The unrelated fibroblast cell line GM01661 (Coriell Biorepository) was used as experimental controls. All cells were propagated in media composed of Dulbecco's modified Eagle's medium (DMEM; Life Technologies), supplemented with 10% fetal bovine serum (FBS; Thermo Scientific), 25.0 mM glucose, penicillin-streptomycin, sodium pyruvate, non-essential amino acids, and GlutaMAX (all from Life Technologies). This complete growth media containing 10% FBS will henceforth be referred to as normal serum media. Alternatively, cells were cultured in a nonpermissive growth media composed of DMEM containing 0.1% FBS and the same supplements listed above. This nonpermissive growth media with 0.1% FBS will hereafter be termed low serum media.

Cells were maintained at 37°C in a humidified, 5% CO_2 incubator and were used for experiments at an intermediate passage number between passage twelve and seventeen. For all experiments, GAN or control cells were seeded into 35 mm dishes containing normal serum media. Sixteen hours later, the cells were washed with PBS and then incubated in either normal or low serum media

for 72 hours. After this three day incubation, the cells were then utilized for the specified experiment.

Immunofluorescence and image acquisition

GAN or control cells were seeded on 35 mm glass bottom coverslip dishes and then grown in low serum media for 72 hours. The cells were subsequently rinsed with PBS and fixed in 4% paraformaldehyde (PFA) for 10 minutes at room temperature. To stop the fixation process, the cells were washed 3 times for 5 minutes each in PBS containing 100 mM glycine. After fixation, cells were permeabilized and blocked in blocking buffer (4% bovine serum albumin and 0.2% saponin in PBS) for 10 minutes at room temperature. The fixed cells were incubated with primary antibody diluted in blocking buffer for 1 hour at room temperature, washed 3 times in blocking buffer for 5 minutes each, and then processed with secondary antibody as was done for the primary. After washing, the cells were rinsed with PBS twice and then stored in PBS for imaging. The antibodies used were mouse anti-vimentin (EMD Millipore), goat anti-mouse Alexa Fluor 568 conjugate, mouse anti-alpha-tubulin Alexa Fluor 488 conjugate, and rabbit anti-GFP Alexa Fluor 647 conjugate (all from Life Technologies).

The immunostained cells were imaged using the confocal Olympus Fluoview FV-1000 MPE system (Olympus America, Central Valley, PA) available at the Indiana Center for Biological Microscopy facility (Indianapolis, IN). Images were obtained in a sequential illumination mode using 488nm, 568nm, and 633nm lasers with Olympus water immersion objective lenses of either 20x

(UApoN340 20xW, NA 0.7) or 60x (UPlanSAPO 60xW, NA 1.2). Each image was acquired as a Z stack with 0.85μm between each frame. Images were comprised of 512x512 pixels (634 x 634 μm2) and compiled using Olympus FluoView Viewer (Version 2.0) imaging software.

GAN phenotypic scoring

To measure the abnormal vimentin phenotype of GAN patient fibroblasts, I developed a new phenotypic scoring method using immunofluorescence that quantifies the restricted distribution of vimentin in patient cells. This measurement is based upon the unaltered tubulin structure in GAN patient fibroblasts, which is indistinguishable from controls, being used as a marker for the total cellular area. Once the total area was obtained, this was then be divided by the vimentin area to generate a ratio of vimentin area to total cellular area, which represents the cellular area that vimentin occupies. This area was then subtracted from one to obtain the cellular area without vimentin, or the vimentin free area (VFA)

To generate the area measurements, the image files were analyzed using ImageJ (NIH). The Z projection of the sum slices was used and any background was removed with the ROF denoise function. Automatic thresholding was then applied with the 'Percentile' algorithm to generate a binary image containing only positive or negative signal for each channel of tubulin or vimentin (Figure 6). The areas generated from these binary images, which represent the area of either tubulin or vimentin in each field of view, were then measured. The total area of

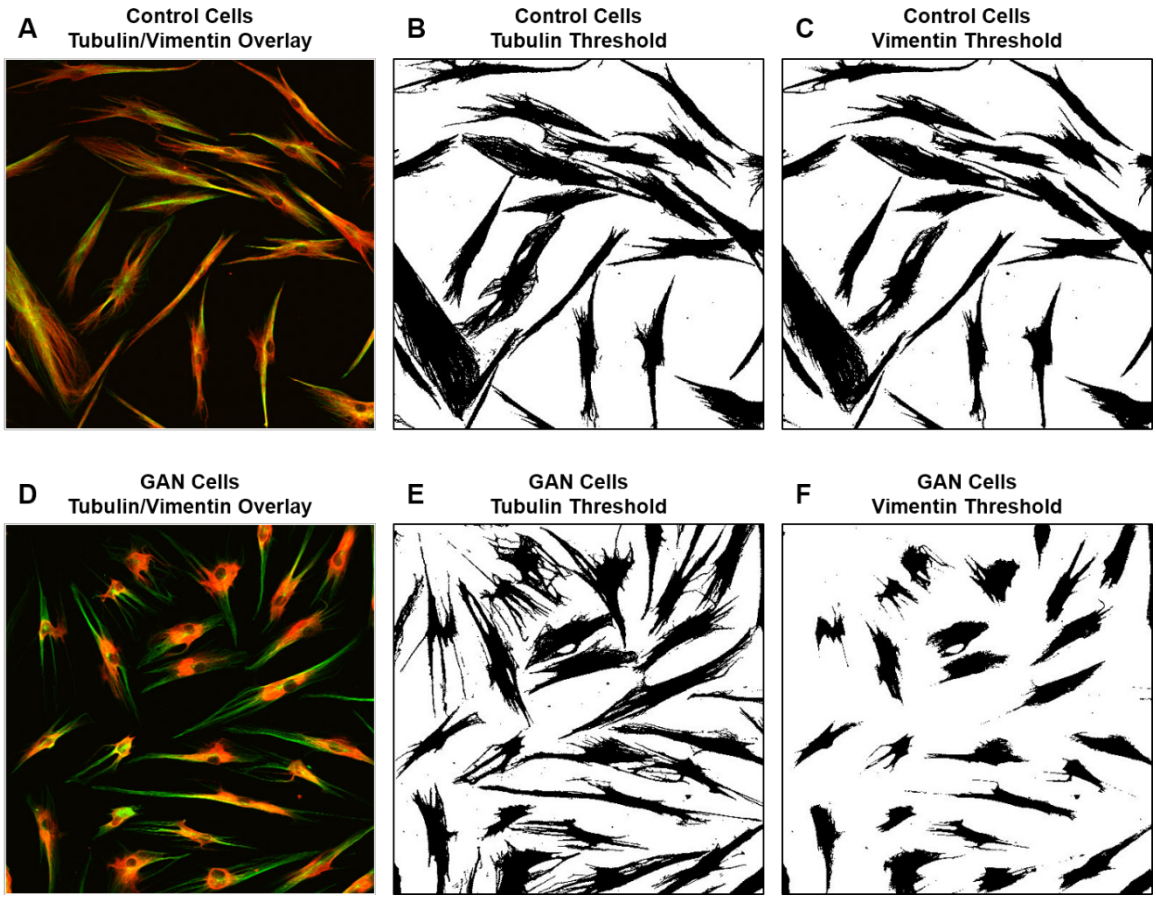

Figure 6: Generation of threshold images to obtain tubulin and vimentin areas for quantification of the VFA. (A) Control cells with a tubulin (green) and vimentin (red) overlay. (B) Thresholded image of the tubulin signal in control cells. (C) Thresholded image of the vimentin signal in control cells. (D) GAN cells with a tubulin (green) and vimentin (red) overlay. (E) Thresholded image of the tubulin signal in GAN cells. (F) Thresholded image of the vimentin signal in GAN cells.

tubulin was then divided by the total area of vimentin, and this ratio was subsequently subtracted from one to generate the VFA.

Each experiment was comprised of four separate replicates for each condition. Every replicate consisted of at least seven images of different fields that were used to generate an average VFA for each experiment. Four separate replicates were then averaged to generate the VFA for each condition.

Western blot analysis

GAN or control cells were seeded into 35 mm dishes and subsequently grown in normal serum media or low serum media for 72 hours. The cells were then washed twice with ice cold PBS and then scraped into ice cold RIPA Buffer (50 mM Tris-HCl, pH 8.0, 150 mM NaCl, 1% Triton X-100, 0.1% SDS, 0.5% sodium deoxycholate), containing Halt protease and phosphatase cocktail inhibitor (Thermo Scientific). Protein concentrations were determined using the BCA protein assay kit (Thermo Scientific), and equal protein amounts were combined with Laemmli sample buffer. The whole cell lysates were separated on 12% SDS-PAGE gels and subsequently transferred to polyvinyl difluoride (PVDF) membranes (EMD Millipore). The membranes were then blocked at room temperature for one hour in PBS-0.05% Tween-20 (PBST) supplemented with 5% blotting-grade nonfat dry milk (Bio-Rad). After blocking, the primary antibody was diluted in 5% milk and incubated with the membranes at 4°C overnight. The membranes were washed with PBST four times for five minutes per wash, and then the corresponding horseradish peroxidase–conjugated secondary antibody was incubated with the membranes for 1 hour at room temperature. After washing with PBST four times for five minutes per wash, the blots were developed using SuperSignal West Pico chemiluminescent substrate (Thermo Scientific). Western blot signal intensities were determined by densitometry using ImageJ (NIH) software. The reported western blot quantifications were obtained from three independent experiments using the same cell line.

The primary antibodies used were anti-gigaxonin, anti-galectin-1, anti-tubulin, and anti-GAPDH (Sigma-Aldrich), anti-vimentin and anti-phospho-vimentin Ser83 (Cell Signaling Technology), anti-H-Ras, anti-K-Ras, and anti-N-Ras (Santa Cruz Biotechnology), anti-MEK1 and anti-MEK2 (Bethyl Laboratories), anti-phospho-vimentin Ser39, anti-phospho-vimentin Ser51, and anti-phospho-vimentin Ser72 (MBL International Corporation), and anti-ubiquitin (Abcam). Secondary antibodies included horseradish peroxidase-conjugated goat anti-rabbit and goat anti-mouse (Bio-Rad), and goat anti-rat (Santa Cruz Biotechnology).

Lentiviral production and transduction

The lentiviral vector pCSCIGW (gift of Dr. Ken Cornetta and Dr. Daniela Bischof, Vector Production Facility, Indiana University School of Medicine), which contains an internal ribosome entry site (IRES), was used for lentivirus production. To allow simultaneous expression of two proteins from the same transcript, a FLAG-tagged WT gigaxonin cDNA sequence was inserted into the upstream reading frame of the IRES and an eGFP sequence was inserted downstream of the IRES. Lentiviruses were produced by cotransfecting the resulting pCSCIGW-gigaxonin-IRES-eGFP transfer plasmid, the packaging plasmids of pMDL and pRSV-Rev, and the envelope plasmid of pMDG1, into 293T cells (Life Technologies) using a calcium phosphate transfection system (Life Technologies). After 3 days, the culture supernatant was collected and filtered. The target GAN cells were then incubated with the viral supernatant

supplemented with 8 μg/mL polybrene (Santa Cruz Biotechnology), and after 8 hours, the virus containing media was replaced with growth media. The transduced cells were grown for a total of 3 days and then sorted by fluorescence-activated cell sorting according to GFP expression. Additional sorting was done again 3 weeks after transduction to generate a stable cell line of GAN cells expressing gigaxonin.

TAT-Giga expression, purification, and treatment

The GAN cDNA sequence was cloned into the pTAT vector (gift from Steve Dowdy, Washington University), which contains an N-terminal 6X His tag followed by a transactivator of transcription (TAT) sequence, to generate a complete His-TAT-GAN cDNA construct (termed TAT-Giga). The TAT-Giga construct was sequenced to ensure fidelity and transformed into BL21(DE3)pLysE cells. The transformed cells were grown for 14-16 hours in LB broth supplemented with ampicillin (100 μg/mL) at 37°C and then seeded into fresh media until the culture reached an optical density of 0.5 at 600 nm. To induce the expression of TAT-Giga, 250 μM of IPTG was added, and the culture was subsequently incubated at 16°C for four hours. TAT-Giga was then isolated and purified using a His-tagged protein purification protocol (250, 251). Briefly, the cells were harvested by centrifugation at 4,500 g for 10 minutes at 4°C, resuspended in lysis buffer (PBS, pH 7.4, with 500 mM NaCl and Sigma P8849 protease inhibitor cocktail), and sonicated in a rosette cooling cell. The lysate was then clarified by centrifugation at 22,500 g for 20 minutes at 4°C and passed

through a 0.75 μm filter. Imidazole was added to the soluble protein lysate to reach a final concentration of 10 mM.

The soluble protein lysate containing the His-tagged TAT-Giga was passed over a 5 mL HisTrap FF nickel affinity column (GE Healthcare) using an Akta Basic UPC 100 FPLC chromatography system (Amersham Biosciences). To elute the His-tagged TAT-Giga protein from the column, the imidazole concentration of the elution buffer was gradually increased up to 500 mM. The elution fractions with an imidazole concentration from 40-80 mM were collected and concentrated using a spin concentrator with a 10,000 MW cutoff (Millipore). The concentrated protein was then loaded onto a PD-10 desalting column (GE Healthcare) and eluted into PBS with 5% glycerol. The protein concentration of the resultant TAT-Giga protein sample was then determined by a BCA assay (Thermo Scientific).

For treatment with the purified TAT-Giga protein, GAN cells were seeded into 35mm dishes containing normal serum media. Sixteen hours later, the cells were washed with PBS and then incubated in low serum media (0.1% FBS) containing 0.15 μg/mL or 0.75 μg/mL TAT-Giga for the low and high dose samples, respectively. PBS was added to the control samples. After 72 hours, the cells were isolated and subjected to immunofluorescence or Western blot analysis as above.

Proteasome inhibition

Control cells were seeded into 35mm dishes containing normal serum media. Sixteen hours later, the cells were washed with PBS and then incubated in low serum media (0.1% FBS) with 0.01 μM MG132 (EMD Millipore). After 72 hours, the cells were isolated and subjected to Western blot analysis as above.

Small interfering RNA (siRNA) inhibition

Cells were seeded into 35mm dishes containing normal serum media. Sixteen hours later, the cells were washed with PBS and incubated in normal serum media without penicillin-streptomycin. For all treatments, 50 nM of siRNA was diluted in 125 μL of DMEM and 5 μL Lipofectamine 2000 (Life Technologies) was diluted in in 125 μL of DMEM. The diluted solutions were mixed together and incubated for 20 minutes at room temperature before being added to each well. After 6 hours, the media containing the siRNA complexes was removed, the cells were washed, and low serum media was added. The cells were grown in low serum conditions for 72 hours before being isolated and subjected to Western blot or immunofluorescence analysis as above. The siRNAs used were from Sigma-Aldrich and included siRNAs targeted against gigaxonin (SASI_Hs01_00217960), galectin-1 (SASI_Hs01_00132990), H-Ras (SASI_Hs01_00231174), K-Ras (SASI_Hs01_00082296), N-Ras (SASI_Hs01_00017654), MEK1 (SASI_Hs01_00090167), and MEK2 (SASI_Hs01_00109852).

Statistics

Data represent mean ± standard deviation from at least 3 independent experiments, with representative blots and images shown. Calculations and graphs were compiled using Microsoft Excel. Statistical comparisons were made using a 2-tailed Student's t test, and a *P* value of 0.05 or less was considered significant.

CHAPTER III: RESULTS

GAN cells have altered vimentin distribution in low serum

GAN patient fibroblasts have a readily inducible phenotype of vimentin filament aggregates. When grown in culture conditions containing 10% FBS, GAN cells have a mostly normal IF structure, as only 5-10% of GAN cells form a vimentin aggregate (84). However, growing the same cells in low serum conditions of 0.1% FBS results in the formation of vimentin aggregates in about 70-80% of GAN cells (82, 84, 85). Although the formation of vimentin aggregates is a consistent finding in GAN patient cells, the quantification of such aggregates is wildly inconsistent, as the same patient cell line was described as containing aggregates in less than 20% of cells in one study (82) and in 90% of the same cells in another study (83). This inconsistency cannot be attributed to either differences in cell culture or clonal variation between the studies, as the same culture conditions were used and there is little clonal variation in GAN cells (82). Instead, these discrepancies most likely result from the ambiguous definition of an aggregate and how this definition is applied between different studies. Without the ability to control for this human error, the phenotypic scoring of aggregates in GAN cells cannot be accurately applied as a universal readout of this disease.

In conjunction with the phenotypic vimentin aggregates, I found that GAN cells also display an abnormal vimentin distribution. Like the formation of the aggregates, this distinct phenotype is also inducible by serum restriction. In the

permissive growth condition of normal serum (10% FBS), most GAN cells have a vimentin structure that is indistinguishable from control cells (Figure 7). However,

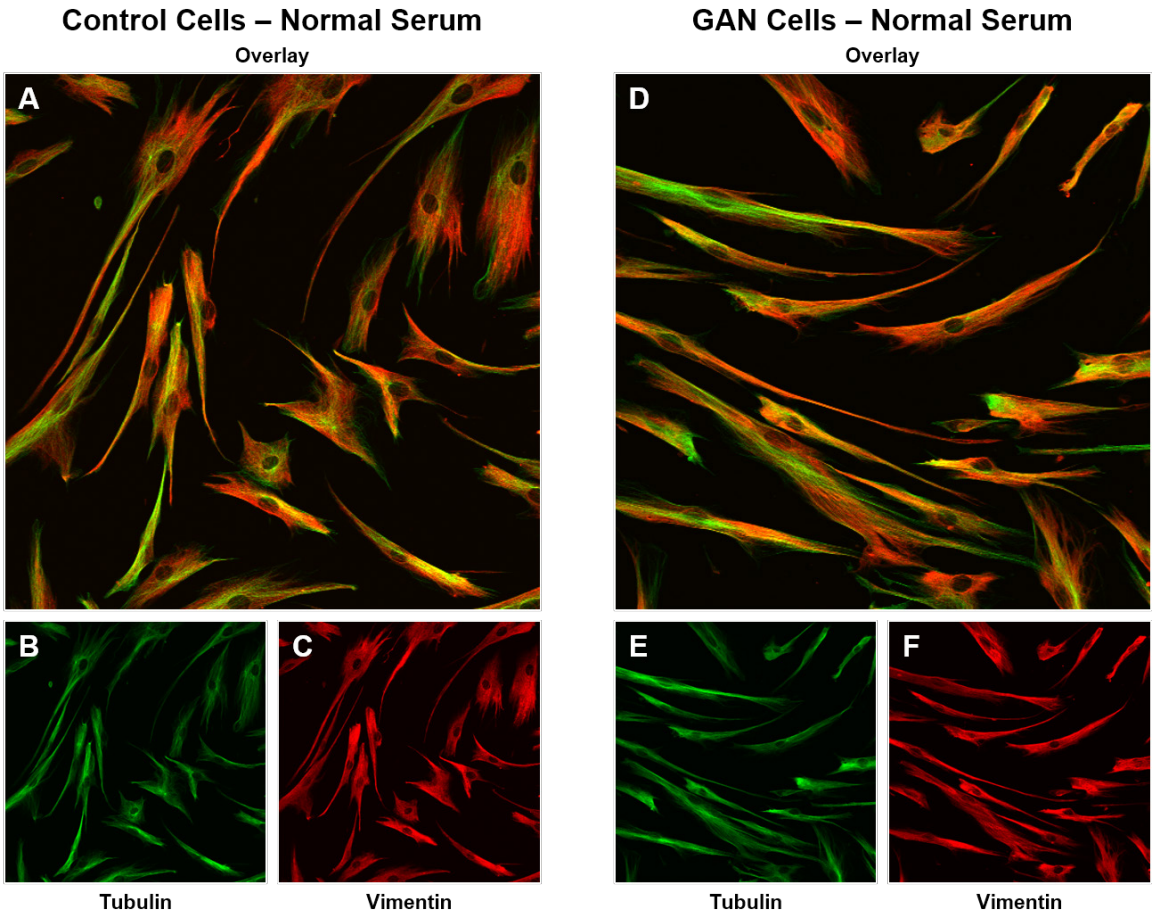

Figure 7: Vimentin distribution in normal serum (10% FBS) conditions. (A) Representative double immunofluorescence of control cells in normal serum with an overlay of tubulin (green) and vimentin (red). (B) Single immunofluorescence of tubulin in control cells. (C) Single immunofluorescence of vimentin in control cells. (D) Representative double immunofluorescence of GAN cells in normal serum with an overlay of tubulin (green) and vimentin (red). (E) Tubulin in GAN cells. (F) Vimentin in GAN cells.

in the restrictive growth condition of low serum (0.1% FBS), GAN cells display a collapsed vimentin network that lacks vimentin in the cell periphery, therefore leading to a concentration of vimentin in the perinuclear region (Figure 8D-F).

Control cells do not show a similar phenotype, as their cytoskeletal distribution remains unchanged in response to serum conditions (Figure 8A-C). This GAN-

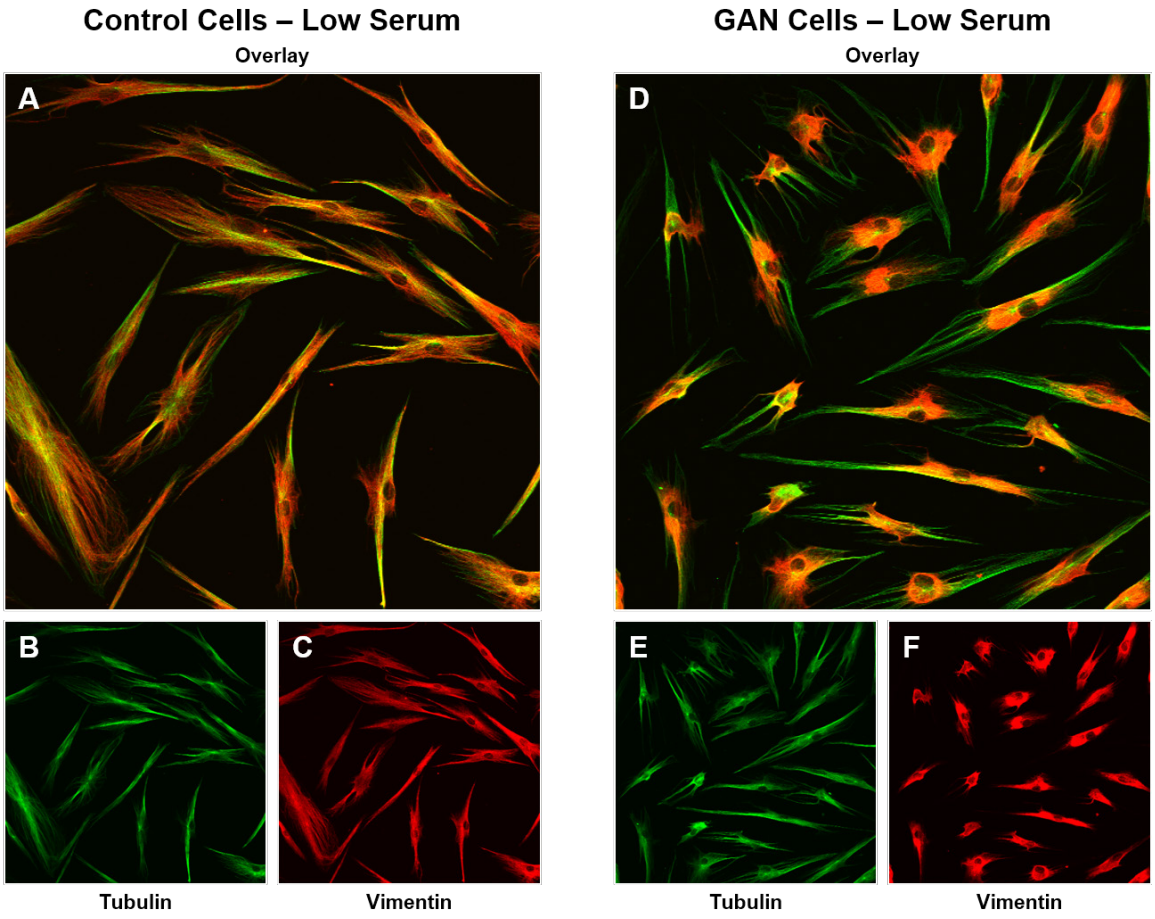

Figure 8: Vimentin distribution in low serum (0.1% FBS) conditions. (A) Representative double immunofluorescence of control cells in low serum with an overlay of tubulin (green) and vimentin (red). (B) Single immunofluorescence of tubulin in control cells. (C) Single immunofluorescence of vimentin in control cells. (D) Representative double immunofluorescence of GAN cells in low serum with an overlay of tubulin (green) and vimentin (red). (E) Tubulin in GAN cells. (F) Vimentin in GAN cells.

specific phenotype is observable using tubulin, which is unaltered in GAN cells, as a cytoskeletal control for visualization of the total cellular area. Using these cytoskeletal markers, I developed a new methodology to describe the GAN

phenotype of a retracted vimentin network, which I termed the vimentin free area (VFA). The VFA was obtained by using algorithmic thresholding in ImageJ to obtain the area of vimentin and tubulin signals (for a detailed methodology please see Materials and Methods). As the tubulin structure is unaltered in GAN cells, the tubulin area was defined as total cellular area. The vimentin area was then divided by the tubulin area to give a ratio of the cellular area that vimentin occupies. This vimentin to tubulin ratio was subtracted from one to give the cellular area that lacks a vimentin signal, termed the VFA.

When quantified, the VFA had similar results to the data obtained by previous publications that counted the number of cells with aggregates (84). In normal serum conditions, there is no significant difference in the distribution of vimentin, as control cells had 10.8% ± 0.9% VFA and the two observed GAN cell lines had VFAs of 11.0% ± 2.7% and 8.2% ± 1.1%, respectively (Figure 9). In contrast, there was a substantial difference in the VFA in low serum conditions, as control cells had 5.2% ± 1.0% VFA whereas both GAN cell lines had significantly elevated VFAs of 35.3% ± 1.5% and 20.6% ± 1.0%, respectively. These results demonstrate that in addition to the formation of vimentin aggregates, GAN fibroblasts also have an altered phenotype of perinuclear restricted vimentin distribution as quantified by the VFA. Utilizing this computerized scoring of vimentin distribution allows for efficient and reproducible quantification of the GAN phenotype while also permitting intermediate nuisances in the phenotype that were not accounted for in the previous binary scoring of vimentin aggregates.

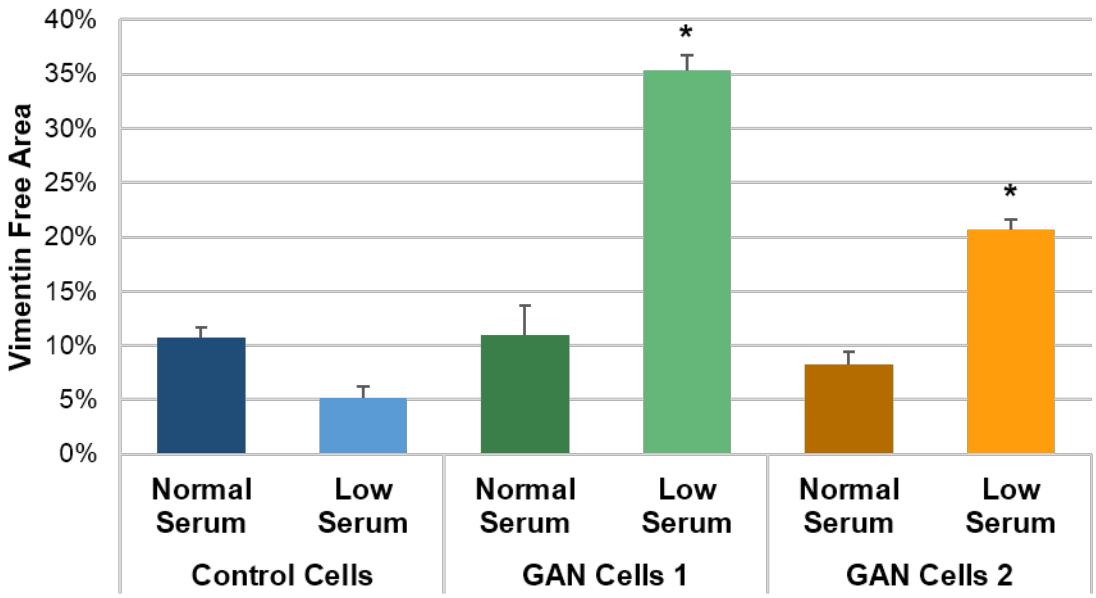

Figure 9: Quantification of the VFA in normal and low serum. The GAN phenotype of a collapsed vimentin network was quantified by the VFA. The VFA was then compared between control cells and two distinct GAN cell lines in different serum conditions (*$P < 0.05$ compared to control cells, n=4 replicates per condition).

GAN cells have elevated Gal-1 and phosphorylated vimentin in low serum

A previous study by Mussche and colleagues (89) utilized differential proteomics to demonstrate that GAN cells have increased protein levels of galectin-1 (Gal-1) . Here I show that Gal-1 levels are elevated in GAN cells, but only significantly in low serum conditions (Figure 10A). Control cells that express Giga significantly decreased the amount of Gal-1 when moved from normal to low serum, thus indicating a significant down-regulation of Gal-1 in low serum conditions (Figure 10B). Conversely, both GAN cell lines tested had no detectable levels of Giga and did not display a similar decrease in Gal-1 when placed in low serum conditions. When quantified, the GAN cell lines respectively had 2.8 and 3.0 times the amount of Gal-1 in low serum when compared to

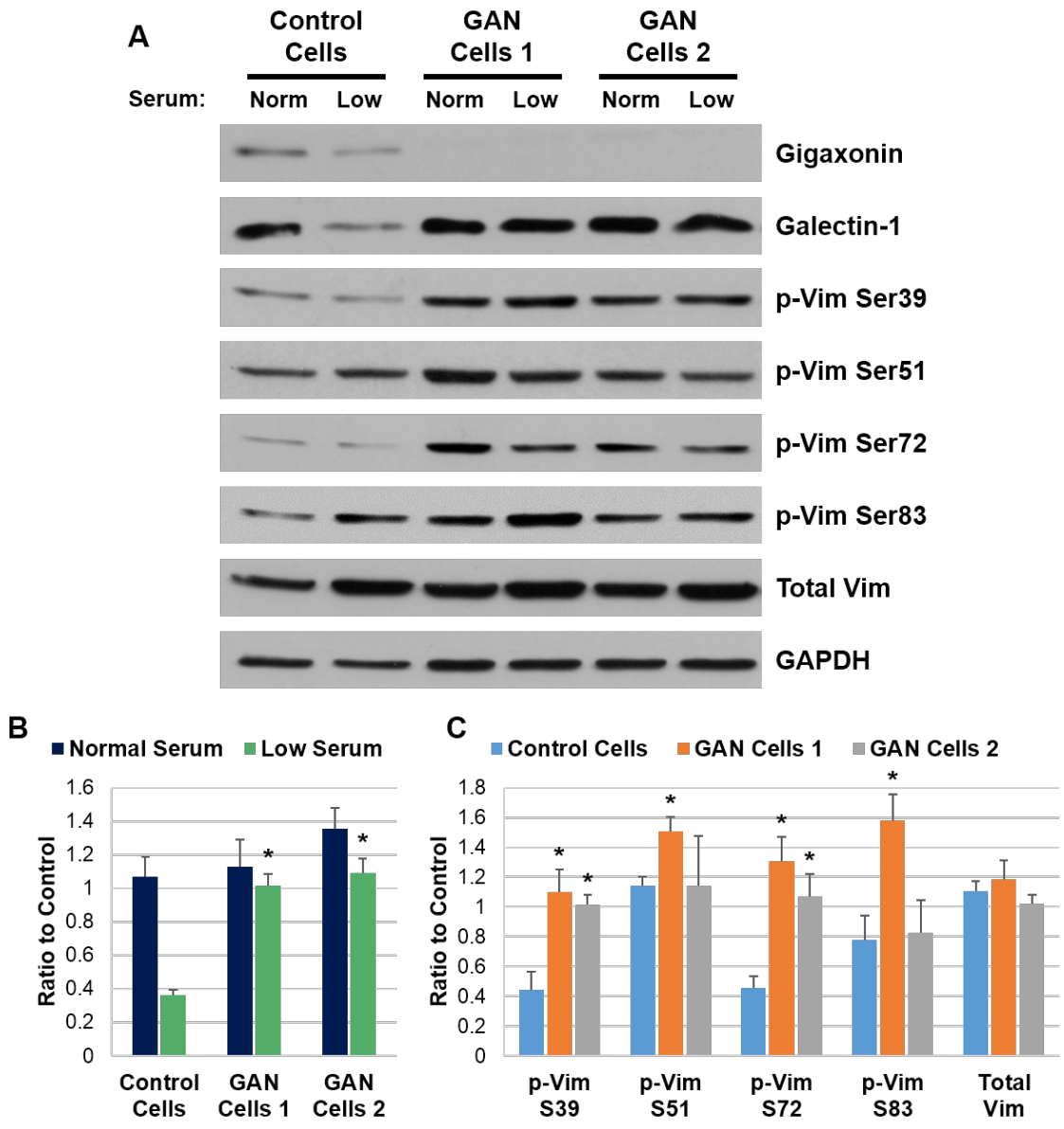

Figure 10: GAN cells have increased levels of Gal-1 and phosphorylated vimentin in low serum. (A) Comparison of protein levels of Gal-1 and phosphorylated vimentin at four serine residues in control cells and two distinct GAN patient cell lines. Representative blots shown. (B) Quantification of Gal-1 protein levels in normal and low serum (*$P < 0.05$ compared to control cells in low serum, n=3). (C) Quantification of vimentin protein levels in low serum (*$P < 0.05$ compared to control cells, n=3).

control cells. These results can be correlated to the observed vimentin abnormalities observed in the same GAN fibroblasts, as significant differences in Gal-1 protein levels and phenotype are specifically observed in GAN cells when compared to controls in low serum. Due to this low serum specific aggravation of the GAN phenotype and Gal-1 protein levels, low serum conditions were utilized in all further experiments.

Examination of vimentin protein levels showed no difference in total vimentin between control and GAN cells, as previously reported (86, 88, 89). However, further assessment using phosphorylation site-specific vimentin antibodies showed a general hyperphosphorylation of vimentin in GAN cell lines that was specifically observed in low serum (Figure 10C). When quantified, vimentin phosphorylation was significantly increased at Ser39 and Ser72 in both GAN cell line 1 and GAN cell line 2. The highest increase was at Ser72, as the GAN cell lines respectively had 2.9 and 2.3 times the amount of phospho-vimentin at Ser72 when compared to control cells in low serum. In addition to these two sites, GAN cell line 1 also had significantly elevated levels of vimentin phosphorylation at both Ser51 and Ser83. With all four tested sites displaying increased phosphorylation, GAN cell line 1 displayed consistent vimentin hyperphosphorylation and therefore was used as the representative GAN cell line in all subsequent experiments. Taken together, these results show a low serum specific hyperphosphorylation of vimentin and accumulation of Gal-1 in GAN cells that correlates with the altered vimentin structure in the same condition.

Giga controls the proteasome mediated degradation of Gal-1

As Giga is purported to function as an E3 ligase adaptor, I hypothesized that the increased Gal-1 protein levels in GAN cells was caused by the lack of Giga-mediated targeting to a protein degradation pathway. To determine the role of Giga in the protein degradation of Gal-1, wild-type Giga was replaced in GAN cells using two separate techniques. First, the wild-type Giga encoding *GAN* gene was introduced into GAN cells using lentiviral transduction. The transduced cells showed high levels of Giga expression and had a corresponding decrease of Gal-1 protein levels when compared to the non-transduced GAN cells (Figure 11). This Giga mediated decrease in Gal-1 was specific, as the levels of other probed proteins, including total vimentin, remained unchanged when Giga was introduced. Although the total amount of vimentin remained unchanged, the levels of vimentin phosphorylation were significantly reduced at Ser39, Ser51, Ser72, and Ser83. These results demonstrated that introducing the wild-type *GAN* gene into patient cells decreases the elevated protein levels of Gal-1 and reverses vimentin hyperphosphorylation.

In addition to replacing the wild-type *GAN* gene into patient cells, the wild-type Giga protein was introduced into GAN cells using the transactivator of transcription (TAT) cell penetrating peptide. A fusion protein was created with wild-type Giga and an N-terminal TAT sequence, which facilitated movement of the TAT-Giga fusion protein across the intact cell membrane, thus replacing functional Giga into GAN cells. TAT-Giga was administered to two separate GAN cell lines, and in both cases, Gal-1 levels decreased when wild-type Giga was

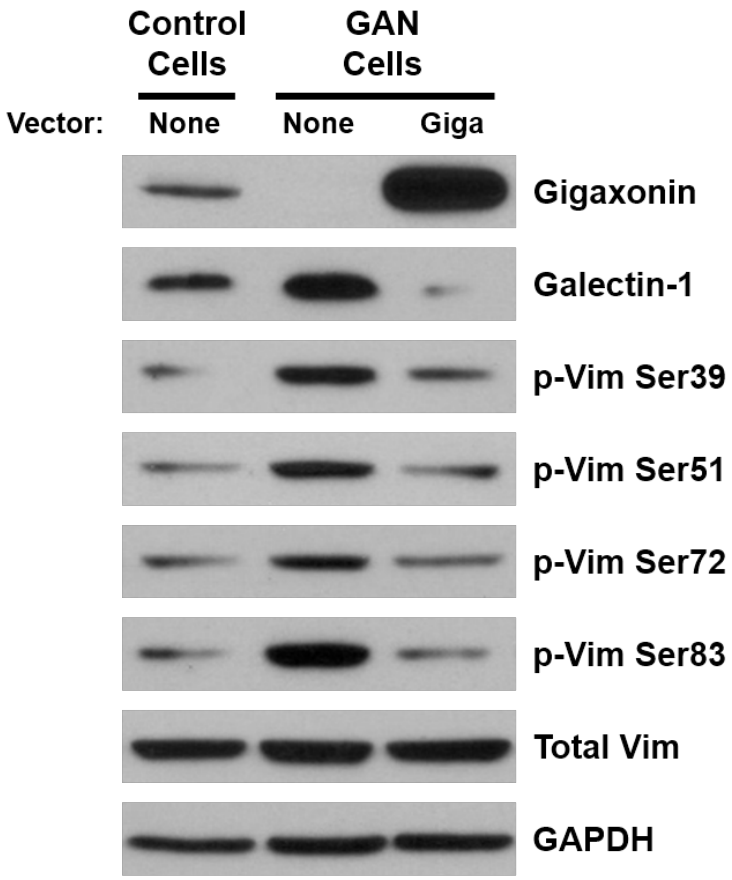

Figure 11: Restoring the wild-type *GAN* gene decreases Gal-1 and reverses vimentin hyperphosphorylation in GAN cells. Wild-type Giga expression was introduced into GAN cells via a lentiviral construct. The expression of Gal-1 and vimentin phosphorylation at specific serine residues was then compared between control cells, GAN cells, and GAN cells transduced with the Giga expressing lentiviral vector. All cells were grown in low serum conditions. Representative blots shown (n=3).

replaced into the cells (Figure 12). The decrease in Gal-1 was also dose-dependent, as the high dose of TAT-Giga (0.75 µg/mL) showed a more profound decrease in Gal-1 levels as compared to the low dose of TAT-Giga (0.15 µg/mL). Therefore, the levels of Gal-1 can also be decreased upon addition of functional Giga to GAN cells, thus demonstrating an inverse relationship between Giga and Gal-1 and suggesting Gal-1 as a substrate of Giga.

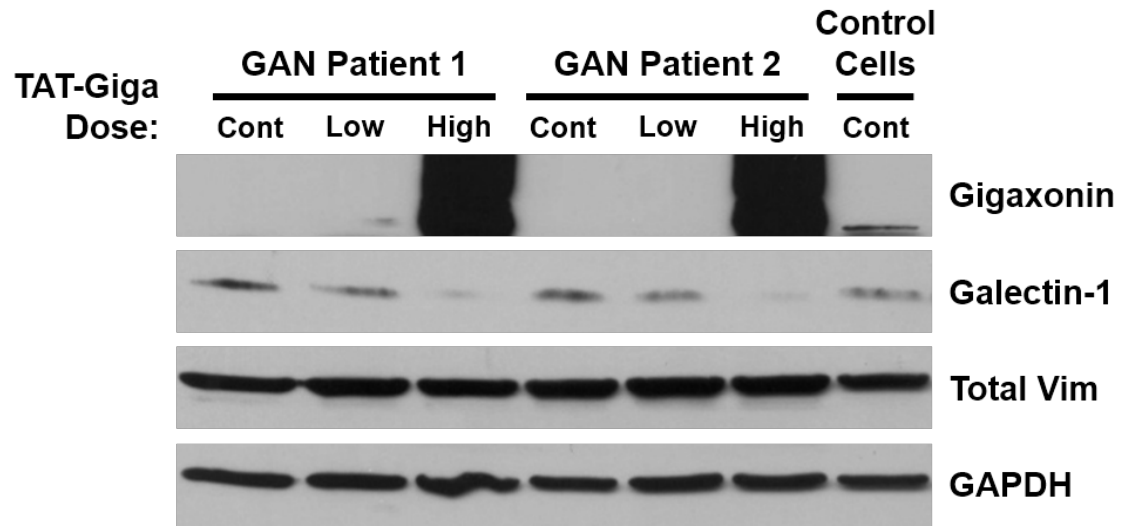

Figure 12: Replacing wild-type Giga protein into GAN cells decreases Gal-1 protein levels. Wild-type Giga was replaced into two separate GAN patient cell lines via TAT-Giga protein replacement therapy. The expression of Gal-1 and total vimentin was then compared between control cells, untreated GAN cells, and GAN cells treated with a low dose or high dose of TAT-Giga. All cells were grown in low serum conditions. Representative blots shown (n=2).

To further confirm this role, Giga protein expression was knocked down in control cells using siRNA. Immunoblotting demonstrated efficient knockdown of Giga to undetectable levels, while also showing a corresponding increase of Gal-1 protein levels that was not seen with a scrambled siRNA control (Figure 13A). This result reaffirmed the inverse correlation between the protein levels of Giga and Gal-1 that was previously observed in GAN cells, as both control cells exposed to Giga siRNA and GAN cells that do not express Giga had significantly elevated protein levels of Gal-1. This further confirmation of an inverse relationship suggested a possible role for Giga as an E3 substrate adaptor that binds to Gal-1 and facilitates its ubiquitination and degradation in the proteasome. In support of this relationship, a recent proteomics survey demonstrated that Gal-1 is ubiquitinated on 5 distinct lysine residues (252).

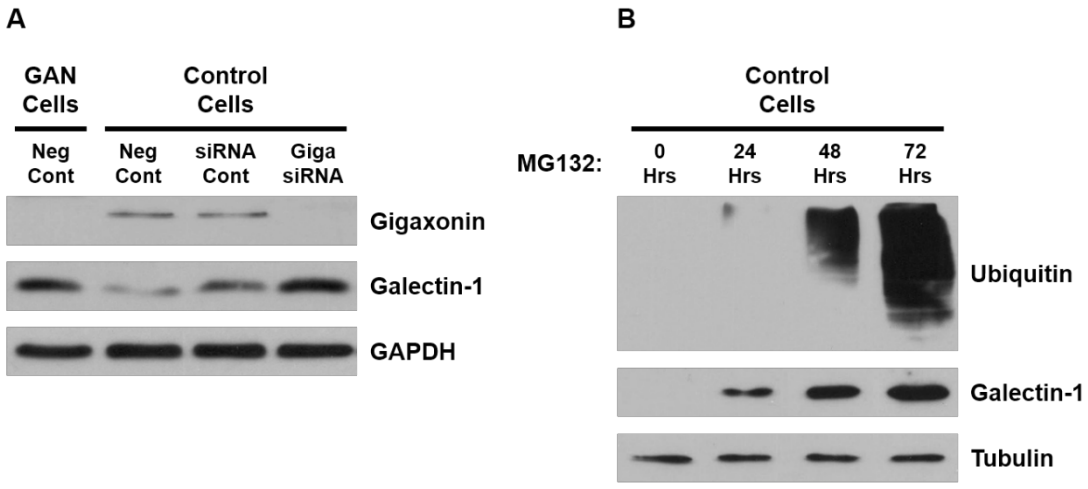

Figure 13: Giga controls the proteasome mediated degradation of Gal-1. (A) Giga siRNA was added to control cells and grown in low serum conditions. The protein levels of Gal-1 were then compared between untreated control cells (Neg Cont), control cells administered an siRNA control, control cells treated with Giga siRNA, and GAN cells. (B) Proteasome function was inhibited with MG132 in control cells and protein levels of Gal-1 were observed over time.

Furthermore, inhibiting the proteasome with MG132 in control cells generated a classical poly-ubiquitin ladder and lead to an accumulation of Gal-1 (Figure 13B). This suggests that in the presence of Giga, Gal-1 is ubiquitinated and undergoes proteasome-mediated degradation. Taken together, these results identify an inverse relationship between Giga and Gal-1 that is indicative of a substrate adaptor-substrate relationship and also suggests that the Giga mediated degradation of Gal-1 occurs in the proteasome.

Restoration of Giga corrects GAN phenotype

As mutations in Giga are known to cause intermediate filament abnormalities in GAN cells, such as perinuclear vimentin accumulation in fibroblasts, I hypothesized that introduction of functional Giga would correct this

GAN phenotype. To replace functional Giga, GAN cells were transduced with a lentiviral construct that utilized an internal ribosomal entry site to express wild-type Giga and eGFP from the same mRNA transcript. Triple immunofluorescence of tubulin, vimentin, and eGFP showed that those cells expressing eGFP, as a marker for the simultaneously expressed Giga, exhibited a normal filamentous vimentin distribution throughout the cytoplasm (Figure 14C-D). This was in stark contrast to the non-transduced GAN cells, as evident by the lack of eGFP signal, which had central vimentin accumulations (Figure 14A-B). When quantified, the perinuclear vimentin accumulations of the non-transduced GAN cells resulted in 35.8% ± 0.8% VFA, while the Giga/eGFP expressing GAN cells had a significantly lower VFA of 15.2% ± 1.3% (Figure 14E). This shows that replacing Giga in GAN cells can decrease the VFA by restoring vimentin distribution.

Similar phenotypic correction was also observed when wild-type Giga was administered to GAN cells using TAT-mediated protein replacement therapy. After treatment with TAT-Giga, double immunofluorescence studies of vimentin and tubulin showed that vimentin distribution was largely restored in GAN cells (Figure 15A-C). When compared to untreated GAN cells that showed accumulated vimentin in the perinuclear region and are lacking vimentin in the cell periphery, the TAT-Giga treated cells displayed a more even distribution of vimentin throughout the cellular area that is phenotypically closer to the control cells. Quantification of this experiment using the previously characterized formation of VFA showed that untreated GAN cells exhibited 32.5% ± 1.7% VFA, which decreased in a dose dependent manner to 20.7% ± 0.5% and 11.4% ±

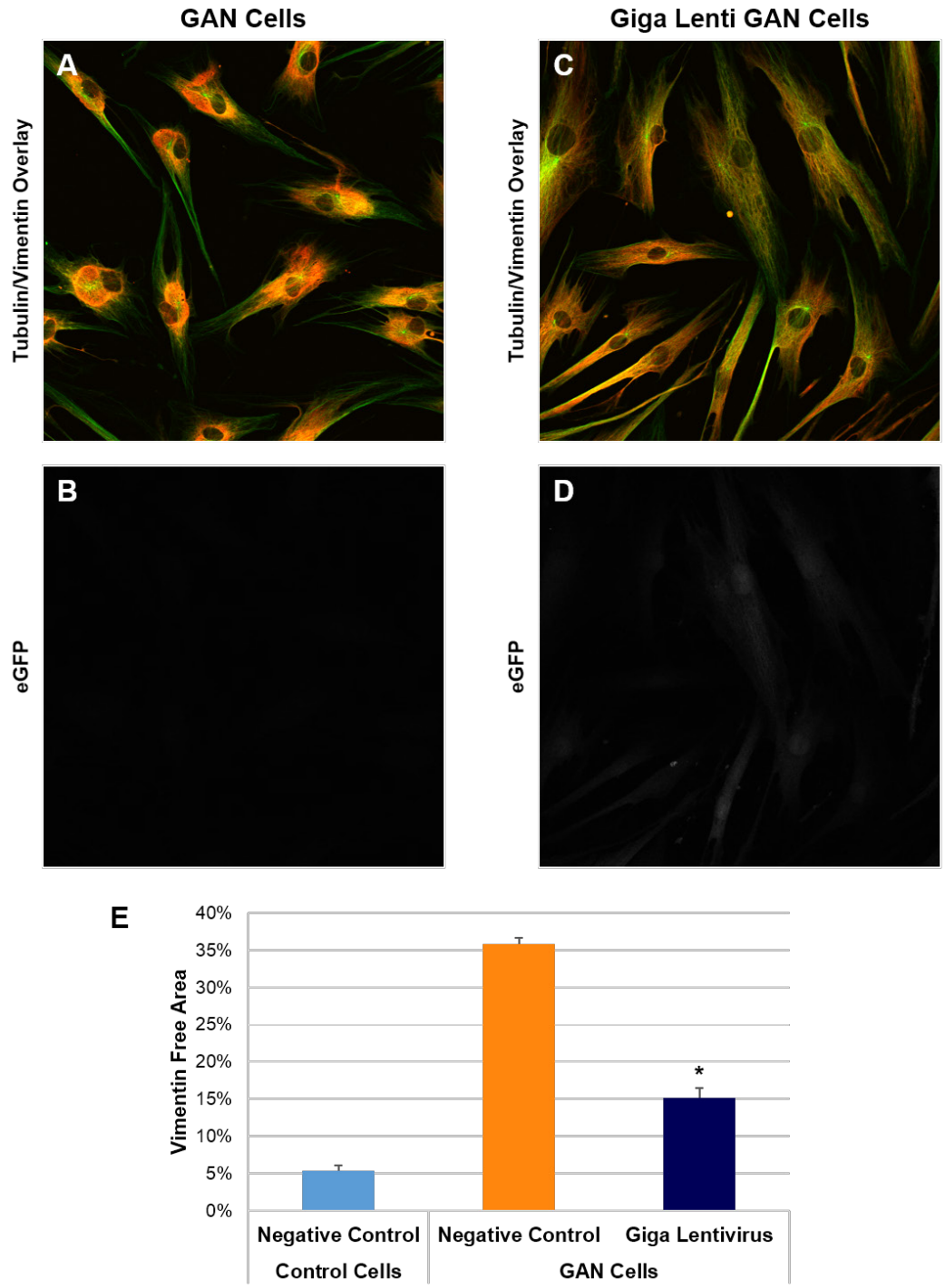

Figure 14: Restoring wild-type GAN gene corrects the GAN phenotype. (A) Non-transduced GAN cells stained for tubulin (green) and vimentin (red). (B) Lack of eGFP in non-transduced GAN cells. (C) GAN cells transduced with the *GAN* gene and stained for tubulin (green) and vimentin (red). (D) eGFP expression in transduced GAN cells. (E) Quantification of the VFA in normal, GAN, and transduced GAN cells (*$P < 0.05$ compared to GAN negative control cells, n=4 per condition). All cells were grown in low serum conditions.

1.0% VFA in GAN cells treated with a low dose (0.15 µg/mL) and high dose (0.75 µg/mL) of TAT-Giga, respectively (Figure 15D). Together, these results demonstrate that replacing either the functional Giga protein, or the wild-type *GAN* gene, can restore vimentin distribution in GAN cells. In addition, this data validates VFA scoring as a dynamic and correctable phenotypic readout for GAN.

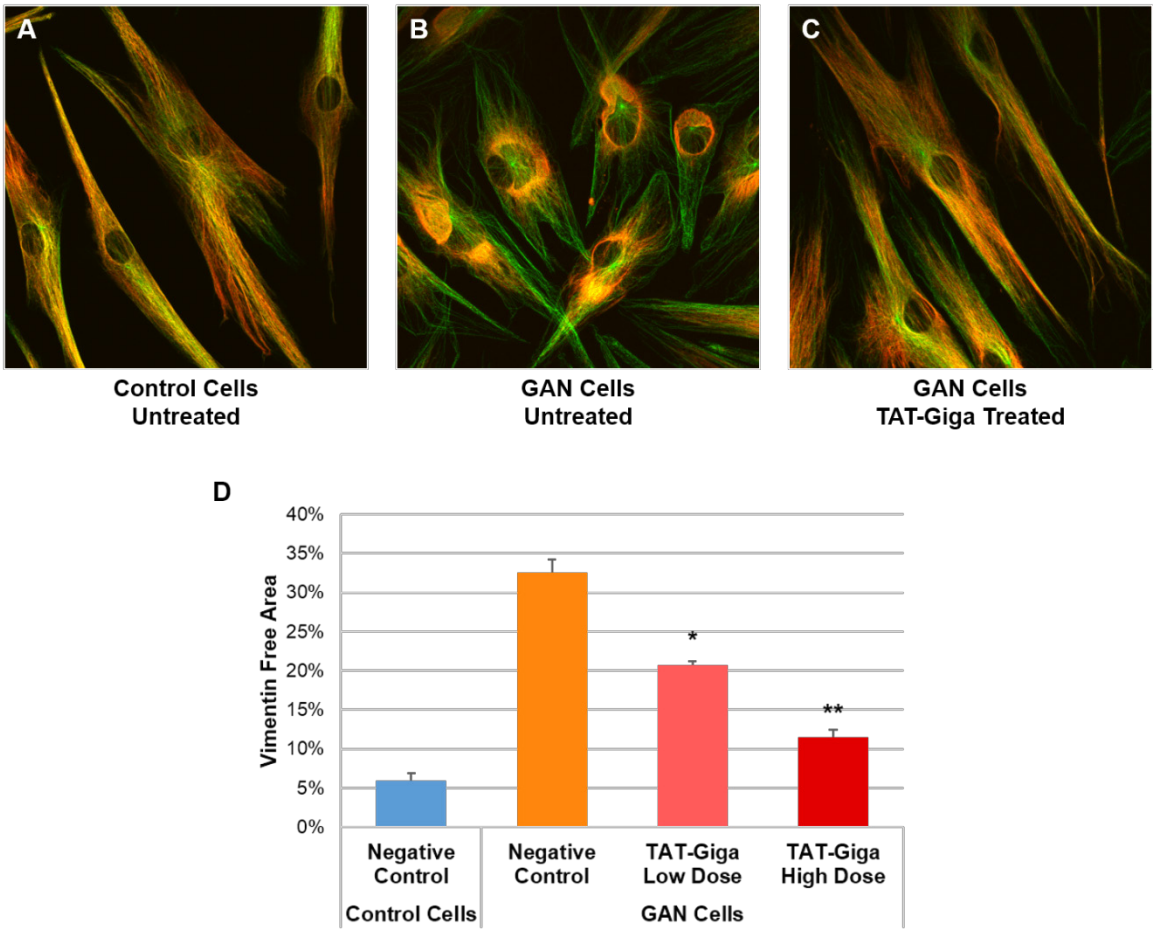

Figure 15: Restoring Giga corrects the GAN phenotype. (A) Representative tubulin (green) and vimentin (red) overlay image of control cells. (B) Overlay image of untreated GAN cells. (C) Overlay of TAT-Giga treated GAN cells. (D) Quantification of the VFA in control, GAN, and TAT-Giga treated GAN cells (*P < 0.05 compared to GAN negative control cells, n=4 per condition). All cells were grown in low serum conditions.

Gal-1 knockdown decreases vimentin phosphorylation and restores vimentin distribution

Since restoring Giga expression in GAN cells decreased the elevated levels of Gal-1, abated vimentin hyperphosphorylation, and corrected vimentin distribution, I hypothesized that directly decreasing Gal-1 levels in GAN cells would similarly rectify the GAN phenotype. Addition of a Gal-1 siRNA to GAN cells resulted in efficient and specific knockdown of Gal-1, as measured by immunoblotting, which was not observed with a scrambled siRNA control (Figure 16). In conjunction with decreased protein levels of Gal-1, GAN cells treated with

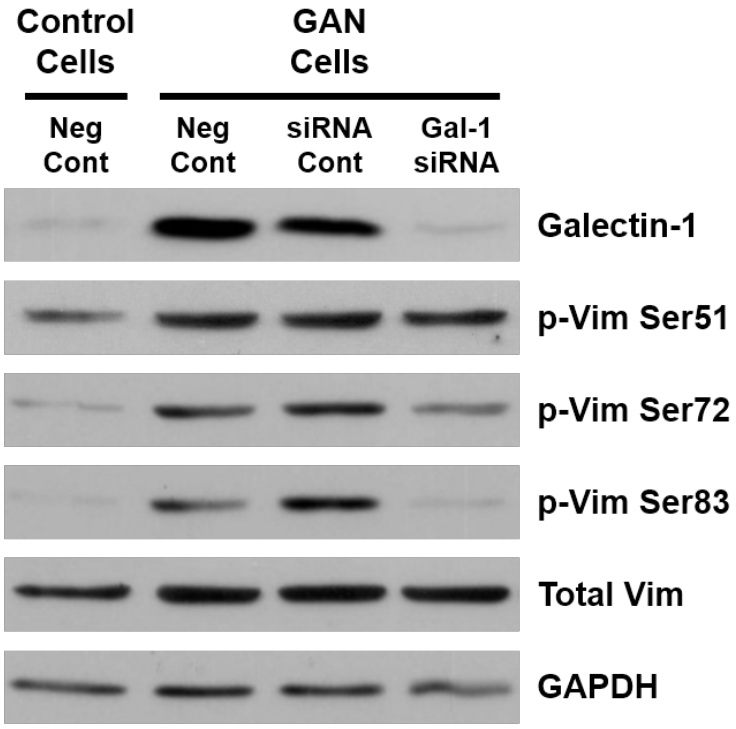

Figure 16: Gal-1 knockdown reduces vimentin phosphorylation. Gal-1 siRNA was administered to GAN cells in low serum conditions. The protein levels of specific vimentin phosphorylation sites were then compared between control cells, untreated GAN cells (Neg Cont), GAN cells given an siRNA control, and GAN cells treated with a Gal-1 siRNA. Representative blots shown (n=3).

Gal-1 siRNA also displayed significantly reduced levels of vimentin phosphorylation at Ser72 and Ser83 to levels commensurate with those of control cells. Phosphorylation at these sites, as noted previously in Figure 10A, is elevated in GAN cells and remains elevated when a scrambled siRNA control is added to the cells. This data suggests that a specific knockdown of Gal-1 can affect the phosphorylation state of vimentin at multiple different serine sites without altering the total vimentin protein levels. Furthermore, GAN cells treated with Gal-1 siRNA demonstrated increased vimentin distribution to the cell periphery and increased colocalization of tubulin and vimentin as measured by immunofluorescence (Figure 17A-C). In contrast, addition of the siRNA control had no effect on the GAN cell phenotype, as they displayed a collapsed vimentin network that lacked vimentin in the cell periphery. Quantification of this data showed GAN cells administered the siRNA control had 36.3% ± 1.4% VFA, while Gal-1 siRNA treated GAN cells had a significantly lower VFA of 14.7% ± 0.4% that was much closer to the 3.9% ± 1.3% VFA observed in control cells (Figure 17D). Taken together, these results show that a knockdown of Gal-1 decreases vimentin phosphorylation, while also showing a corresponding decrease in VFA. The increased colocalization observed in Gal-1 knockdown GAN cells not only reveals that decreasing the levels of Gal-1 can correct the GAN phenotype, but more importantly that Gal-1 accumulation is critical to the formation of GAN.

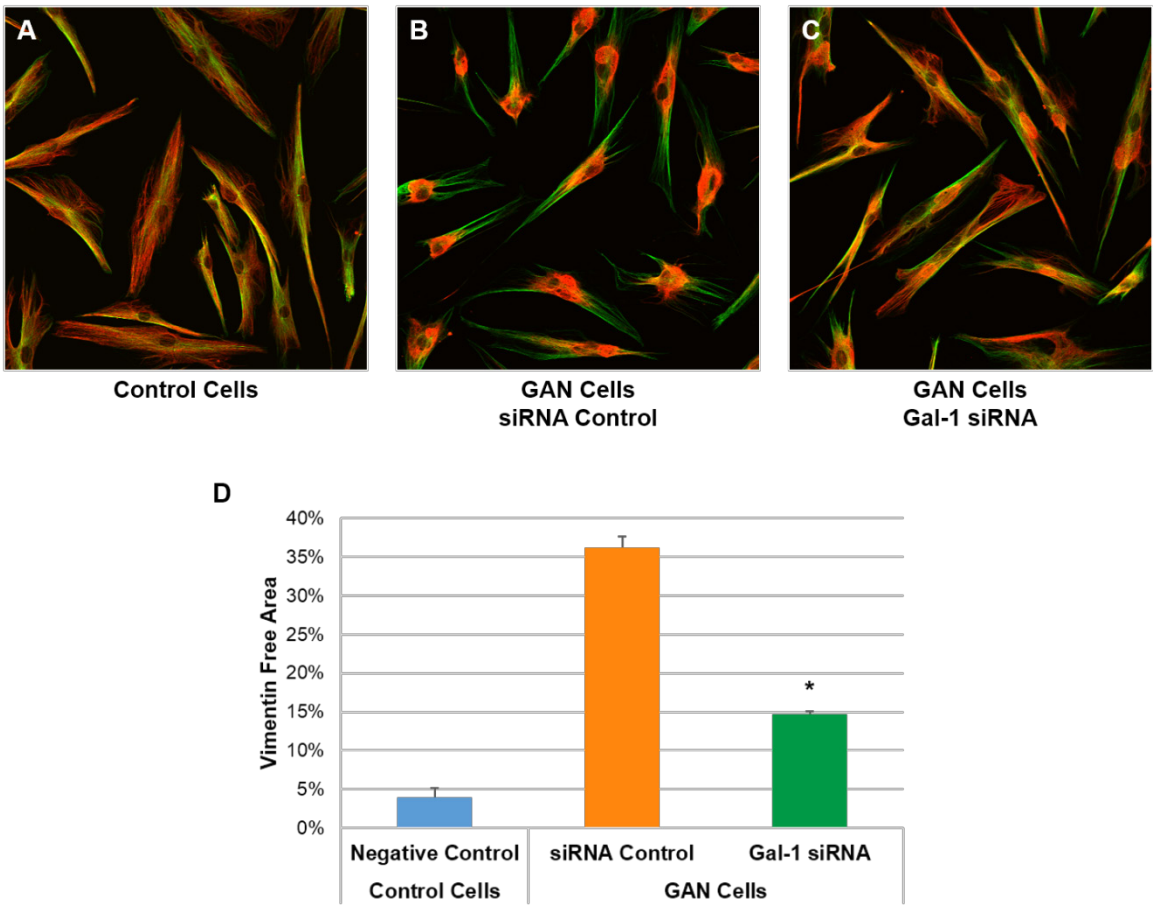

Figure 17: Gal-1 knockdown corrects vimentin distribution. (A) Representative tubulin (green) and vimentin (red) overlay image of control cells. (B) Overlay image of siRNA control treated GAN cells. (C) Overlay of Gal-1 siRNA treated GAN cells. (D) Quantification of the VFA in control cells, siRNA control treated GAN cells, and Gal-1 siRNA treated GAN cells (*$P < 0.05$ compared to GAN siRNA control cells, n=4 per condition). All cells were grown in low serum conditions.

H-Ras siRNA decreases vimentin phosphorylation and improves vimentin distribution

As the previous data demonstrated the integral role of Gal-1 in the formation of GAN, I sought to determine the signaling proteins downstream of Gal-1 that were critical to formation of the GAN phenotype. Gal-1 has previously been shown to specifically bind to and stabilize H-Ras, while having little to no

affinity for the other two Ras isoforms of K-Ras and N-Ras (165). With this data, I hypothesized that accumulated Gal-1 signals specifically through H-Ras to mediate vimentin hyperphosphorylation and vimentin disorganization in GAN cells. To test this, specific siRNAs corresponding to each Ras isoform was added to GAN cells individually, and an efficient knockdown was observed for H-Ras, K-Ras, and N-Ras (Figure 18). Immunoblotting shows increased levels of

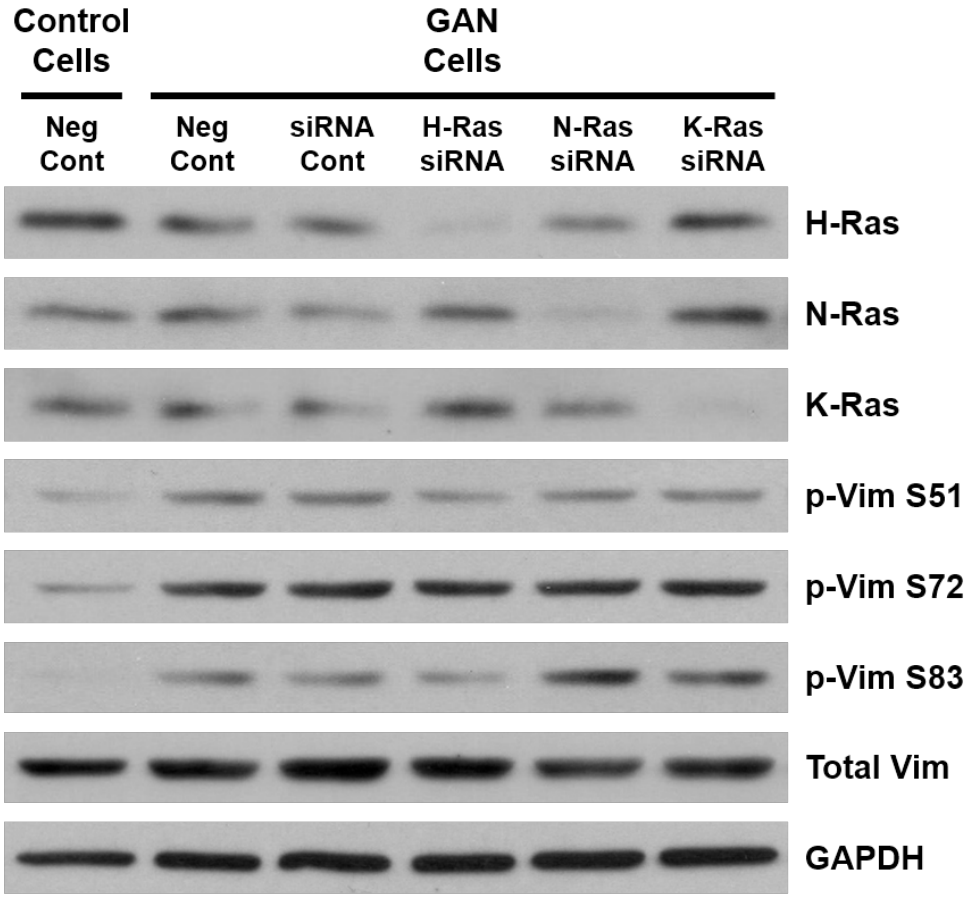

Figure 18: H-Ras specific knockdown exclusively reduces vimentin phosphorylation. Specific Ras isoform siRNA was administered to GAN cells grown in low serum conditions. The protein levels of specific vimentin phosphorylation sites were then compared between control cells, untreated GAN cells (Neg Cont), GAN cells given an siRNA control, and GAN cells treated with a Ras isoform siRNA. Representative blots shown (n=3).

phosphorylated vimentin in GAN cells, as noted previously, that remain elevated with addition of an siRNA control. Upon addition of the siRNA for each Ras isoform, only the H-Ras specific siRNA showed a decrease in vimentin phosphorylation at Ser51 and Ser83. Conversely, both the K-Ras and N-Ras siRNAs had little to no effect on the phosphorylation state of vimentin, as they remained unchanged from the GAN cells treated with an siRNA control; therefore, K-Ras and N-Ras do not contribute to the increased vimentin phosphorylation of GAN cells. Together, these results suggest that accumulated Gal-1 signals specifically through the H-Ras isoform to generate the vimentin hyperphosphorylation observed in GAN cells.

Immunofluorescence was subsequently performed to determine if the H-Ras specific decrease in vimentin phosphorylation translated into a correction of the GAN phenotype. Indeed, only those cells treated with the H-Ras siRNA showed increased vimentin distribution and an improved phenotype that more resembled the normal cytoskeletal structure of the control cells (Figure 19A-C). This phenotypic observation was confirmed by VFA quantification, which showed that the 35.2% ± 1.4% VFA area observed for GAN cells with siRNA control was significantly decreased to 22.6% ± 0.8% VFA upon addition of H-Ras siRNA (Figure 19D). Unlike the H-Ras siRNA, addition of either the K-Ras or the N-Ras siRNA had no discernable effect on the GAN phenotype, as both conditions resulted in the perinuclear vimentin accumulation that is seen in GAN cells transfected with an siRNA control. Upon quantification, GAN cells treated with K-Ras and N-Ras siRNAs had VFAs of 31.2% ± 2.2% and 31.0% ± 1.3%,

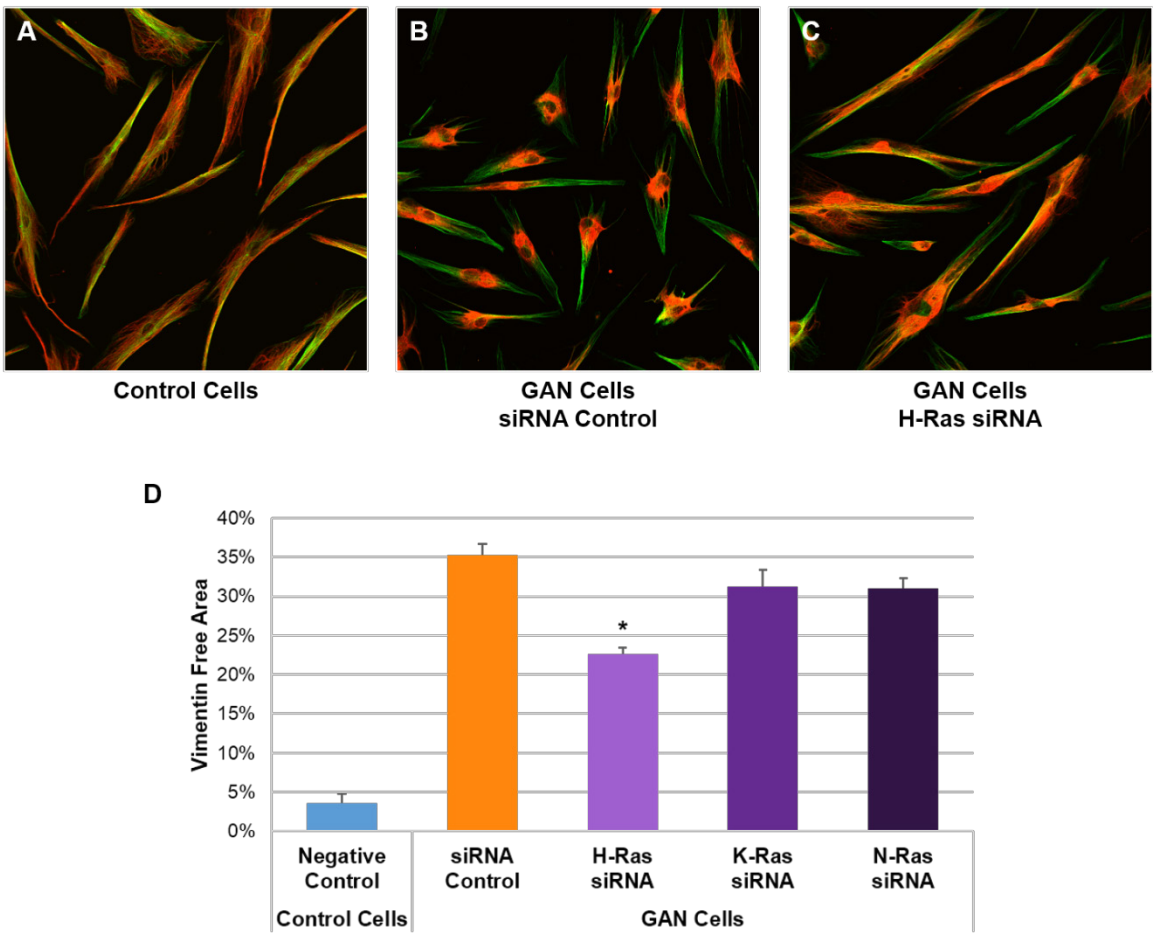

Figure 19: H-Ras siRNA improves vimentin distribution. (A) Representative tubulin (green) and vimentin (red) overlay image of control cells. (B) Overlay image of siRNA control treated GAN cells. (C) Overlay of H-Ras siRNA treated GAN cells. (D) Quantification of the VFA in control cells, siRNA control treated GAN cells, and Ras isoform siRNA treated GAN cells (*$P < 0.05$ compared to GAN siRNA control cells, n=4 per condition). All cells were grown in low serum conditions.

respectively, and these values were not significantly different from the 35.2% ± 1.4% VFA observed in GAN cells with the siRNA control. This data collectively demonstrates that only siRNA against the H-Ras specific Ras isoform has the ability to decrease vimentin hyperphosphorylation and improve vimentin distribution. Therefore, the H-Ras isoform is suggested to be critical to the formation of GAN and functions downstream of Gal-1 to cause the

hyperphosphorylation of vimentin and the altered vimentin distribution observed in GAN cells.

MEK1/2 knockdown reduces vimentin phosphorylation and improves vimentin distribution

As the previous data demonstrated that the GAN phenotype was dependent on H-Ras signaling, I sought to determine the downstream Ras effectors that contribute to the formation of GAN. The utilization of Ras effectors is altered by Gal-1 such that Ras signaling is diverted to Raf-1 at the expense of PI3K, thus leading to activation of the downstream Raf-1 effectors of mitogen-activated protein kinase kinase 1 and 2 (MEK1 and MEK2). I therefore hypothesized that MEK1 and MEK2 contribute to the vimentin hyperphosphorylation and vimentin disorganization observed in GAN cells. To determine their involvement in GAN, the levels of MEK1 and MEK2 proteins were decreased by separate siRNAs that ablated the expression of each protein (Figure 20). The decreased protein levels of MEK1 and MEK2 also generated reduced levels of vimentin phosphorylation at Ser83, thus demonstrating the involvement of MEK1 and MEK2 in the phosphorylation of vimentin at that specific site.

When these cells were observed by immunofluorescence, the combination of MEK1/2 siRNAs displayed significantly improved vimentin distribution (Figure 21A-C). This was reflected in the VFA quantification, as the siRNA control treated GAN cells had a VFA of 35.3% ± 0.6%, while the MEK1/2 siRNA treated GAN

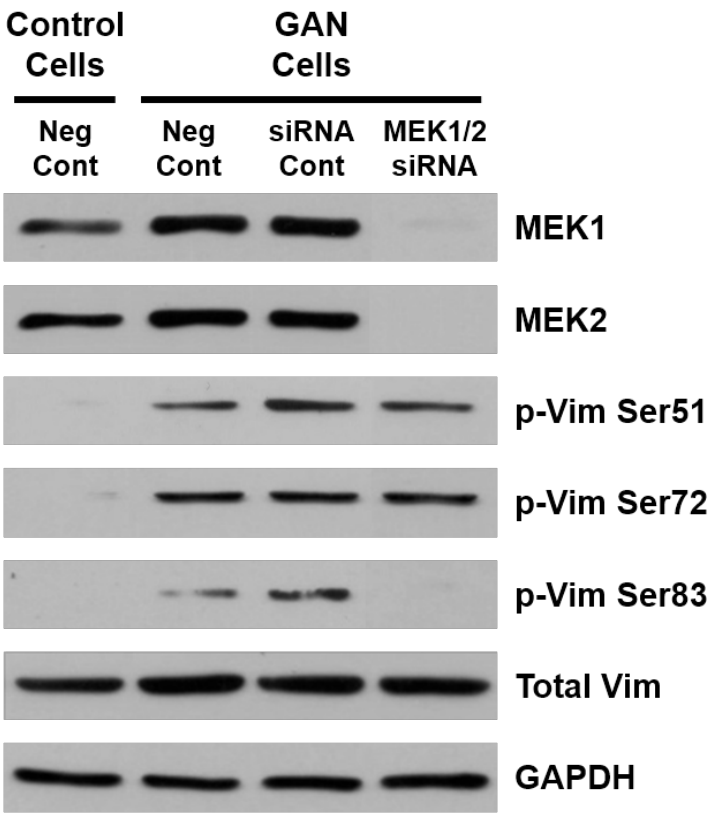

Figure 20: MEK1/2 siRNA reduces vimentin phosphorylation at Ser83. MEK1 and MEK2 siRNA was administered to GAN cells grown in low serum conditions. The protein levels of specific vimentin phosphorylation sites were then compared between control cells, untreated GAN cells (Neg Cont), GAN cells given an siRNA control, and GAN cells treated with a combination of MEK1/2 siRNAs. Representative blots shown (n=3).

cells had a VFA of 24.6% ± 0.4% (Figure 21D). Taken together, this data demonstrates that MEK1 and MEK2 are critical to the formation of the GAN phenotype, as they contribute to the hyperphosphorylation and disorganization of vimentin.

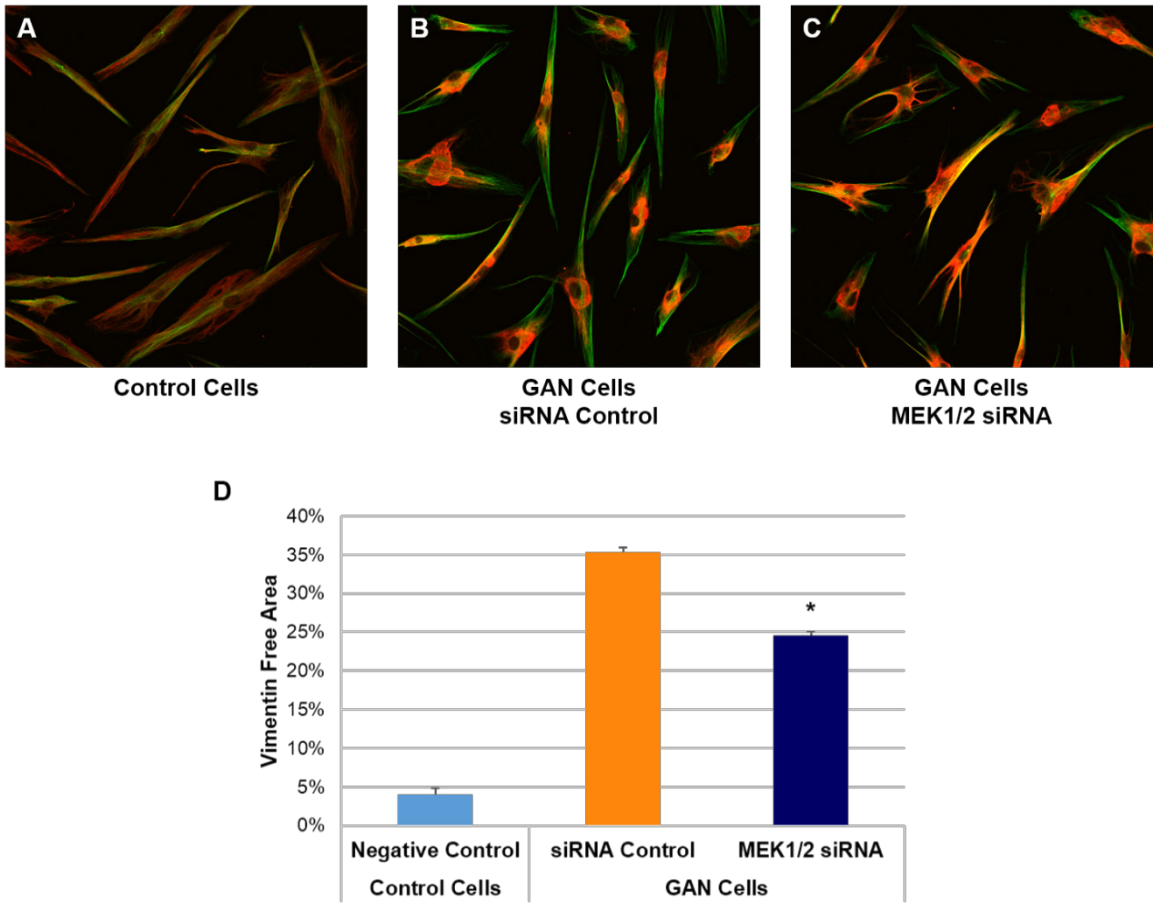

Figure 21: MEK1/2 siRNA improves vimentin distribution. (A) Representative tubulin (green) and vimentin (red) overlay image of control cells. (B) Overlay image of siRNA control treated GAN cells. (C) Overlay of MEK1/2 siRNA treated GAN cells. (D) Quantification of the VFA in control cells, siRNA control treated GAN cells, and MEK1/2 siRNA treated GAN cells (*P < 0.05 compared to GAN siRNA control cells, n=4 per condition). All cells were grown in low serum conditions.

CHAPTER IV: DISCUSSION

GAN is a progressive neurodegenerative disease that is characterized by giant axons filled with disorganized NFs. Although many different neurodegenerative diseases display similar NF phenotypes, GAN is unique in that seemingly all classes of IFs are affected, as IF abnormalities have been noted in the patient hair cells, fibroblasts, myocytes, and additional cell types. These systemic IF phenotypes are therefore not attributable to a mutation in one class of IF, but rather are caused by a defect in a ubiquitous protein that controls cytoskeletal organization.

GAN has been linked to autosomal recessive mutations of the *GAN* gene, which codes for the Giga protein. Based on sequence similarity, Giga is predicted to function as a substrate adaptor for a multisubunit E3 ubiquitin ligase and loss of this function in GAN patients would lead to an accumulation of any substrate. However, substrates of Giga have proven difficult to identify and potential substrates that have been proposed show no relationship to the observed phenotype of IF abnormalities. A recent proteomics study identified five proteins, including Gal-1, that were significantly increased in GAN patient cell, thus making them potential substrates of Giga (89).

Gal-1 functions to stabilize activated Ras and promotes its signaling through Raf-1, which then activates multiple protein kinases that are known to phosphorylate intermediate filaments. Generally, the phosphorylation of intermediate filaments promotes the disassembly of the normal filament

structure, leading to a retraction of IFs away from the cell periphery and toward the center of the cell. This phenotype is similar to that observed in GAN patient cells, which lead us to hypothesize that Giga regulates IF phosphorylation and structure by modulating the Ras pathway through the degradation of Gal-1. The following section will review the principal results of this study and discuss their impact in the context of GAN.

GAN cells have altered vimentin distribution in low serum

Without a functional mouse model to study the disease, the fibroblasts of GAN patients represent the main modality used to study GAN. These cells can be utilized because, like the neurons of the patients, they contain a disorganized IF structure. In GAN patient fibroblasts, this disorganization manifests as cytoplasmic vimentin aggregates near the nucleus. This distinctive feature has previously been used to quantify the vimentin phenotype as a percentage of cells containing aggregates. Such methodology, however, has demonstrated limited utility due to high variability in the percentages of GAN cells with aggregates being reported for the same cell lines (82, 83). These inconsistent findings are most likely due to the arbitrary definition of an aggregate and the human error involved in making this nuanced decision.

Although this aggregate phenotype is the most striking feature of GAN cells, the formation of the aggregate is simultaneous accompanied by a retraction of vimentin from the periphery. In this study, I developed a new scoring system based on this retraction of vimentin from the periphery of GAN cells, which I

quantified as the vimentin free area (VFA). This quantification system uses automated thresholding based on freely available software to obtain the area of vimentin staining in relation to the total cellular area. Utilizing this computerized scoring system removes any previous ambiguity to what was defined as an aggregate and allows consistent reproducible results that can be produced on multiple imaging platforms.

This phenotype of an altered vimentin distribution resembles what is observed during distinct stages of the cell cycle. In mitosis, a vast rearrangement of the IF is observed, which allows the disassembly of the cellular structural components and subsequent segregation into the daughter cells. Throughout this process, a general vimentin hyperphosphorylation is observed in concert with the disassembly of the IF structure. This phosphorylation-induced disassembly is first observed in late prophase, when vimentin is retracted from the cellular periphery to form a centrosomal vimentin aggregate. As this is a similar phenotype to the one observed in GAN, I hypothesized vimentin hyperphosphorylation also causes the formation of VFA in GAN patient cells.

GAN cells have elevated Gal-1 and phosphorylated vimentin in low serum

The GAN phenotype of induced vimentin retraction and aggregate formation in low serum conditions has been well described, but a molecular mechanism leading to this serum-based aggravation has not been determined. Here, I demonstrated that GAN cells have elevated levels of Gal-1 exclusively in low serum conditions, and that this pathway can account for the GAN phenotypic

discrepancy based on serum conditions. When grown in low serum, cells are synchronized in G0 resting phase and no longer undergo cell division. This occurs due to the scarcity of growth factors supplied by the 0.1% FBS supplemented into the low serum media. Without these growth factors, there is little activation of signaling pathways, such as Ras. For control cells, the low protein levels of Gal-1 reinforces the lack of Ras signaling, as there is little Gal-1 to stabilize any Ras activated by the low basal level of growth factors. Together, these conditions generate limited Gal-1 stabilized Ras activation, which leads to the decreased vimentin phosphorylation observed in control cells grown in low serum. This low level of vimentin phosphorylation allows the control cells to maintain the normal vimentin structure and distribution that is required in non-dividing cells.

In contrast, the GAN cells maintain high levels of Gal-1 in the absence of Giga when grown in low serum. These elevated levels of Gal-1 allow any amount of Ras activated by the low concentration of serum growth factors to be maintained in the activated state. This activated Ras can then signal through Raf-1 to induce vimentin phosphorylation, and this is observed as GAN cells have significantly elevated phosphorylated vimentin levels at serine residues 39, 51, 72, and 83. As seen during the cell cycle, vimentin phosphorylation correlates with a retraction of vimentin from the periphery of the cell and the formation of a centrosomal aggregate. This phenotype is mirrored in GAN cells. Accordingly, I propose that elevated levels of Gal-1 lock Ras in an activated state that leads to vimentin hyperphosphorylation in GAN cells grown in low serum.

The serum-based differences in Gal-1 protein levels and vimentin phosphorylation are also reflected in the phenotypes of both cell types. For control cells, a decrease in VFA is observed that mirrors the decrease of Gal-1 when they are moved from normal to low serum conditions. This is indicative of the cell cycle state of control cells in the two serum condition. In low serum, the lack of growth factors coupled with low Gal-1 expression lead to generally low levels of vimentin phosphorylation. This allows for the control cells to maintain a normal filamentous IF structure that is characteristic of an interphase cell. However, in normal serum conditions, a subset of control cell are progressing through the cell cycle and therefore will transiently have a retracted vimentin network as they progress through prophase. This is reflected in the VFA measurement for control cells, as they have increased VFA in normal serum as compared to low, thus indicating increased cell cycle activity in normal serum.

GAN cells grown in normal serum are indistinguishable from control cells when scored by VFA. This is of particular note, as it seems to reflect the similar levels of Gal-1 expressed between the two cell lines in these culture conditions. When GAN cells are moved into low serum, however, their VFA drastically increases and appears to be related to the increased levels of Gal-1 that are maintained by GAN cells in this condition. As reflected by their increased VFA in low serum, the GAN cells appear to become locked into an IF phenotype that is reminiscent of cycling cells in late prophase. This raises the possibility that the low serum condition synchronizes control cells in the G0 resting phase, but synchronizes GAN cells in prophase. Together, these results demonstrate low

serum specific increases in Gal-1 and vimentin phosphorylation in GAN cells that can account for the phenotypic differences between GAN and control fibroblasts.

Giga controls the proteasome mediated degradation of Gal-1

As a proposed substrate adaptor, Giga should have an inverse relationship with a potential substrate, like Gal-1. For example, increasing the protein levels of a substrate adaptor should facilitate the proteasome mediated degradation of any substrate, leading to decreased protein levels of the substrate. This relationship was demonstrated for Giga and Gal-1, as replacing wild-type Giga through either lentiviral transduction or protein replacement therapy caused a significant decrease in the protein levels of Gal-1. These findings suggest that Gal-1 is in fact a substrate of Giga.

This inverse relationship was observed in every experiment, with one exception arising when comparing normal and low serum protein levels of Giga and Gal-1 in control cells. In this experiment Giga is expressed at equivalent levels in both growth conditions, but Gal-1 only appears to be degraded in low serum. This appears to create a contradiction in normal serum, as Giga is expressed but Gal-1 does not appear to be degraded. However, this scenario may be explained by the substrate adaptor binding to the substrate being regulated by post-translational modifications. Generally, post-translational modification of the substrate is a prerequisite for substrate adaptor binding and degradation (101, 253). This modification-specific degradation allows for the targeting of a specific pool of substrates to be degraded, while also maintaining a

basal level of the substrate that is not subjected to degradation. Additionally, post-translational modification of the substrate adaptors themselves have also been shown to be required for substrate binding in some cases (101). As Giga is present in control cells at equivalent levels in both normal and low serum, this scenario presents a possible pathway in which Giga and/or Gal-1 are modified exclusively in low serum to facilitate their interaction and subsequently induce the degradation of Gal-1.

Gal-1 knockdown decreases vimentin phosphorylation and restores vimentin distribution

Directly decreasing the protein levels of Gal-1 in GAN cells resulted in decreased vimentin phosphorylation and also a significant decrease in the VFA of these cells. Together these results suggest the direct involvement of Gal-1 in the formation of GAN, and such involvement could explain multiple different aspects of the disease. First, Gal-1 is widely expressed in most cells, which could explain why IF abnormalities are seen in various different GAN cell types (148, 159). For all cells that express Gal-1, the lack of Giga expression in GAN patients could lead to Gal-1 accumulation and aberrant signaling leading to similar IF abnormalities seen in patient fibroblasts. Although Gal-1 is expressed in most cell types, its expression is the highest in primary sensory and motor neurons of the spinal cord and brain stem (157). These sensory and motor neurons also happen to be the most affected cells in GAN patients and the neurodegeneration of these cells leads to progressive loss of ambulatory ability in patients. The inability to

regulate Gal-1 protein levels in these specific cells that inherently have high expression levels could generate the particularly high levels of dysfunction observed in GAN patient sensory and motor neurons. Additionally, Gal-1 expression is much lower throughout the brain, which may explain why the brain is largely unaffected and allows most patients to maintain normal mentation (158). Similar low levels of Gal-1 expression outside the nervous system may also justify why other organ system appear to be unaffected in GAN patients.

In addition to multiple aspects of GAN being related to the spatial expression of Gal-1, the temporal expression of Gal-1 also appears to be related to the progression of the disease. The expression of Gal-1 in sensory neurons is first detected after neuronal differentiation and Gal-1 levels remain high throughout the process of neuronal maturation (158). After synaptogenesis, however, Gal-1 is normally observed at much lower levels (158). In humans, the process of synaptogenesis occurs throughout the initial stages of development, but a peak synapse density occurs during the juvenile period of three to five years of age (254). Therefore, synaptogenesis occurs around the time that GAN patients initially present with symptomatic gait disturbances. This presents an intriguing possibility that Gal-1 is normally involved in the growth and development of neurons, but is down-regulated after neuronal maturation. The down-regulation of Gal-1 after synaptogenesis could be related to Giga function, thus leading to aberrantly high levels of Gal-1 in GAN patients after the normal neuronal maturation ends. In this case, the accumulated Gal-1 could then facilitate abnormal IF hyperphosphorylation as is seen in GAN patient fibroblasts.

H-Ras siRNA decreases vimentin phosphorylation and improves vimentin distribution

Since Gal-1 siRNA improved the GAN phenotype, I proceeded further down the proposed signaling pathway to target the main Gal-1 binding partner: Ras. Treatment of GAN cells with siRNA directed against the three Ras isoforms demonstrated that only the H-Ras siRNA decreased the vimentin hyperphosphorylation and formation of VFA. This result was in agreement with previous reports that demonstrated that Gal-1 only bound and stabilized H-Ras and had no affinity for K-Ras or N-Ras. Together, these results demonstrate a pathway where increased H-Ras signaling, due to Gal-1 stabilization, leads to the increased vimentin phosphorylation and VFA in GAN patient cells.

A Gal-1 mediated hyperphosphorylation of IFs could explain many aspects of the giant axons observed in patients, including the location of the enlarged axons in the distal region of the nerve. The phosphorylation of NFs occurs in a proximal to distal gradient, with the highest levels of phosphorylation observed in the most distal axonal region (206, 255). This distal region of the axon is also where the axonal enlargements are concentrated in GAN neurons (18, 82). As hyperphosphorylation of NFs has been demonstrated to cause their bundling and accumulation, it is possible that the normal cellular machinery responsible for phosphorylation is dysfunctional in GAN patients, thus leading to the formation of distal neuronal aggregates (244, 247, 248). NF phosphorylation also alters their transport by interrupting the association with kinesin, leading to a slower rate of anterograde transport (235, 240, 244). With this slowing of anterograde transport,

NF phosphorylation has also been shown to lead to distal accumulations of NFs (256). Altogether, NF hyperphosphorylation could contribute to the formation of distal axonal enlargements by increased NF bundling and interrupted anterograde NF transport.

Future directions

This thesis research presents a model for the underlying cause of GAN in which the loss of Giga leads to an accumulation of Gal-1 and subsequent hyperphosphorylation of IFs. Although this study provided multiple lines of experimentation concluding that Giga functions as a substrate adaptor to control the degradation of Gal-1, I was unable to demonstrate the direct binding required to verify this function. This is most likely due to the transient nature of this reaction and the inherently low expression levels of Giga. Future studies will need to address this binding to solidify Giga as a substrate adaptor that targets Gal-1 for degradation. If Giga and Gal-1 binding is verified, additional studies should be performed to determine if the Giga and Gal-1 binding is induced by post-translational modifications. This idea is suggested by the observation that Gal-1 down-regulation occurs in low serum conditions in control cells without an increase in Giga protein. The modification of either or both partners could specifically facilitate this interaction in low serum conditions, and without the signal in normal serum, the binding may not occur.

After verification of Giga's function as a substrate adaptor, additional binding partners of Giga should be identified. Most substrate adaptors have the

ability to bind more than one substrate, so in addition to Gal-1, it is likely Giga also controls the degradation of additional proteins. This scenario is supported by comparing the western blot results of the lentiviral experiments restoring Giga expression to those of the Gal-1 siRNA experiments. When wild-type Giga expression was restored with the lentiviral construct, a generalized decrease in vimentin phosphorylation was observed in GAN cells. This decrease included all four tested vimentin phosphorylation sites at serine residues 39, 51, 72, and 83. In contrast, only two vimentin phosphorylation sites were significantly decreased with the Gal-1 siRNA. These differences in the vimentin phosphorylation state between the two experiments may be attributed to what each treatment accomplished. In the first case of the Giga lentivirus, replacing the wild-type protein into the GAN cells enabled the functional Giga to facilitate the degradation of all potential substrates and lead to reduced vimentin phosphorylation at all four tested serine residues. Conversely, treatment with the Gal-1 siRNA merely decreased the protein levels of one potential Giga substrates and only lead to reduced vimentin phosphorylation at two of the four tested serine residues. These results suggest that Gal-1 mediated signaling contributes to increased vimentin phosphorylation at two specific residues, but other potential Giga substrates may be responsible for the hyperphosphorylation of vimentin at addition sites.

Further evidence of additional Giga substrates was demonstrated by the immunofluorescence results of Giga restoration compared to Gal-1 siRNA treatment in GAN cells. First, Giga restoration via lentiviral transduction or protein

replacement therapy generated treated patient cells that were indistinguishable from controls, as they not only had corrected vimentin distribution, but also completely lack the vimentin aggregates that are observed in untreated GAN cells (data not shown). In contrast, treating the GAN cells with a Gal-1 specific siRNA only resulted in corrected vimentin distribution, while having little effect on the formation of vimentin aggregates (data not shown). These vimentin aggregates clearance with Giga replacement and the persistence of aggregates with Gal-1 siRNA suggest that additional Giga substrates, besides Gal-1, may be involved in the formation of the aggregates.

Additional Giga substrates may include the first purported substrates of MAP1B, TBCB, and MAP8 (93, 124-126). Although the validity of these three MAPs as Giga substrates has been brought into question by previous publications (85, 86, 89), my data demonstrates elevated levels of MAP1B and TBCB in GAN cells that is suggestive of these proteins being Giga substrates (Figure 22). These elevated levels of MAP1B and TBCB are low serum specific and follow the same serum based expression pattern as that of Gal-1. In control cells, the protein levels of both MAP1B and TBCB are decreased as the cells are moved from normal to low serum. In GAN cells, however, no such low serum decrease is observed, therefore leading to elevated levels of MAP1B and TBCB. Accumulation of MAPs such as MAP1B and TBCB are known to alter the microtubule structure and dynamics by promoting the assembly and/or disassembly of microtubules (134, 135, 141, 142). GAN cells, however, present a phenotypically normal microtubule network that has no apparent direct link to the

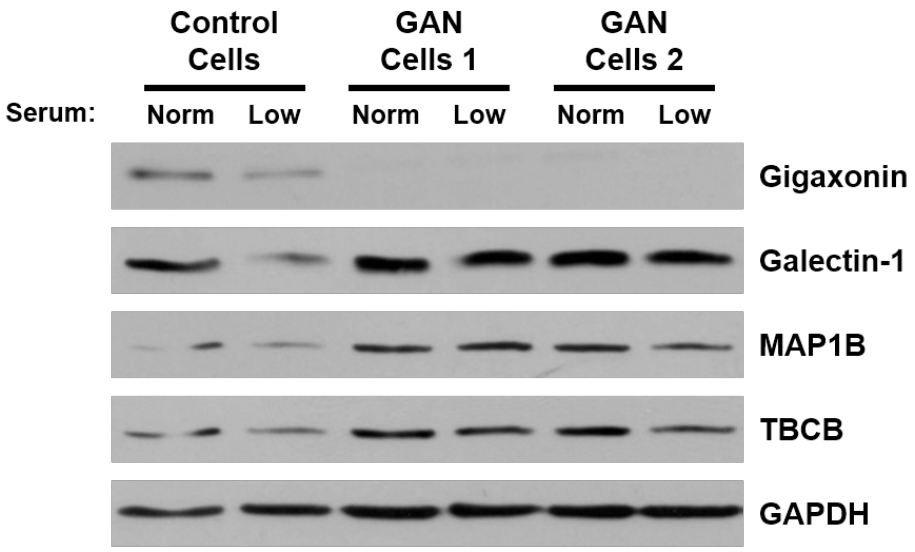

Figure 22: Elevated protein levels of MAP1B-LC and TBCB specifically in low serum conditions. Comparison of the protein levels of Gal-1, MAP1B, and TBCB in control cells and two distinct GAN patient cell lines. Representative blots shown (n=3).

abnormal IF structure of patient cells, which has previously led to the dismissal of MAP1B and TBCB as being relevant in GAN (82-84).

Although the microtubule structure appears to not be directly affected by an accumulation of MAP1B and TBCB, increased protein levels of related MAPs, such as MAP2, MAP4, or tau, were shown to alter cellular transport by interfering with molecular motors (257-259). This interference occurs as the MAPs compete with the molecular motors for microtubule binding sides and impede the attachment of the motors to the microtubule track (258, 259). The attachment of the kinesin motor is preferentially disrupted, thus leading to decreased anterograde transport and a subsequent perinuclear accumulation of kinesin cargo near the microtubule organizing center (258, 260). Such kinesin cargo includes IFs, which form perinuclear IF aggregates when kinesin motility is

disrupted by the overexpression of multiple MAPs (258, 260, 261). Therefore, while not directly affecting the microtubule structure, the accumulation of MAP1B and TBCB could indirectly alter the IF structure by obstructing the movement of IF on associated kinesin motors and ultimately result in the formation of perinuclear vimentin aggregates that resemble those observed in GAN patient fibroblasts. This scenario suggests that the GAN phenotype could occur as a consequence of two separate mechanisms resulting from the loss of Giga function: the accumulation of MAPs, such as MAP1B and TBCB, leads to the formation of perinuclear vimentin aggregates, and/or elevated levels of Gal-1 cause vimentin phosphorylation and the subsequent retraction of vimentin from the cell periphery. Future studies should address whether MAP1B and TBCB are Giga substrates and determine their roles not only in the formation of vimentin aggregates, but also in the generation of the overall GAN phenotype.

Additional insight into the retraction of vimentin from the GAN cell periphery was obtained by using an H-Ras specific siRNA, which reduced vimentin phosphorylation and improved vimentin distribution in GAN cells. These results are highly suggestive of H-Ras contributing to the GAN phenotype, but it failed to directly demonstrate increased Ras signaling in GAN. Multiple assays were used in attempt to directly address this in GAN cells, but all produced inconsistent results using our fibroblast cell models. This result may be due to nuances in the cell model and experiment assay that did not fully quantify Ras activity, or because of transient nature of the Ras nanoclusters that are formed in the presence of Gal-1. Future studies should directly reinvestigate whether there

is increased Ras activity in GAN cells and further determine the exact downstream pathway in which H-Ras facilitates the formation of GAN. If the Ras pathway involvement is confirmed, it would suggest that small molecule inhibitors of downstream Ras effectors may prove effective in the treatment of GAN. Taken together, this study demonstrates that Giga regulates IF phosphorylation and structure by decreasing Ras signaling through the degradation of Gal-1, and provides a framework for utilizing Ras pathway inhibitors as a therapy for this currently immedicable genetic disease.

REFERENCES

1. Berg BO, Rosenberg SH, and Asbury AK. Giant axonal neuropathy. *Pediatrics.* 1972;49(6):894-9.
2. Treiber-Held S, Budjarjo-Welim H, Reimann D, Richter J, Kretzschmar HA, and Hanefeld F. Giant axonal neuropathy: a generalized disorder of intermediate filaments with longitudinal grooves in the hair. *Neuropediatrics.* 1994;25(2):89-93.
3. Koop O, Schirmacher A, Nelis E, Timmerman V, De Jonghe P, Ringelstein B, Rasic VM, Evrard P, Gartner J, Claeys KG, et al. Genotype-phenotype analysis in patients with giant axonal neuropathy (GAN). *Neuromuscular disorders : NMD.* 2007;17(8):624-30.
4. Opal P, and Goldman RD. Explaining intermediate filament accumulation in giant axonal neuropathy. *Rare diseases.* 2013;1(e25378.
5. Guazzi GC, Malandrini A, Gerli R, and Federico A. Giant axonal neuropathy in 2 siblings: a generalized disorder of intermediate filaments. *European neurology.* 1991;31(1):50-6.
6. Ouvrier RA. Giant axonal neuropathy. A review. *Brain & development.* 1989;11(4):207-14.
7. Igisu H, Ohta M, Tabira T, Hosokawa S, and Goto I. Giant axonal neuropathy. A clinical entity affecting the central as well as the peripheral nervous system. *Neurology.* 1975;25(8):717-21.
8. Yang Y, Allen E, Ding J, and Wang W. Giant axonal neuropathy. *Cellular and molecular life sciences : CMLS.* 2007;64(5):601-9.
9. Kuhlenbaumer G, Young P, Oberwittler C, Hunermund G, Schirmacher A, Domschke K, Ringelstein B, and Stogbauer F. Giant axonal neuropathy (GAN): case report and two novel mutations in the gigaxonin gene. *Neurology.* 2002;58(8):1273-6.
10. Fois A, Balestri P, Farnetani MA, Berardi R, Mattei R, Laurenzi E, Alessandrini C, Gerli R, Ribuffo A, and Calvieri S. Giant axonal neuropathy. Endocrinological and histological studies. *European journal of pediatrics.* 1985;144(3):274-80.
11. Koch T, Schultz P, Williams R, and Lampert P. Giant axonal neuropathy: a childhood disorder of microfilaments. *Annals of neurology.* 1977;1(5):438-51.
12. Demir E, Bomont P, Erdem S, Cavalier L, Demirci M, Kose G, Muftuoglu S, Cakar AN, Tan E, Aysun S, et al. Giant axonal neuropathy: clinical and genetic study in six cases. *Journal of neurology, neurosurgery, and psychiatry.* 2005;76(6):825-32.
13. Brockmann K, Pouwels PJ, Dechent P, Flanigan KM, Frahm J, and Hanefeld F. Cerebral proton magnetic resonance spectroscopy of a patient with giant axonal neuropathy. *Brain & development.* 2003;25(1):45-50.

14. Alkan A, Kutlu R, Sigirci A, Baysal T, Altinok T, and Yakinci C. Giant axonal neuropathy: MRS findings. *Journal of neuroimaging : official journal of the American Society of Neuroimaging.* 2003;13(4):371-5.
15. Carpenter S, Karpati G, Andermann F, and Gold R. Giant axonal neuropathy. A clinically and morphologically distinct neurological disease. *Archives of neurology.* 1974;31(5):312-6.
16. Boizot A, Talmat-Amar Y, Morrogh D, Kuntz NL, Halbert C, Chabrol B, Houlden H, Stojkovic T, Schulman BA, Rautenstrauss B, et al. The instability of the BTB-KELCH protein Gigaxonin causes Giant Axonal Neuropathy and constitutes a new penetrant and specific diagnostic test. *Acta neuropathologica communications.* 2014;2(47.
17. Nalini A, Gayathri N, Yasha TC, Ravishankar S, Urtizberea A, Huehne K, and Rautenstrauss B. Clinical, pathological and molecular findings in two siblings with giant axonal neuropathy (GAN): report from India. *European journal of medical genetics.* 2008;51(5):426-35.
18. Kretzschmar HA, Berg BO, and Davis RL. Giant axonal neuropathy. A neuropathological study. *Acta neuropathologica.* 1987;73(2):138-44.
19. Taratuto AL, Sevlever G, Saccoliti M, Caceres L, and Schultz M. Giant axonal neuropathy (GAN): an immunohistochemical and ultrastructural study report of a Latin American case. *Acta neuropathologica.* 1990;80(6):680-3.
20. Schroder JM, Bohl J, and von Bardeleben U. Changes of the ratio between myelin thickness and axon diameter in human developing sural, femoral, ulnar, facial, and trochlear nerves. *Acta neuropathologica.* 1988;76(5):471-83.
21. Asbury AK, Gale MK, Cox SC, Baringer JR, and Berg BO. Giant axonal neuropathy--a unique case with segmental neurofilamentous masses. *Acta neuropathologica.* 1972;20(3):237-47.
22. Donaghy M, King RH, Thomas PK, and Workman JM. Abnormalities of the axonal cytoskeleton in giant axonal neuropathy. *Journal of neurocytology.* 1988;17(2):197-208.
23. Peiffer J, Schlote W, Bischoff A, Boltshauser E, and Muller G. Generalized giant axonal neuropathy: a filament-forming disease of neuronal, endothelial, glial, and schwann cells in a patient without kinky hair. *Acta neuropathologica.* 1977;40(3):213-8.
24. Tandan R, Little BW, Emery ES, Good PS, Pendlebury WW, and Bradley WG. Childhood giant axonal neuropathy. Case report and review of the literature. *Journal of the neurological sciences.* 1987;82(1-3):205-28.
25. Houlden H, Groves M, Miedzybrodzka Z, Roper H, Willis T, Winer J, Cole G, and Reilly MM. New mutations, genotype phenotype studies and manifesting carriers in giant axonal neuropathy. *Journal of neurology, neurosurgery, and psychiatry.* 2007;78(11):1267-70.
26. Ishikawa H, Bischoff R, and Holtzer H. Mitosis and intermediate-sized filaments in developing skeletal muscle. *The Journal of cell biology.* 1968;38(3):538-55.

27. Fuchs E, and Weber K. Intermediate filaments: structure, dynamics, function, and disease. *Annual review of biochemistry.* 1994;63(345-82.
28. Herrmann H, Strelkov SV, Burkhard P, and Aebi U. Intermediate filaments: primary determinants of cell architecture and plasticity. *The Journal of clinical investigation.* 2009;119(7):1772-83.
29. Steinert PM, and Roop DR. Molecular and cellular biology of intermediate filaments. *Annual review of biochemistry.* 1988;57(593-625.
30. Strelkov SV, Herrmann H, and Aebi U. Molecular architecture of intermediate filaments. *BioEssays : news and reviews in molecular, cellular and developmental biology.* 2003;25(3):243-51.
31. Chang L, and Goldman RD. Intermediate filaments mediate cytoskeletal crosstalk. *Nature reviews Molecular cell biology.* 2004;5(8):601-13.
32. Eriksson JE, Dechat T, Grin B, Helfand B, Mendez M, Pallari HM, and Goldman RD. Introducing intermediate filaments: from discovery to disease. *The Journal of clinical investigation.* 2009;119(7):1763-71.
33. Burke B, and Stewart CL. The nuclear lamins: flexibility in function. *Nature reviews Molecular cell biology.* 2013;14(1):13-24.
34. Herrmann H, and Aebi U. Intermediate filaments: molecular structure, assembly mechanism, and integration into functionally distinct intracellular Scaffolds. *Annual review of biochemistry.* 2004;73(749-89.
35. Parry DA, Strelkov SV, Burkhard P, Aebi U, and Herrmann H. Towards a molecular description of intermediate filament structure and assembly. *Experimental cell research.* 2007;313(10):2204-16.
36. Parry DA, Steven AC, and Steinert PM. The coiled-coil molecules of intermediate filaments consist of two parallel chains in exact axial register. *Biochemical and biophysical research communications.* 1985;127(3):1012-8.
37. Steinert PM, Zimmerman SB, Starger JM, and Goldman RD. Ten-nanometer filaments of hamster BHK-21 cells and epidermal keratin filaments have similar structures. *Proceedings of the National Academy of Sciences of the United States of America.* 1978;75(12):6098-101.
38. Portet S, Mucke N, Kirmse R, Langowski J, Beil M, and Herrmann H. Vimentin intermediate filament formation: in vitro measurement and mathematical modeling of the filament length distribution during assembly. *Langmuir : the ACS journal of surfaces and colloids.* 2009;25(15):8817-23.
39. Meier M, Padilla GP, Herrmann H, Wedig T, Hergt M, Patel TR, Stetefeld J, Aebi U, and Burkhard P. Vimentin coil 1A-A molecular switch involved in the initiation of filament elongation. *Journal of molecular biology.* 2009;390(2):245-61.
40. Kirmse R, Portet S, Mucke N, Aebi U, Herrmann H, and Langowski J. A quantitative kinetic model for the in vitro assembly of intermediate filaments from tetrameric vimentin. *The Journal of biological chemistry.* 2007;282(25):18563-72.
41. Herrmann H, Haner M, Brettel M, Muller SA, Goldie KN, Fedtke B, Lustig A, Franke WW, and Aebi U. Structure and assembly properties of the

intermediate filament protein vimentin: the role of its head, rod and tail domains. *Journal of molecular biology.* 1996;264(5):933-53.
42. Zackroff RV, and Goldman RD. In vitro assembly of intermediate filaments from baby hamster kidney (BHK-21) cells. *Proceedings of the National Academy of Sciences of the United States of America.* 1979;76(12):6226-30.
43. Herrmann H, and Aebi U. Intermediate filament assembly: fibrillogenesis is driven by decisive dimer-dimer interactions. *Current opinion in structural biology.* 1998;8(2):177-85.
44. Georgakopoulou S, Moller D, Sachs N, Herrmann H, and Aebi U. Near-UV circular dichroism reveals structural transitions of vimentin subunits during intermediate filament assembly. *Journal of molecular biology.* 2009;386(2):544-53.
45. Goldman R, Goldman A, Green K, Jones J, Lieska N, and Yang HY. Intermediate filaments: possible functions as cytoskeletal connecting links between the nucleus and the cell surface. *Annals of the New York Academy of Sciences.* 1985;455(1-17.
46. Franke WW, Schmid E, Osborn M, and Weber K. Different intermediate-sized filaments distinguished by immunofluorescence microscopy. *Proceedings of the National Academy of Sciences of the United States of America.* 1978;75(10):5034-8.
47. Sun TT, and Green H. Immunofluorescent staining of keratin fibers in cultured cells. *Cell.* 1978;14(3):469-76.
48. Lazarides E. Intermediate filaments as mechanical integrators of cellular space. *Nature.* 1980;283(5744):249-56.
49. Goldman RD, Khuon S, Chou YH, Opal P, and Steinert PM. The function of intermediate filaments in cell shape and cytoskeletal integrity. *The Journal of cell biology.* 1996;134(4):971-83.
50. Weinstein DE, Shelanski ML, and Liem RK. Suppression by antisense mRNA demonstrates a requirement for the glial fibrillary acidic protein in the formation of stable astrocytic processes in response to neurons. *The Journal of cell biology.* 1991;112(6):1205-13.
51. Helfand BT, Mendez MG, Pugh J, Delsert C, and Goldman RD. A role for intermediate filaments in determining and maintaining the shape of nerve cells. *Molecular biology of the cell.* 2003;14(12):5069-81.
52. Sarria AJ, Lieber JG, Nordeen SK, and Evans RM. The presence or absence of a vimentin-type intermediate filament network affects the shape of the nucleus in human SW-13 cells. *Journal of cell science.* 1994;107 (Pt 6)(1593-607.
53. Gao Y, and Sztul E. A novel interaction of the Golgi complex with the vimentin intermediate filament cytoskeleton. *The Journal of cell biology.* 2001;152(5):877-94.
54. Milner DJ, Mavroidis M, Weisleder N, and Capetanaki Y. Desmin cytoskeleton linked to muscle mitochondrial distribution and respiratory function. *The Journal of cell biology.* 2000;150(6):1283-98.

55. Li Z, Colucci-Guyon E, Pincon-Raymond M, Mericskay M, Pournin S, Paulin D, and Babinet C. Cardiovascular lesions and skeletal myopathy in mice lacking desmin. *Developmental biology.* 1996;175(2):362-6.
56. Milner DJ, Weitzer G, Tran D, Bradley A, and Capetanaki Y. Disruption of muscle architecture and myocardial degeneration in mice lacking desmin. *The Journal of cell biology.* 1996;134(5):1255-70.
57. Soellner P, Quinlan RA, and Franke WW. Identification of a distinct soluble subunit of an intermediate filament protein: tetrameric vimentin from living cells. *Proceedings of the National Academy of Sciences of the United States of America.* 1985;82(23):7929-33.
58. Starger JM, Brown WE, Goldman AE, and Goldman RD. Biochemical and immunological analysis of rapidly purified 10-nm filaments from baby hamster kidney (BHK-21) cells. *The Journal of cell biology.* 1978;78(1):93-109.
59. Albers K, and Fuchs E. Expression of mutant keratin cDNAs in epithelial cells reveals possible mechanisms for initiation and assembly of intermediate filaments. *The Journal of cell biology.* 1989;108(4):1477-93.
60. Ngai J, Coleman TR, and Lazarides E. Localization of newly synthesized vimentin subunits reveals a novel mechanism of intermediate filament assembly. *Cell.* 1990;60(3):415-27.
61. Miller RK, Vikstrom K, and Goldman RD. Keratin incorporation into intermediate filament networks is a rapid process. *The Journal of cell biology.* 1991;113(4):843-55.
62. Yoon M, Moir RD, Prahlad V, and Goldman RD. Motile properties of vimentin intermediate filament networks in living cells. *The Journal of cell biology.* 1998;143(1):147-57.
63. Windoffer R, and Leube RE. Detection of cytokeratin dynamics by time-lapse fluorescence microscopy in living cells. *Journal of cell science.* 1999;112 (Pt 24)(4521-34.
64. Helfand BT, Chang L, and Goldman RD. The dynamic and motile properties of intermediate filaments. *Annual review of cell and developmental biology.* 2003;19(445-67.
65. Prahlad V, Yoon M, Moir RD, Vale RD, and Goldman RD. Rapid movements of vimentin on microtubule tracks: kinesin-dependent assembly of intermediate filament networks. *The Journal of cell biology.* 1998;143(1):159-70.
66. Goldman RD. The role of three cytoplasmic fibers in BHK-21 cell motility. I. Microtubules and the effects of colchicine. *The Journal of cell biology.* 1971;51(3):752-62.
67. Helfand BT, Mikami A, Vallee RB, and Goldman RD. A requirement for cytoplasmic dynein and dynactin in intermediate filament network assembly and organization. *The Journal of cell biology.* 2002;157(5):795-806.
68. Gyoeva FK, and Gelfand VI. Coalignment of vimentin intermediate filaments with microtubules depends on kinesin. *Nature.* 1991;353(6343):445-8.

69. Coulombe PA, Kerns ML, and Fuchs E. Epidermolysis bullosa simplex: a paradigm for disorders of tissue fragility. *The Journal of clinical investigation.* 2009;119(7):1784-93.
70. Coulombe PA, Hutton ME, Letai A, Hebert A, Paller AS, and Fuchs E. Point mutations in human keratin 14 genes of epidermolysis bullosa simplex patients: genetic and functional analyses. *Cell.* 1991;66(6):1301-11.
71. Muller FB, Kuster W, Wodecki K, Almeida H, Jr., Bruckner-Tuderman L, Krieg T, Korge BP, and Arin MJ. Novel and recurrent mutations in keratin KRT5 and KRT14 genes in epidermolysis bullosa simplex: implications for disease phenotype and keratin filament assembly. *Human mutation.* 2006;27(7):719-20.
72. Brownlees J, Ackerley S, Grierson AJ, Jacobsen NJ, Shea K, Anderton BH, Leigh PN, Shaw CE, and Miller CC. Charcot-Marie-Tooth disease neurofilament mutations disrupt neurofilament assembly and axonal transport. *Human molecular genetics.* 2002;11(23):2837-44.
73. Figlewicz DA, Krizus A, Martinoli MG, Meininger V, Dib M, Rouleau GA, and Julien JP. Variants of the heavy neurofilament subunit are associated with the development of amyotrophic lateral sclerosis. *Human molecular genetics.* 1994;3(10):1757-61.
74. Eriksson M, Brown WT, Gordon LB, Glynn MW, Singer J, Scott L, Erdos MR, Robbins CM, Moses TY, Berglund P, et al. Recurrent de novo point mutations in lamin A cause Hutchinson-Gilford progeria syndrome. *Nature.* 2003;423(6937):293-8.
75. Scaffidi P, and Misteli T. Reversal of the cellular phenotype in the premature aging disease Hutchinson-Gilford progeria syndrome. *Nature medicine.* 2005;11(4):440-5.
76. Boltshauser E, Bischoff A, and Isler W. Giant axonal neuropathy. Report of a case with normal hair. *Journal of the neurological sciences.* 1977;31(2):269-78.
77. Prineas JW, Ouvrier RA, Wright RG, Walsh JC, and McLeod JG. Gian axonal neuropathy--a generalized disorder of cytoplasmic microfilament formation. *Journal of neuropathology and experimental neurology.* 1976;35(4):458-70.
78. Takebe Y, Koide N, and Takahashi G. Giant axonal neuropathy: report of two siblings with endocrinological and histological studies. *Neuropediatrics.* 1981;12(4):392-404.
79. Sabatelli M, Bertini E, Ricci E, Salviati G, Magi S, Papacci M, and Tonali P. Peripheral neuropathy with giant axons and cardiomyopathy associated with desmin type intermediate filaments in skeletal muscle. *Journal of the neurological sciences.* 1992;109(1):1-10.
80. Rybojad M, Moraillon I, Bonafe JL, Cambon L, and Evrard P. [Pilar dysplasia: an early marker of giant axonal neuropathy]. *Annales de dermatologie et de venereologie.* 1998;125(12):892-3.
81. Pena SD. Giant axonal neuropathy: intermediate filament aggregates in cultured skin fibroblasts. *Neurology.* 1981;31(11):1470-3.

82. Klymkowsky MW, and Plummer DJ. Giant axonal neuropathy: a conditional mutation affecting cytoskeletal organization. *The Journal of cell biology.* 1985;100(1):245-50.
83. Pena SD, Opas M, Turksen K, Kalnins VI, and Carpenter S. Immunocytochemical studies of intermediate filament aggregates and their relationship to microtubules in cultured skin fibroblasts from patients with giant axonal neuropathy. *European journal of cell biology.* 1983;31(2):227-34.
84. Bomont P, and Koenig M. Intermediate filament aggregation in fibroblasts of giant axonal neuropathy patients is aggravated in non dividing cells and by microtubule destabilization. *Human molecular genetics.* 2003;12(8):813-22.
85. Cleveland DW, Yamanaka K, and Bomont P. Gigaxonin controls vimentin organization through a tubulin chaperone-independent pathway. *Human molecular genetics.* 2009;18(8):1384-94.
86. Mahammad S, Murthy SN, Didonna A, Grin B, Israeli E, Perrot R, Bomont P, Julien JP, Kuczmarski E, Opal P, et al. Giant axonal neuropathy-associated gigaxonin mutations impair intermediate filament protein degradation. *The Journal of clinical investigation.* 2013;123(5):1964-75.
87. Bousquet O, Basseville M, Vila-Porcile E, Billette de Villemeur T, Hauw JJ, Landrieu P, and Portier MM. Aggregation of a subpopulation of vimentin filaments in cultured human skin fibroblasts derived from patients with giant axonal neuropathy. *Cell motility and the cytoskeleton.* 1996;33(2):115-29.
88. Pena SD. Giant axonal neuropathy: an inborn error of organization of intermediate filaments. *Muscle Nerve.* 1982;5(2):166-72.
89. Mussche S, De Paepe B, Smet J, Devreese K, Lissens W, Rasic VM, Murnane M, Devreese B, and Van Coster R. Proteomic analysis in giant axonal neuropathy: New insights into disease mechanisms. *Muscle & Nerve.* 2012;46(2):246-56.
90. Ben Hamida C, Cavalier L, Belal S, Sanhaji H, Nadal N, Barhoumi C, M'Rissa N, Marzouki N, Mandel JL, Ben Hamida M, et al. Homozygosity mapping of giant axonal neuropathy gene to chromosome 16q24.1. *Neurogenetics.* 1997;1(2):129-33.
91. Bomont P, Cavalier L, Blondeau F, Ben Hamida C, Belal S, Tazir M, Demir E, Topaloglu H, Korinthenberg R, Tuysuz B, et al. The gene encoding gigaxonin, a new member of the cytoskeletal BTB/kelch repeat family, is mutated in giant axonal neuropathy. *Nature genetics.* 2000;26(3):370-4.
92. Ganay T, Boizot A, Burrer R, Chauvin JP, and Bomont P. Sensory-motor deficits and neurofilament disorganization in gigaxonin-null mice. *Molecular neurodegeneration.* 2011;6(25.
93. Ding J, Liu JJ, Kowal AS, Nardine T, Bhattacharya P, Lee A, and Yang Y. Microtubule-associated protein 1B: a neuronal binding partner for gigaxonin. *The Journal of cell biology.* 2002;158(3):427-33.

94. Mussche S, Devreese B, Nagabhushan Kalburgi S, Bachaboina L, Fox JC, Shih HJ, Van Coster R, Samulski RJ, and Gray SJ. Restoration of cytoskeleton homeostasis after gigaxonin gene transfer for giant axonal neuropathy. *Human gene therapy.* 2013;24(2):209-19.
95. Leung CL, Pang Y, Shu C, Goryunov D, and Liem RK. Alterations in lipid metabolism gene expression and abnormal lipid accumulation in fibroblast explants from giant axonal neuropathy patients. *BMC genetics.* 2007;8(6.
96. Bruno C, Bertini E, Federico A, Tonoli E, Lispi ML, Cassandrini D, Pedemonte M, Santorelli FM, Filocamo M, Dotti MT, et al. Clinical and molecular findings in patients with giant axonal neuropathy (GAN). *Neurology.* 2004;62(1):13-6.
97. Bomont P, Ioos C, Yalcinkaya C, Korinthenberg R, Vallat JM, Assami S, Munnich A, Chabrol B, Kurlemann G, Tazir M, et al. Identification of seven novel mutations in the GAN gene. *Human mutation.* 2003;21(4):446.
98. Perez-Torrado R, Yamada D, and Defossez PA. Born to bind: the BTB protein-protein interaction domain. *BioEssays : news and reviews in molecular, cellular and developmental biology.* 2006;28(12):1194-202.
99. Xu L, Wei Y, Reboul J, Vaglio P, Shin TH, Vidal M, Elledge SJ, and Harper JW. BTB proteins are substrate-specific adaptors in an SCF-like modular ubiquitin ligase containing CUL-3. *Nature.* 2003;425(6955):316-21.
100. Adams J, Kelso R, and Cooley L. The kelch repeat superfamily of proteins: propellers of cell function. *Trends in cell biology.* 2000;10(1):17-24.
101. Petroski MD, and Deshaies RJ. Function and regulation of cullin-RING ubiquitin ligases. *Nature reviews Molecular cell biology.* 2005;6(1):9-20.
102. Pickart CM. Mechanisms underlying ubiquitination. *Annual review of biochemistry.* 2001;70(503-33.
103. Pickart CM. Back to the future with ubiquitin. *Cell.* 2004;116(2):181-90.
104. Nalepa G, Rolfe M, and Harper JW. Drug discovery in the ubiquitin-proteasome system. *Nature reviews Drug discovery.* 2006;5(7):596-613.
105. Tai HC, and Schuman EM. Ubiquitin, the proteasome and protein degradation in neuronal function and dysfunction. *Nature reviews Neuroscience.* 2008;9(11):826-38.
106. Ciechanover A, Heller H, Elias S, Haas AL, and Hershko A. ATP-dependent conjugation of reticulocyte proteins with the polypeptide required for protein degradation. *Proceedings of the National Academy of Sciences of the United States of America.* 1980;77(3):1365-8.
107. Haas AL, and Rose IA. The mechanism of ubiquitin activating enzyme. A kinetic and equilibrium analysis. *The Journal of biological chemistry.* 1982;257(17):10329-37.
108. Hershko A, and Ciechanover A. The ubiquitin system. *Annual review of biochemistry.* 1998;67(425-79.
109. Hochstrasser M. Ubiquitin-dependent protein degradation. *Annual review of genetics.* 1996;30(405-39.

110. McGrath JP, Jentsch S, and Varshavsky A. UBA 1: an essential yeast gene encoding ubiquitin-activating enzyme. *The EMBO journal.* 1991;10(1):227-36.
111. van Wijk SJ, and Timmers HT. The family of ubiquitin-conjugating enzymes (E2s): deciding between life and death of proteins. *FASEB journal : official publication of the Federation of American Societies for Experimental Biology.* 2010;24(4):981-93.
112. Nakayama KI, and Nakayama K. Ubiquitin ligases: cell-cycle control and cancer. *Nature reviews Cancer.* 2006;6(5):369-81.
113. Feldman RM, Correll CC, Kaplan KB, and Deshaies RJ. A complex of Cdc4p, Skp1p, and Cdc53p/cullin catalyzes ubiquitination of the phosphorylated CDK inhibitor Sic1p. *Cell.* 1997;91(2):221-30.
114. Kipreos ET, Lander LE, Wing JP, He WW, and Hedgecock EM. cul-1 is required for cell cycle exit in C. elegans and identifies a novel gene family. *Cell.* 1996;85(6):829-39.
115. Zheng N, Schulman BA, Song L, Miller JJ, Jeffrey PD, Wang P, Chu C, Koepp DM, Elledge SJ, Pagano M, et al. Structure of the Cul1-Rbx1-Skp1-F boxSkp2 SCF ubiquitin ligase complex. *Nature.* 2002;416(6882):703-9.
116. Schulman BA, Carrano AC, Jeffrey PD, Bowen Z, Kinnucan ER, Finnin MS, Elledge SJ, Harper JW, Pagano M, and Pavletich NP. Insights into SCF ubiquitin ligases from the structure of the Skp1-Skp2 complex. *Nature.* 2000;408(6810):381-6.
117. Pintard L, Willems A, and Peter M. Cullin-based ubiquitin ligases: Cul3-BTB complexes join the family. *The EMBO journal.* 2004;23(8):1681-7.
118. Geyer R, Wee S, Anderson S, Yates J, and Wolf DA. BTB/POZ domain proteins are putative substrate adaptors for cullin 3 ubiquitin ligases. *Molecular cell.* 2003;12(3):783-90.
119. Pintard L, Willis JH, Willems A, Johnson JL, Srayko M, Kurz T, Glaser S, Mains PE, Tyers M, Bowerman B, et al. The BTB protein MEL-26 is a substrate-specific adaptor of the CUL-3 ubiquitin-ligase. *Nature.* 2003;425(6955):311-6.
120. Furukawa M, He YJ, Borchers C, and Xiong Y. Targeting of protein ubiquitination by BTB-Cullin 3-Roc1 ubiquitin ligases. *Nature cell biology.* 2003;5(11):1001-7.
121. Furukawa M, and Xiong Y. BTB protein Keap1 targets antioxidant transcription factor Nrf2 for ubiquitination by the Cullin 3-Roc1 ligase. *Molecular and cellular biology.* 2005;25(1):162-71.
122. Cullinan SB, Gordan JD, Jin J, Harper JW, and Diehl JA. The Keap1-BTB protein is an adaptor that bridges Nrf2 to a Cul3-based E3 ligase: oxidative stress sensing by a Cul3-Keap1 ligase. *Molecular and cellular biology.* 2004;24(19):8477-86.
123. Zhang DD, Lo SC, Sun Z, Habib GM, Lieberman MW, and Hannink M. Ubiquitination of Keap1, a BTB-Kelch substrate adaptor protein for Cul3, targets Keap1 for degradation by a proteasome-independent pathway. *The Journal of biological chemistry.* 2005;280(34):30091-9.

124. Allen E, Ding J, Wang W, Pramanik S, Chou J, Yau V, and Yang Y. Gigaxonin-controlled degradation of MAP1B light chain is critical to neuronal survival. *Nature.* 2005;438(7065):224-8.
125. Wang W, Ding J, Allen E, Zhu P, Zhang L, Vogel H, and Yang Y. Gigaxonin interacts with tubulin folding cofactor B and controls its degradation through the ubiquitin-proteasome pathway. *Current biology : CB.* 2005;15(22):2050-5.
126. Ding J, Allen E, Wang W, Valle A, Wu C, Nardine T, Cui B, Yi J, Taylor A, Jeon NL, et al. Gene targeting of GAN in mouse causes a toxic accumulation of microtubule-associated protein 8 and impaired retrograde axonal transport. *Human molecular genetics.* 2006;15(9):1451-63.
127. Zhuang M, Calabrese MF, Liu J, Waddell MB, Nourse A, Hammel M, Miller DJ, Walden H, Duda DM, Seyedin SN, et al. Structures of SPOP-substrate complexes: insights into molecular architectures of BTB-Cul3 ubiquitin ligases. *Molecular cell.* 2009;36(1):39-50.
128. Hoeck JD, Jandke A, Blake SM, Nye E, Spencer-Dene B, Brandner S, and Behrens A. Fbw7 controls neural stem cell differentiation and progenitor apoptosis via Notch and c-Jun. *Nature neuroscience.* 2010;13(11):1365-72.
129. Klotz K, Cepeda D, Tan Y, Sun D, Sangfelt O, and Spruck C. SCF(Fbxw7/hCdc4) targets cyclin E2 for ubiquitin-dependent proteolysis. *Experimental cell research.* 2009;315(11):1832-9.
130. Welcker M, Orian A, Grim JE, Eisenman RN, and Clurman BE. A nucleolar isoform of the Fbw7 ubiquitin ligase regulates c-Myc and cell size. *Current biology : CB.* 2004;14(20):1852-7.
131. Wei J, Mialki RK, Dong S, Khoo A, Mallampalli RK, Zhao Y, and Zhao J. A new mechanism of RhoA ubiquitination and degradation: roles of SCF(FBXL19) E3 ligase and Erk2. *Biochimica et biophysica acta.* 2013;1833(12):2757-64.
132. Wu C, and Ghosh S. beta-TrCP mediates the signal-induced ubiquitination of IkappaBbeta. *The Journal of biological chemistry.* 1999;274(42):29591-4.
133. Zhao J, Wei J, Mialki R, Zou C, Mallampalli RK, and Zhao Y. Extracellular signal-regulated kinase (ERK) regulates cortactin ubiquitination and degradation in lung epithelial cells. *The Journal of biological chemistry.* 2012;287(23):19105-14.
134. Pedrotti B, and Islam K. Microtubule associated protein 1B (MAP1B) promotes efficient tubulin polymerisation in vitro. *FEBS letters.* 1995;371(1):29-31.
135. Togel M, Wiche G, and Propst F. Novel features of the light chain of microtubule-associated protein MAP1B: microtubule stabilization, self interaction, actin filament binding, and regulation by the heavy chain. *The Journal of cell biology.* 1998;143(3):695-707.
136. Meixner A, Haverkamp S, Wassle H, Fuhrer S, Thalhammer J, Kropf N, Bittner RE, Lassmann H, Wiche G, and Propst F. MAP1B is required for axon guidance and Is involved in the development of the central and

peripheral nervous system. *The Journal of cell biology.* 2000;151(6):1169-78.
137. Gonzalez-Billault C, Avila J, and Caceres A. Evidence for the role of MAP1B in axon formation. *Molecular biology of the cell.* 2001;12(7):2087-98.
138. Gonzalez-Billault C, Owen R, Gordon-Weeks PR, and Avila J. Microtubule-associated protein 1B is involved in the initial stages of axonogenesis in peripheral nervous system cultured neurons. *Brain research.* 2002;943(1):56-67.
139. Kortazar D, Carranza G, Bellido J, Villegas JC, Fanarraga ML, and Zabala JC. Native tubulin-folding cofactor E purified from baculovirus-infected Sf9 cells dissociates tubulin dimers. *Protein expression and purification.* 2006;49(2):196-202.
140. Carranza G, Castano R, Fanarraga ML, Villegas JC, Goncalves J, Soares H, Avila J, Marenchino M, Campos-Olivas R, Montoya G, et al. Autoinhibition of TBCB regulates EB1-mediated microtubule dynamics. *Cellular and molecular life sciences : CMLS.* 2013;70(2):357-71.
141. Kortazar D, Fanarraga ML, Carranza G, Bellido J, Villegas JC, Avila J, and Zabala JC. Role of cofactors B (TBCB) and E (TBCE) in tubulin heterodimer dissociation. *Experimental cell research.* 2007;313(3):425-36.
142. Tian G, Lewis SA, Feierbach B, Stearns T, Rommelaere H, Ampe C, and Cowan NJ. Tubulin subunits exist in an activated conformational state generated and maintained by protein cofactors. *The Journal of cell biology.* 1997;138(4):821-32.
143. Orban-Nemeth Z, Simader H, Badurek S, Trancikova A, and Propst F. Microtubule-associated protein 1S, a short and ubiquitously expressed member of the microtubule-associated protein 1 family. *The Journal of biological chemistry.* 2005;280(3):2257-65.
144. Ding J, Valle A, Allen E, Wang W, Nardine T, Zhang Y, Peng L, and Yang Y. Microtubule-associated protein 8 contains two microtubule binding sites. *Biochemical and biophysical research communications.* 2006;339(1):172-9.
145. Johnson-Kerner BL, Ahmad FS, Diaz AG, Greene JP, Gray SJ, Samulski RJ, Chung WK, Van Coster R, Maertens P, Noggle SA, et al. Intermediate filament protein accumulation in motor neurons derived from giant axonal neuropathy iPSCs rescued by restoration of gigaxonin. *Human molecular genetics.* 2014.
146. Dequen F, Bomont P, Gowing G, Cleveland DW, and Julien JP. Modest loss of peripheral axons, muscle atrophy and formation of brain inclusions in mice with targeted deletion of gigaxonin exon 1. *Journal of neurochemistry.* 2008;107(1):253-64.
147. Barondes SH, Castronovo V, Cooper DN, Cummings RD, Drickamer K, Feizi T, Gitt MA, Hirabayashi J, Hughes C, Kasai K, et al. Galectins: a family of animal beta-galactoside-binding lectins. *Cell.* 1994;76(4):597-8.
148. Liu FT, Patterson RJ, and Wang JL. Intracellular functions of galectins. *Biochimica et biophysica acta.* 2002;1572(2-3):263-73.

149. Camby I, Le Mercier M, Lefranc F, and Kiss R. Galectin-1: a small protein with major functions. *Glycobiology.* 2006;16(11):137R-57R.
150. Ahmad N, Gabius HJ, Sabesan S, Oscarson S, and Brewer CF. Thermodynamic binding studies of bivalent oligosaccharides to galectin-1, galectin-3, and the carbohydrate recognition domain of galectin-3. *Glycobiology.* 2004;14(9):817-25.
151. Astorgues-Xerri L, Riveiro ME, Tijeras-Raballand A, Serova M, Neuzillet C, Albert S, Raymond E, and Faivre S. Unraveling galectin-1 as a novel therapeutic target for cancer. *Cancer treatment reviews.* 2014;40(2):307-19.
152. Wells V, and Mallucci L. Identification of an autocrine negative growth factor: mouse beta-galactoside-binding protein is a cytostatic factor and cell growth regulator. *Cell.* 1991;64(1):91-7.
153. Adams L, Scott GK, and Weinberg CS. Biphasic modulation of cell growth by recombinant human galectin-1. *Biochimica et biophysica acta.* 1996;1312(2):137-44.
154. Yang RY, Hsu DK, and Liu FT. Expression of galectin-3 modulates T-cell growth and apoptosis. *Proceedings of the National Academy of Sciences of the United States of America.* 1996;93(13):6737-42.
155. Matarrese P, Tinari A, Mormone E, Bianco GA, Toscano MA, Ascione B, Rabinovich GA, and Malorni W. Galectin-1 sensitizes resting human T lymphocytes to Fas (CD95)-mediated cell death via mitochondrial hyperpolarization, budding, and fission. *The Journal of biological chemistry.* 2005;280(8):6969-85.
156. Poirier F, Timmons PM, Chan CT, Guenet JL, and Rigby PW. Expression of the L14 lectin during mouse embryogenesis suggests multiple roles during pre- and post-implantation development. *Development.* 1992;115(1):143-55.
157. Regan LJ, Dodd J, Barondes SH, and Jessell TM. Selective expression of endogenous lactose-binding lectins and lactoseries glycoconjugates in subsets of rat sensory neurons. *Proceedings of the National Academy of Sciences of the United States of America.* 1986;83(7):2248-52.
158. Hynes MA, Gitt M, Barondes SH, Jessell TM, and Buck LB. Selective expression of an endogenous lactose-binding lectin gene in subsets of central and peripheral neurons. *The Journal of neuroscience : the official journal of the Society for Neuroscience.* 1990;10(3):1004-13.
159. Sango K, Tokashiki A, Ajiki K, Horie M, Kawano H, Watabe K, Horie H, and Kadoya T. Synthesis, localization and externalization of galectin-1 in mature dorsal root ganglion neurons and Schwann cells. *The European journal of neuroscience.* 2004;19(1):55-64.
160. Harrison FL, and Wilson TJ. The 14 kDa beta-galactoside binding lectin in myoblast and myotube cultures: localization by confocal microscopy. *Journal of cell science.* 1992;101 (Pt 3)(635-46.
161. Cho M, and Cummings RD. Galectin-1, a beta-galactoside-binding lectin in Chinese hamster ovary cells. II. Localization and biosynthesis. *The Journal of biological chemistry.* 1995;270(10):5207-12.

162. Schwarz FP, Ahmed H, Bianchet MA, Amzel LM, and Vasta GR. Thermodynamics of bovine spleen galectin-1 binding to disaccharides: correlation with structure and its effect on oligomerization at the denaturation temperature. *Biochemistry.* 1998;37(17):5867-77.
163. Hughes RC. Secretion of the galectin family of mammalian carbohydrate-binding proteins. *Biochimica et biophysica acta.* 1999;1473(1):172-85.
164. Moiseeva EP, Williams B, Goodall AH, and Samani NJ. Galectin-1 interacts with beta-1 subunit of integrin. *Biochemical and biophysical research communications.* 2003;310(3):1010-6.
165. Paz A, Haklai R, Elad-Sfadia G, Ballan E, and Kloog Y. Galectin-1 binds oncogenic H-Ras to mediate Ras membrane anchorage and cell transformation. *Oncogene.* 2001;20(51):7486-93.
166. Ehrhardt A, Ehrhardt GR, Guo X, and Schrader JW. Ras and relatives--job sharing and networking keep an old family together. *Experimental hematology.* 2002;30(10):1089-106.
167. Boriack-Sjodin PA, Margarit SM, Bar-Sagi D, and Kuriyan J. The structural basis of the activation of Ras by Sos. *Nature.* 1998;394(6691):337-43.
168. Cherfils J, and Zeghouf M. Regulation of small GTPases by GEFs, GAPs, and GDIs. *Physiological reviews.* 2013;93(1):269-309.
169. Vetter IR, and Wittinghofer A. The guanine nucleotide-binding switch in three dimensions. *Science.* 2001;294(5545):1299-304.
170. Downward J. Targeting RAS signalling pathways in cancer therapy. *Nature reviews Cancer.* 2003;3(1):11-22.
171. Wennerberg K, Rossman KL, and Der CJ. The Ras superfamily at a glance. *Journal of cell science.* 2005;118(Pt 5):843-6.
172. Umanoff H, Edelmann W, Pellicer A, and Kucherlapati R. The murine N-ras gene is not essential for growth and development. *Proceedings of the National Academy of Sciences of the United States of America.* 1995;92(5):1709-13.
173. Johnson L, Greenbaum D, Cichowski K, Mercer K, Murphy E, Schmitt E, Bronson RT, Umanoff H, Edelmann W, Kucherlapati R, et al. K-ras is an essential gene in the mouse with partial functional overlap with N-ras. *Genes & development.* 1997;11(19):2468-81.
174. Koera K, Nakamura K, Nakao K, Miyoshi J, Toyoshima K, Hatta T, Otani H, Aiba A, and Katsuki M. K-ras is essential for the development of the mouse embryo. *Oncogene.* 1997;15(10):1151-9.
175. Esteban LM, Vicario-Abejon C, Fernandez-Salguero P, Fernandez-Medarde A, Swaminathan N, Yienger K, Lopez E, Malumbres M, McKay R, Ward JM, et al. Targeted genomic disruption of H-ras and N-ras, individually or in combination, reveals the dispensability of both loci for mouse growth and development. *Molecular and cellular biology.* 2001;21(5):1444-52.
176. Hancock JF. Ras proteins: different signals from different locations. *Nature reviews Molecular cell biology.* 2003;4(5):373-84.
177. Jaumot M, Yan J, Clyde-Smith J, Sluimer J, and Hancock JF. The linker domain of the Ha-Ras hypervariable region regulates interactions with

exchange factors, Raf-1 and phosphoinositide 3-kinase. *The Journal of biological chemistry.* 2002;277(1):272-8.
178. Yan J, Roy S, Apolloni A, Lane A, and Hancock JF. Ras isoforms vary in their ability to activate Raf-1 and phosphoinositide 3-kinase. *The Journal of biological chemistry.* 1998;273(37):24052-6.
179. Voice JK, Klemke RL, Le A, and Jackson JH. Four human ras homologs differ in their abilities to activate Raf-1, induce transformation, and stimulate cell motility. *The Journal of biological chemistry.* 1999;274(24):17164-70.
180. Suire S, Hawkins P, and Stephens L. Activation of phosphoinositide 3-kinase gamma by Ras. *Current biology : CB.* 2002;12(13):1068-75.
181. Hamilton M, and Wolfman A. Ha-ras and N-ras regulate MAPK activity by distinct mechanisms in vivo. *Oncogene.* 1998;16(11):1417-28.
182. Walsh AB, and Bar-Sagi D. Differential activation of the Rac pathway by Ha-Ras and K-Ras. *The Journal of biological chemistry.* 2001;276(19):15609-15.
183. Willumsen BM, Christensen A, Hubbert NL, Papageorge AG, and Lowy DR. The p21 ras C-terminus is required for transformation and membrane association. *Nature.* 1984;310(5978):583-6.
184. Reiss Y, Goldstein JL, Seabra MC, Casey PJ, and Brown MS. Inhibition of purified p21ras farnesyl:protein transferase by Cys-AAX tetrapeptides. *Cell.* 1990;62(1):81-8.
185. Choy E, Chiu VK, Silletti J, Feoktistov M, Morimoto T, Michaelson D, Ivanov IE, and Philips MR. Endomembrane trafficking of ras: the CAAX motif targets proteins to the ER and Golgi. *Cell.* 1999;98(1):69-80.
186. Boyartchuk VL, Ashby MN, and Rine J. Modulation of Ras and a-factor function by carboxyl-terminal proteolysis. *Science.* 1997;275(5307):1796-800.
187. Kim E, Ambroziak P, Otto JC, Taylor B, Ashby M, Shannon K, Casey PJ, and Young SG. Disruption of the mouse Rce1 gene results in defective Ras processing and mislocalization of Ras within cells. *The Journal of biological chemistry.* 1999;274(13):8383-90.
188. Hrycyna CA, Sapperstein SK, Clarke S, and Michaelis S. The Saccharomyces cerevisiae STE14 gene encodes a methyltransferase that mediates C-terminal methylation of a-factor and RAS proteins. *The EMBO journal.* 1991;10(7):1699-709.
189. Dai Q, Choy E, Chiu V, Romano J, Slivka SR, Steitz SA, Michaelis S, and Philips MR. Mammalian prenylcysteine carboxyl methyltransferase is in the endoplasmic reticulum. *The Journal of biological chemistry.* 1998;273(24):15030-4.
190. Apolloni A, Prior IA, Lindsay M, Parton RG, and Hancock JF. H-ras but not K-ras traffics to the plasma membrane through the exocytic pathway. *Molecular and cellular biology.* 2000;20(7):2475-87.
191. Willumsen BM, Cox AD, Solski PA, Der CJ, and Buss JE. Novel determinants of H-Ras plasma membrane localization and transformation. *Oncogene.* 1996;13(9):1901-9.

192. Hancock JF, Paterson H, and Marshall CJ. A polybasic domain or palmitoylation is required in addition to the CAAX motif to localize p21ras to the plasma membrane. *Cell.* 1990;63(1):133-9.
193. Simons K, and Toomre D. Lipid rafts and signal transduction. *Nature reviews Molecular cell biology.* 2000;1(1):31-9.
194. Prior IA, Muncke C, Parton RG, and Hancock JF. Direct visualization of Ras proteins in spatially distinct cell surface microdomains. *The Journal of cell biology.* 2003;160(2):165-70.
195. Prior IA, and Hancock JF. Compartmentalization of Ras proteins. *Journal of cell science.* 2001;114(Pt 9):1603-8.
196. Niv H, Gutman O, Kloog Y, and Henis YI. Activated K-Ras and H-Ras display different interactions with saturable nonraft sites at the surface of live cells. *The Journal of cell biology.* 2002;157(5):865-72.
197. Prior IA, Harding A, Yan J, Sluimer J, Parton RG, and Hancock JF. GTP-dependent segregation of H-ras from lipid rafts is required for biological activity. *Nature cell biology.* 2001;3(4):368-75.
198. Rotblat B, Prior IA, Muncke C, Parton RG, Kloog Y, Henis YI, and Hancock JF. Three separable domains regulate GTP-dependent association of H-ras with the plasma membrane. *Molecular and cellular biology.* 2004;24(15):6799-810.
199. Elad-Sfadia G, Haklai R, Ballan E, Gabius HJ, and Kloog Y. Galectin-1 augments Ras activation and diverts Ras signals to Raf-1 at the expense of phosphoinositide 3-kinase. *The Journal of biological chemistry.* 2002;277(40):37169-75.
200. Belanis L, Plowman SJ, Rotblat B, Hancock JF, and Kloog Y. Galectin-1 is a novel structural component and a major regulator of h-ras nanoclusters. *Molecular biology of the cell.* 2008;19(4):1404-14.
201. Rotblat B, Belanis L, Liang H, Haklai R, Elad-Zefadia G, Hancock JF, Kloog Y, and Plowman SJ. H-Ras nanocluster stability regulates the magnitude of MAPK signal output. *PloS one.* 2010;5(8):e11991.
202. Ashery U, Yizhar O, Rotblat B, Elad-Sfadia G, Barkan B, Haklai R, and Kloog Y. Spatiotemporal organization of Ras signaling: rasosomes and the galectin switch. *Cellular and molecular neurobiology.* 2006;26(4-6):471-95.
203. Guzman C, Solman M, Ligabue A, Blazevits O, Andrade DM, Reymond L, Eggeling C, and Abankwa D. The efficacy of Raf kinase recruitment to the GTPase H-ras depends on H-ras membrane conformer-specific nanoclustering. *The Journal of biological chemistry.* 2014;289(14):9519-33.
204. Janosch P, Kieser A, Eulitz M, Lovric J, Sauer G, Reichert M, Gounari F, Buscher D, Baccarini M, Mischak H, et al. The Raf-1 kinase associates with vimentin kinases and regulates the structure of vimentin filaments. *FASEB journal : official publication of the Federation of American Societies for Experimental Biology.* 2000;14(13):2008-21.
205. Snider NT, and Omary MB. Post-translational modifications of intermediate filament proteins: mechanisms and functions. *Nature reviews Molecular cell biology.* 2014;15(3):163-77.

206. Sihag RK, Inagaki M, Yamaguchi T, Shea TB, and Pant HC. Role of phosphorylation on the structural dynamics and function of types III and IV intermediate filaments. *Experimental cell research.* 2007;313(10):2098-109.
207. Inagaki M, Nishi Y, Nishizawa K, Matsuyama M, and Sato C. Site-specific phosphorylation induces disassembly of vimentin filaments in vitro. *Nature.* 1987;328(6131):649-52.
208. Chou YH, Rosevear E, and Goldman RD. Phosphorylation and disassembly of intermediate filaments in mitotic cells. *Proceedings of the National Academy of Sciences of the United States of America.* 1989;86(6):1885-9.
209. Eriksson JE, He T, Trejo-Skalli AV, Harmala-Brasken AS, Hellman J, Chou YH, and Goldman RD. Specific in vivo phosphorylation sites determine the assembly dynamics of vimentin intermediate filaments. *Journal of cell science.* 2004;117(Pt 6):919-32.
210. Busch T, Armacki M, Eiseler T, Joodi G, Temme C, Jansen J, von Wichert G, Omary MB, Spatz J, and Seufferlein T. Keratin 8 phosphorylation regulates keratin reorganization and migration of epithelial tumor cells. *Journal of cell science.* 2012;125(Pt 9):2148-59.
211. Chen DN, Zeng J, Wang F, Zheng W, Tu WW, Zhao JS, and Xu J. Hyperphosphorylation of intermediate filament proteins is involved in microcystin-LR-induced toxicity in HL7702 cells. *Toxicology letters.* 2012;214(2):192-9.
212. Lee EJ, Park MK, Kim HJ, Kang JH, Kim YR, Kang GJ, Byun HJ, and Lee CH. 12-O-Tetradecanoylphorbol-13-Acetate Induces Keratin 8 Phosphorylation and Reorganization via Expression of Transglutaminase-2. *Biomolecules & therapeutics.* 2014;22(2):122-8.
213. Lei S, Tian YP, Xiao WD, Li S, Rao XC, Zhang JL, Yang J, Hu XM, and Chen W. ROCK is involved in vimentin phosphorylation and rearrangement induced by dengue virus. *Cell biochemistry and biophysics.* 2013;67(3):1333-42.
214. Goto H, Kosako H, Tanabe K, Yanagida M, Sakurai M, Amano M, Kaibuchi K, and Inagaki M. Phosphorylation of vimentin by Rho-associated kinase at a unique amino-terminal site that is specifically phosphorylated during cytokinesis. *The Journal of biological chemistry.* 1998;273(19):11728-36.
215. Izawa I, and Inagaki M. Regulatory mechanisms and functions of intermediate filaments: a study using site- and phosphorylation state-specific antibodies. *Cancer science.* 2006;97(3):167-74.
216. Lamb NJ, Fernandez A, Feramisco JR, and Welch WJ. Modulation of vimentin containing intermediate filament distribution and phosphorylation in living fibroblasts by the cAMP-dependent protein kinase. *The Journal of cell biology.* 1989;108(6):2409-22.
217. Sin WC, Chen XQ, Leung T, and Lim L. RhoA-binding kinase alpha translocation is facilitated by the collapse of the vimentin intermediate filament network. *Molecular and cellular biology.* 1998;18(11):6325-39.

218. Meriane M, Mary S, Comunale F, Vignal E, Fort P, and Gauthier-Rouviere C. Cdc42Hs and Rac1 GTPases induce the collapse of the vimentin intermediate filament network. *The Journal of biological chemistry.* 2000;275(42):33046-52.
219. Evans RM, and Fink LM. An alteration in the phosphorylation of vimentin-type intermediate filaments is associated with mitosis in cultured mammalian cells. *Cell.* 1982;29(1):43-52.
220. Evans RM. Peptide mapping of phosphorylated vimentin. Evidence for a site-specific alteration in mitotic cells. *The Journal of biological chemistry.* 1984;259(9):5372-5.
221. Evans RM. Phosphorylation of vimentin in mitotically selected cells. In vitro cyclic AMP-independent kinase and calcium-stimulated phosphatase activities. *The Journal of cell biology.* 1989;108(1):67-78.
222. Chou YH, Bischoff JR, Beach D, and Goldman RD. Intermediate filament reorganization during mitosis is mediated by p34cdc2 phosphorylation of vimentin. *Cell.* 1990;62(6):1063-71.
223. Chou YH, Opal P, Quinlan RA, and Goldman RD. The relative roles of specific N- and C-terminal phosphorylation sites in the disassembly of intermediate filament in mitotic BHK-21 cells. *Journal of cell science.* 1996;109 (Pt 4)(817-26.
224. Rosevear ER, McReynolds M, and Goldman RD. Dynamic properties of intermediate filaments: disassembly and reassembly during mitosis in baby hamster kidney cells. *Cell motility and the cytoskeleton.* 1990;17(3):150-66.
225. Inagaki N, Ito M, Nakano T, and Inagaki M. Spatiotemporal distribution of protein kinase and phosphatase activities. *Trends in biochemical sciences.* 1994;19(11):448-52.
226. Foisner R. Dynamic organisation of intermediate filaments and associated proteins during the cell cycle. *BioEssays : news and reviews in molecular, cellular and developmental biology.* 1997;19(4):297-305.
227. Tsujimura K, Ogawara M, Takeuchi Y, Imajoh-Ohmi S, Ha MH, and Inagaki M. Visualization and function of vimentin phosphorylation by cdc2 kinase during mitosis. *The Journal of biological chemistry.* 1994;269(49):31097-106.
228. Yamaguchi T, Goto H, Yokoyama T, Sillje H, Hanisch A, Uldschmid A, Takai Y, Oguri T, Nigg EA, and Inagaki M. Phosphorylation by Cdk1 induces Plk1-mediated vimentin phosphorylation during mitosis. *The Journal of cell biology.* 2005;171(3):431-6.
229. Inagaki M, Inagaki N, Takahashi T, and Takai Y. Phosphorylation-dependent control of structures of intermediate filaments: a novel approach using site- and phosphorylation state-specific antibodies. *Journal of biochemistry.* 1997;121(3):407-14.
230. Goto H, Yasui Y, Kawajiri A, Nigg EA, Terada Y, Tatsuka M, Nagata K, and Inagaki M. Aurora-B regulates the cleavage furrow-specific vimentin phosphorylation in the cytokinetic process. *The Journal of biological chemistry.* 2003;278(10):8526-30.

231. Carden MJ, Trojanowski JQ, Schlaepfer WW, and Lee VM. Two-stage expression of neurofilament polypeptides during rat neurogenesis with early establishment of adult phosphorylation patterns. *The Journal of neuroscience : the official journal of the Society for Neuroscience.* 1987;7(11):3489-504.
232. Sanchez I, Hassinger L, Sihag RK, Cleveland DW, Mohan P, and Nixon RA. Local control of neurofilament accumulation during radial growth of myelinating axons in vivo. Selective role of site-specific phosphorylation. *The Journal of cell biology.* 2000;151(5):1013-24.
233. Angelides KJ, Smith KE, and Takeda M. Assembly and exchange of intermediate filament proteins of neurons: neurofilaments are dynamic structures. *The Journal of cell biology.* 1989;108(4):1495-506.
234. Colakoglu G, and Brown A. Intermediate filaments exchange subunits along their length and elongate by end-to-end annealing. *The Journal of cell biology.* 2009;185(5):769-77.
235. Yabe JT, Pimenta A, and Shea TB. Kinesin-mediated transport of neurofilament protein oligomers in growing axons. *Journal of cell science.* 1999;112 (Pt 21)(3799-814.
236. Motil J, Chan WK, Dubey M, Chaudhury P, Pimenta A, Chylinski TM, Ortiz DT, and Shea TB. Dynein mediates retrograde neurofilament transport within axons and anterograde delivery of NFs from perikarya into axons: regulation by multiple phosphorylation events. *Cell motility and the cytoskeleton.* 2006;63(5):266-86.
237. Roy S, Coffee P, Smith G, Liem RK, Brady ST, and Black MM. Neurofilaments are transported rapidly but intermittently in axons: implications for slow axonal transport. *The Journal of neuroscience : the official journal of the Society for Neuroscience.* 2000;20(18):6849-61.
238. Wang L, and Brown A. Rapid intermittent movement of axonal neurofilaments observed by fluorescence photobleaching. *Molecular biology of the cell.* 2001;12(10):3257-67.
239. Wang L, Ho CL, Sun D, Liem RK, and Brown A. Rapid movement of axonal neurofilaments interrupted by prolonged pauses. *Nature cell biology.* 2000;2(3):137-41.
240. Kushkuley J, Chan WK, Lee S, Eyer J, Leterrier JF, Letournel F, and Shea TB. Neurofilament cross-bridging competes with kinesin-dependent association of neurofilaments with microtubules. *Journal of cell science.* 2009;122(Pt 19):3579-86.
241. Ackerley S, Grierson AJ, Brownlees J, Thornhill P, Anderton BH, Leigh PN, Shaw CE, and Miller CC. Glutamate slows axonal transport of neurofilaments in transfected neurons. *The Journal of cell biology.* 2000;150(1):165-76.
242. Jung C, Yabe JT, Lee S, and Shea TB. Hypophosphorylated neurofilament subunits undergo axonal transport more rapidly than more extensively phosphorylated subunits in situ. *Cell motility and the cytoskeleton.* 2000;47(2):120-9.

243. Ackerley S, Thornhill P, Grierson AJ, Brownlees J, Anderton BH, Leigh PN, Shaw CE, and Miller CC. Neurofilament heavy chain side arm phosphorylation regulates axonal transport of neurofilaments. *The Journal of cell biology.* 2003;161(3):489-95.
244. Yabe JT, Chylinski T, Wang FS, Pimenta A, Kattar SD, Linsley MD, Chan WK, and Shea TB. Neurofilaments consist of distinct populations that can be distinguished by C-terminal phosphorylation, bundling, and axonal transport rate in growing axonal neurites. *The Journal of neuroscience : the official journal of the Society for Neuroscience.* 2001;21(7):2195-205.
245. Gou JP, Gotow T, Janmey PA, and Leterrier JF. Regulation of neurofilament interactions in vitro by natural and synthetic polypeptides sharing Lys-Ser-Pro sequences with the heavy neurofilament subunit NF-H: neurofilament crossbridging by antiparallel sidearm overlapping. *Medical & biological engineering & computing.* 1998;36(3):371-87.
246. Aranda-Espinoza H, Carl P, Leterrier JF, Janmey P, and Discher DE. Domain unfolding in neurofilament sidearms: effects of phosphorylation and ATP. *FEBS letters.* 2002;531(3):397-401.
247. Shea TB, Yabe JT, Ortiz D, Pimenta A, Loomis P, Goldman RD, Amin N, and Pant HC. Cdk5 regulates axonal transport and phosphorylation of neurofilaments in cultured neurons. *Journal of cell science.* 2004;117(Pt 6):933-41.
248. Chan WK, Yabe JT, Pimenta AF, Ortiz D, and Shea TB. Neurofilaments can undergo axonal transport and cytoskeletal incorporation in a discontinuous manner. *Cell motility and the cytoskeleton.* 2005;62(3):166-79.
249. de Waegh SM, Lee VM, and Brady ST. Local modulation of neurofilament phosphorylation, axonal caliber, and slow axonal transport by myelinating Schwann cells. *Cell.* 1992;68(3):451-63.
250. Vyas PM, Tomamichel WJ, Pride PM, Babbey CM, Wang Q, Mercier J, Martin EM, and Payne RM. A TAT-frataxin fusion protein increases lifespan and cardiac function in a conditional Friedreich's ataxia mouse model. *Human molecular genetics.* 2012;21(6):1230-47.
251. Del Gaizo V, and Payne RM. A novel TAT-mitochondrial signal sequence fusion protein is processed, stays in mitochondria, and crosses the placenta. *Molecular therapy : the journal of the American Society of Gene Therapy.* 2003;7(6):720-30.
252. Kim W, Bennett EJ, Huttlin EL, Guo A, Li J, Possemato A, Sowa ME, Rad R, Rush J, Comb MJ, et al. Systematic and quantitative assessment of the ubiquitin-modified proteome. *Molecular cell.* 2011;44(2):325-40.
253. Lolkema MP, Gervais ML, Snijckers CM, Hill RP, Giles RH, Voest EE, and Ohh M. Tumor suppression by the von Hippel-Lindau protein requires phosphorylation of the acidic domain. *The Journal of biological chemistry.* 2005;280(23):22205-11.
254. Bianchi S, Stimpson CD, Duka T, Larsen MD, Janssen WG, Collins Z, Bauernfeind AL, Schapiro SJ, Baze WB, McArthur MJ, et al. Synaptogenesis and development of pyramidal neuron dendritic

morphology in the chimpanzee neocortex resembles humans. *Proceedings of the National Academy of Sciences of the United States of America.* 2013;110 Suppl 2(10395-401.
255. Nixon RA, Lewis SE, Dahl D, Marotta CA, and Drager UC. Early posttranslational modifications of the three neurofilament subunits in mouse retinal ganglion cells: neuronal sites and time course in relation to subunit polymerization and axonal transport. *Brain research Molecular brain research.* 1989;5(2):93-108.
256. Shea TB, and Yabe J. Occam's Razor slices through the mysteries of neurofilament axonal transport: can it really be so simple? *Traffic.* 2000;1(6):522-3.
257. Bulinski JC, McGraw TE, Gruber D, Nguyen HL, and Sheetz MP. Overexpression of MAP4 inhibits organelle motility and trafficking in vivo. *Journal of cell science.* 1997;110 (Pt 24)(3055-64.
258. Trinczek B, Ebneth A, Mandelkow EM, and Mandelkow E. Tau regulates the attachment/detachment but not the speed of motors in microtubule-dependent transport of single vesicles and organelles. *Journal of cell science.* 1999;112 (Pt 14)(2355-67.
259. Seitz A, Kojima H, Oiwa K, Mandelkow EM, Song YH, and Mandelkow E. Single-molecule investigation of the interference between kinesin, tau and MAP2c. *The EMBO journal.* 2002;21(18):4896-905.
260. Ebneth A, Godemann R, Stamer K, Illenberger S, Trinczek B, and Mandelkow E. Overexpression of tau protein inhibits kinesin-dependent trafficking of vesicles, mitochondria, and endoplasmic reticulum: implications for Alzheimer's disease. *The Journal of cell biology.* 1998;143(3):777-94.
261. Stamer K, Vogel R, Thies E, Mandelkow E, and Mandelkow EM. Tau blocks traffic of organelles, neurofilaments, and APP vesicles in neurons and enhances oxidative stress. *The Journal of cell biology.* 2002;156(6):1051-63.

CURRICULUM VITAE

KYLE BENJAMIN MARTIN

Education

Ph.D. (2008 – 2015)
Indiana University, Indianapolis, IN
Major: Medical & Molecular Genetics

Bachelor of Science (2004 – 2008)
Ohio University, Athens, OH
Major: Biochemistry

Awards and Honors

2014: American Society for Biochemistry and Molecular Biology Travel Award
2014: Indiana University School of Medicine Graduate Student Travel Award
2008: Indiana University School of Medicine Fellowship Travel Grant
2008: Ohio University Provost Undergraduate Research Grant
2007: Ohio University Undergraduate Research/TA Training Program
2007 – 2008: Ohio University Dean's Scholarship
2004 – 2008: Ohio University Alvin Carlson Scholarship
2004 – 2008: Altria Group Scholarship

Publications

1. **Martin KB** and Payne RM. Gigaxonin regulates intermediate filament phosphorylation and structure by modulating the Ras pathway through the degradation of galectin-1. *Manuscript in preparation*

Invited Presentations

1. **Martin KB**. Prevention of the GAN fibroblast phenotype via TAT-Gigaxonin protein replacement therapy. Hannah's Hope Fund GAN Conference. Northwestern University, Chicago, IL. (2012)
2. **Martin KB**. Treatment of Giant Axonal Neuropathy using cell penetrating peptides. Hannah's Hope Fund GAN Conference. Columbia University, New York City, NY. (2011)
3. **Martin KB**. TAT-Gigaxonin Fusion Proteins: A Novel Therapeutic Strategy for GAN. Hannah's Hope Fund GAN Conference. NIH Chemical Genomics Center, Washington D.C. (2009)

Poster Presentations

1. **Martin KB** and Payne RM. Gigaxonin regulates intermediate filament structure by modulating the Ras pathway through the degradation of galectin-1. American Society for Biochemistry and Molecular Biology Annual Meeting. San Diego, CA. (2014)
2. **Martin KB** and Payne RM. Intermediate filament hyperphosphorylation in Giant Axonal Neuropathy. IUPUI Research Day. Indianapolis, IN. (2014)
3. **Martin KB** and Payne RM. TAT-mediated treatment of an ubiquitin-proteasome system defect. Neurobiology of Disease in Children Symposium. Savannah, GA. (2011)
4. **Martin KB** and Payne RM. Treatment of Giant Axonal Neuropathy using cell penetrating peptides. Riley Heart Center Symposium. Indianapolis, IN. (2010)

Teaching Experience

2008: Peer-Led Team Learning Instructor, Ohio University, Athens, OH
Courses: Chemistry 152, 153

2007 – 2008: Teaching Assistant, Ohio University, Athens, OH
Courses: Chemistry 151, 152, 153